Toplinska svojstva filmova poli(etilen-oksida)/natrijevog alginata nakon izlaganja Ca2+ ionima

Pervan, Nikolina

Master's thesis / Diplomski rad

2020

SVEUČILIŠTE U SPLITU

KEMIJSKO-TEHNOLOŠKI FAKULTET

TOPLINSKA SVOJSTVA FILMOVA POLI(ETILEN-OKSIDA)/NATRIJEVOG ALGINATA NAKON IZLAGANJA Ca^{2+} IONIMA

DIPLOMSKI RAD

NIKOLINA PERVAN

Matični broj: 205

Split, rujan 2020.

SVEUČILIŠTE U SPLITU
KEMIJSKO-TEHNOLOŠKI FAKULTET
DIPLOMSKI STUDIJ KEMIJSKE TEHNOLOGIJE
MATERIJALI

TOPLINSKA SVOJSTVA FILMOVA POLI(ETILEN-OKSIDA)/NATRIJEVOG ALGINATA NAKON IZLAGANJA Ca^{2+} IONIMA

DIPLOMSKI RAD

NIKOLINA PERVAN
Matični broj: 205

Split, rujan 2020.

UNIVERSITY OF SPLIT
FACULTY OF CHEMISTRY AND TECHNOLGY
GRADUATE STUDY OF CHEMICAL TEHNOLOGY
MATERIALS

THERMAL PROPERTIES OF POLY(ETHYLENE OXIDE)/SODIUM ALGINATE FILMS AFTER TREATMENT WITH Ca^{2+} IONS

DIPLOMA THESIS

NIKOLINA PERVAN

Parent number: 205

Split, September 2020.

UTJECAJ KALCIJEVOG KLORIDA NA TOPLINSKA SVOJSTVA FILMOVA MJEŠAVINA POLI(ETILEN-OKSIDA) I NATRIJEVOG ALGINATA

Nikolina Pervan, 205

Sažetak: Referentni film poli(etilen oksid)/natrijev alginat mješavine s 80 mas.% poli(etilen oksida) i 20 mas.% natrijevog alginata (80%PEO/20%NaAlg) pripremljen je metodom lijevanja filma iz otopine. Umrežavanje natrijevog alginata u filmu mješavine s Ca^{2+} ionima provedeno je s 1, 2,5, 5, 7,5 i 10% w/v metanolne otopine $CaCl_2$ tijekom 10, 30, 60 i 180 minuta izlaganja, nakon čega su filmovi isprani dva puta. Strukturna promjena NaAlg istražena je primjenom infracrvene spektroskopije s Fourierovom transformacijom (FT-IR) prema kojoj je umrežavanje s Ca^{2+} ionima uspješno provedeno. Diferencijalna pretražna kalorimetrija (DSC) primijenjena je za ispitivanje utjecaja umrežavanja na toplinska svojstva i kristalnost PEO u filmovima mješavina. Umrežavanje s Ca^{2+} ionima ima značajan utjecaj na kristalizaciju PEO i kod određenih uvjeta se smanjuje količina kristalne faze PEO u tretiranim filmovima mješavina. Toplinska stabilnost tretiranih filmova mješavina ispitivana je uporabom neizotermne termogravimetrije (TG). Određeni uvjeti umrežavanja doveli su do poboljšanja toplinske stabilnosti alginata u filmu mješavine i usporavanja razgradnje PEO. Sve provedene analize potvrdile su uspješno umrežavanje s Ca^{2+} ionima. U budućim istraživanjima umrežavanje NaAlg s Ca^{2+} ionima u filmu 80%PEO/20%NaAlg mješavine provodit će se samo s najvećom koncentracijom metanolne otopine $CaCl_2$ (10% w/v) i uz najduže vrijeme izlaganja otopini (180 min). Navedeni uvjeti polučili su najbolje rezultate te dobiveni film pri tim uvjetima ima najveći potencijal kao čvrsti polimerni elektrolit.

Ključne riječi: poli(etilen-oksid), natrijev alginat, kalcijev klorid, umrežavanje, toplinska svojstva, toplinska postojanost

Rad sadrži: 89 stranica, 69 slika, 22 tablice, 52 literaturne reference

Jezik izvornika: engleski

Sastav Povjerenstva za obranu:

1. Prof. dr. sc. Ladislav Vrsalović - predsjednik
2. Doc. dr. sc. Miće Jakić - član
3. Doc. dr. sc. Sanja Perinović Jozić - član-mentor

Datum obrane: 25. rujna 2020.

Rad je u tiskanom i elektroničkom (pdf format) obliku pohranjen u Knjižnici Kemijsko-tehnološkog fakulteta Split, Ruđera Boškovića 35.

INFLUENCE OF CALCIUM CHLORIDE ON THE THERMAL PROPERTIES OF FILMS BLENDS OF POLY(ETHYLENE OXIDE) AND SODIUM ALGINATE
Nikolina Pervan, 205

Abstract: The referent film of poly(ethylene oxide)/sodium alginate blend with 80 wt% of poly(ethylene oxide) and 20 wt% of sodium alginate (80%PEO/20%NaAlg) was prepared by solution casting method. The cross-linkage of sodium alginate in the blend film with Ca^{2+} ions was conducted with 1, 2.5, 5, 7.5 and 10% w/v $CaCl_2$ methanol solution during 10, 30, 60 and 180 minutes exposure time after which the films were rinse twice. The structural change of NaAlg was investigated by Fourier transform infrared spectroscopy (FT-IR) according to which the cross-linkage with Ca^{2+} ions was successful. Differential scanning calorimetry (DSC) has been applied to investigate the influence of cross-linkage treatment to the thermal properties and crystallinity of PEO in the films. The cross-linkage with Ca^{2+} ions has significant effect on the crystallization process of PEO and under the specific conditions it lowers the amount of crystalline phase of PEO in the treated films. Thermal stability of the treated films was investigated using non-isothermal thermogravimetry (TG). The specific conditions make the degradation of alginate in the treated films more stable while at the same time they decrease the rate of the degradation of PEO. All analysis confirmed the successful cross-linkage with Ca^{2+} ions. In the future investigations cross-linkage of NaAlg with Ca^{2+} ions in 80%PEO/20%NaAlg film will be carried out only at the highest concentration of $CaCl_2$ methanol solution (10% w/v) and the highest exposure time to the solution (180 min). These conditions showed the best results and obtained film under these conditions has the greatest potential to be a solid polymer electrolyte.

Keywords: poly(ethylene oxide), sodium alginate, calcium chloride, cross-linkage, thermal properties, thermal stability

DIPLOMA THESIS ASSIGNMENT

1. To prepare referent film of poly(ethylene oxide)/sodium alginate blend with 80 wt% of poly(ethylene oxide) and 20 wt% of sodium alginate by solution casting method.

2. Expose prepared film to calcium chloride methanol solution to induce cross-linking of sodium alginate in the blend film by ion exchange of Na^+ with Ca^{2+} ions.

3. The cross-linkage treatment conduct with different concentration of calcium chloride solution, different time during which the film will be expose or immerse in a solution and different number of the rinsing with methanol after cross-linkage procedure.

4. After the cross-linkage treatment: to analyse the films by Fourier transform infrared spectroscopy, differential scanning calorimetry and non-isothermal thermogravimetry in terms of structural changes and changes of the thermal properties. Find the best conditions for the cross-linkage and at the same time see which film has a potential to be a solid polymer electrolyte.

.

SUMMARY

The referent film of poly(ethylene oxide)/sodium alginate blend with 80 wt% of poly(ethylene oxide) and 20 wt% of sodium alginate (80%PEO/20%NaAlg) was prepared by solution casting method. The cross-linkage of sodium alginate in the blend film with Ca^{2+} ions was conducted with 1, 2.5, 5, 7.5 and 10% w/v $CaCl_2$ methanol solution during 10, 30, 60 and 180 minutes exposure time after which the films were rinse twice. The structural change of NaAlg was investigated by Fourier transform infrared spectroscopy (FT-IR) according to which the cross-linkage with Ca^{2+} ions was successful. Differential scanning calorimetry (DSC) has been applied to investigate the influence of cross-linkage treatment to the thermal properties and crystallinity of PEO in the films. The cross-linkage with Ca^{2+} ions has significant effect on the crystallization process of PEO and under the specific conditions it lowers the amount of crystalline phase of PEO in the treated films. Thermal stability of the treated films was investigated using non-isothermal thermogravimetry (TG). The specific conditions make the degradation of alginate in the treated films more stable while at the same time they decrease the rate of the degradation of PEO. All analysis confirmed the successful cross-linkage with Ca^{2+} ions. In the future investigations cross-linkage of NaAlg with Ca^{2+} ions in 80%PEO/20%NaAlg film will be carried out only at the highest concentration of $CaCl_2$ methanol solution (10% w/v) and the highest exposure time to the solution (180 min). These conditions showed the best results and obtained film under these conditions has the greatest potential to be a solid polymer electrolyte.

Keywords: poly(ethylene oxide), sodium alginate, calcium chloride, cross-linkage, thermal properties, thermal stability

SAŽETAK

Referentni film poli(etilen oksid)/natrijev alginat mješavine s 80 mas.% poli(etilen oksida) i 20 mas.% natrijevog alginata (80%PEO/20%NaAlg) pripremljen je metodom lijevanja filma iz otopine. Umrežavanje natrijevog alginata u filmu mješavine s Ca^{2+} ionima provedeno je s 1, 2,5, 5, 7,5 i 10% w/v metanolne otopine $CaCl_2$ tijekom 10, 30, 60 i 180 minuta izlaganja, nakon čega su filmovi isprani dva puta. Strukturna promjena NaAlg istražena je primjenom infracrvene spektroskopije s Fourierovom transformacijom (FT-IR) prema kojoj je umrežavanje s Ca^{2+} ionima uspješno provedeno. Diferencijalna pretražna kalorimetrija (DSC) primijenjena je za ispitivanje utjecaja umrežavanja na toplinska svojstva i kristalnost PEO u filmovima mješavina. Umrežavanje s Ca^{2+} ionima ima značajan utjecaj na kristalizaciju PEO i kod određenih uvjeta se smanjuje količina kristalne faze PEO u tretiranim filmovima mješavina. Toplinska stabilnost tretiranih filmova mješavina ispitivana je uporabom neizotermne termogravimetrije (TG). Određeni uvjeti umrežavanja doveli su do poboljšanja toplinske stabilnosti alginata u filmu mješavine i usporavanja razgradnje PEO. Sve provedene analize potvrdile su uspješno umrežavanje s Ca^{2+} ionima. U budućim istraživanjima umrežavanje NaAlg s Ca^{2+} ionima u filmu 80%PEO/20%NaAlg mješavine provodit će se samo s najvećom koncentracijom metanolne otopine $CaCl_2$ (10% w/v) i uz najduže vrijeme izlaganja otopini (180 min). Navedeni uvjeti polučili su najbolje rezultate te dobiveni film pri tim uvjetima ima najveći potencijal kao čvrsti polimerni elektrolit.

Ključne riječi: poli(etilen-oksid), natrijev alginat, kalcijev klorid, umrežavanje, toplinska svojstva, toplinska postojanost

CONTENTS

INTRODUCTION

Development of environment friendly and biodegradable materials based on natural polymers increased attention in an attempt to substitute petroleum-based plastics, which present important concerns in terms of pollution and sustainability of nowadays and more importantly of the future of next generations including ours. The problems of overflowing landfills, polluted waters and plastics wastes have also accelerated the need to develop polymers with controllable lifetimes taking into consideration environmentally acceptable manufacturing, application, recycling and disposal methodology.[1]

Our life is closely connected and controlled by electronics which cannot function without batteries, so it can be said that we live in a battery-driven society. From our smartphones, laptops and other electronic devices to children's toys and cars, modern life practically runs on batteries. But they are not just used in consumer goods. When storms knock out the power grid, batteries keep hospital equipment working and trains running, we can still have electricity in our homes. But batteries can seriously damage the environment including human health if not disposed of properly. The exact combination and number of chemicals inside a battery vary with the type of battery, but the list includes cadmium, lead, mercury, nickel, lithium and electrolytes.[2] Being aware of the danger of mentioned chemicals research for less dangerous solution brought to us solid polymer electrolytes (SPE).

The intrinsic phenomenon of a solid material exhibiting liquid-like conductivity without motion of the solvent itself was fascinating from theoretical point of view and the application to electrochemical devices sounded very promising in a time of emerging concerns with energy and pollution. The SPE are thought to be ideal medium for a wide range of electronic processes. They include primary and secondary rechargeable batteries, ambient temperature fuel cells, electrochromic devices, modified electrodes/sensors, solid state reference electrode system, thermoelectric generators, high vacuum electrochemical devices and electrochemical switching.

Polymer electrolytes are key materials for construction of lightweight and flexible batteries. Many types of polymer electrolytes have been investigated. Many polymer compounds for polymer electrolytes have polyether structure, especially, polyethylene oxide (PEO) structure in their main chain and/or side chains.[3] The advantages of using solid polymer electrolyte (SPE) over their counterpart of liquid electrolytes are

flexibility, no leakage, ease of processing as thin films of large surface area, electrochemical stability and volumetric stability over repeated charge-discharge cycles in a given device. A large number of Li^+, Na^+ and H^+ conducting polymer electrolytes formed by the dissolution of alkali metal salts in various polymer hosts have been reported in literature. In order to achieve a good complexed polymer metal-salt system, the choice of polymer host and the metal salt plays a key role. The choice of polymer host depends mainly on factors such as atoms or group of atoms with sufficient electron donor capacity to form coordination bond with cations, low barrier to bond rotations, so that segmental motion of the polymer chain can take place easily, suitable distance between coordinating centres, to facilitate the formation of multiple intrapolymer ion bonds.[4]

PEO exhibits good electrochemical and mechanical properties, but due to the high degree of crystallinity it has low electrical conductivity at room temperature. Conductivity in these systems is associated with ion migrations and with the mobility of the polymer chain segments being more pronounced in the amorphous phase. One way to increase the electrical conductivity of PEO is to blend with other polymers with the aim of reducing its crystallinity. Sodium alginate (NaAlg) is a natural polysaccharide, polyelectrolyte characterized by high chain stiffness, can easily form a film with PEO and at the same time it could remove or at least suppress the crystallization of PEO. Since both polymers are biodegradable and water soluble, their blend also meets the concept of sustainable development. Additional exchange of Na^+ with Ca^{2+} ions could bring to life new properties of this blend and make it more suitable for SPE. Binding together biodegradable polymers and batteries never seemed more possible than nowadays. Exactly that was main encourager of this work.

In this thesis, a study of the structural change of NaAlg in the referent PEO/NaAlg film conducted with different concentration of $CaCl_2$ solution in methanol, different time during which the film was immersed in the solution and different number of the rinse with methanol was investigated. The effect of cross-linkage was analysed by Fourier transform infrared spectroscopy, differential scanning calorimetry and nonisothermal thermogravimetry.

1. THEORY

1.1. History of polymers

The word polymer is derived from the Greek *polus* and *meros*, meaning many and parts. Since most chemists and chemical engineers are now involved in some phase of polymer science or technology, some have called this the polymer age. Actually, we have always lived in a polymer age.

The ancient Greeks classified all matter as animal, vegetable, and mineral. Minerals were emphasized by the alchemists, but medieval artisans emphasized animal and vegetable matter. All are largely polymers and are important to life as we know it. Early humans learned how to process, dye, and weave the natural proteinaceous fibers of wool and silk and the carbohydrate fibers of flax and cotton. Early South American civilizations such as the Aztecs used natural rubber (Hevea brasiliensis) for making elastic articles and for waterproofing fabrics. Until Wöhler synthesized urea from inorganic compounds in 1828, there had been little progress in organic chemistry since the alchemists emphasized the transmutation of base metals to gold and believed in a vital force theory. Despite this essential breakthrough, little progress was made in understanding organic chemistry until the 1850s, when Kekulé developed the presently accepted technique for writing structural formulas. However, polymer scientists displayed a talent for making empirical discoveries before the science was developed. Polymer science was largely empirical, instinctive, and intuitive. Some of important polymer discoveries are chronologically shown in Table 1.[5]

Table 1. Chronological development of commercial polymers

Date	Material
Before 1800	Cotton, wool, silk fibers, glass,paper
1839	Vulcanization of rubber
1892	Viscose rayon fibres
1897	Poly(phenylene sulfide)
1907	Phenol – formaldehyde resins
1913	Poly(vinyl acetate)
1920	Urea – formaldehyde resins
1927	Poly(vinyl chloride)

1928	Nylon
1931	Poly(methyl methacrylate)
1934	Epoxy resins
1937	Polystyrene
1939	Nylon 6
1941	Poly(ethylene terephthalate)
1943	Silicones, polyurethanes
1948	ABS
1957	Polypropylene, polycarbonate
1966	Liquide crystals
1970	Poly(butylene terephthalate)

1.2. Polymers

Polymers are all around us. The soil we grow our foods from is largely polymeric as are the foods we eat. The plants about us are largely polymeric. We are walking exhibits to the widespread nature of polymers—from our hair and fingernails, our skin, bones, tendons and muscles; our socks, shoes, glasses; the morning newspaper; major portions of our automobiles, airplanes, trucks, boats, space craft; our chairs, waste paper baskets, pencils, tables, pictures, coaches, curtains, glass windows; the roads we drive on, the houses we live in, and the buildings we work in; the tapes and CDs we listen to; packaging—all are either totally polymeric or contain a large amount of polymeric materials.[4] Hence, how polymers can be defined?

In 1920, Staudinger proposed the macromolecular hypothesis: "Polymers are molecules made of covalently bonded elementary units, called monomers."[6]

IUPAC definition: "Polymers are substances composed of macromolecules, very large molecules with molecular weights ranging from a few thousand to as high as millions of grams/mole." The IUPAC Gold Book definition of a macromolecule is: "A molecule of high relative molecular mass, the structure of which essentially comprises the multiple repetition of units derived, actually or conceptually, from molecules of low relative molecular mass."[7] Macromolecule is used for individual molecules and polymer is used to denote a substance composed of macromolecules.

When it comes to polymer terminology we have to know difference between monomer molecule and monomer unit also called mer. Monomer molecule is molecule

which can undergo polymerization, thereby contributing constitutional units to the essential structure of a macromolecule. Mer is largest constitutional unit contributed by a single monomer molecule to the structure of a macromolecule.[8]

The entire structure of a polymer is generated during polymerization, the process by which constitutional units are covalently bonded together, Figure 1.[6]
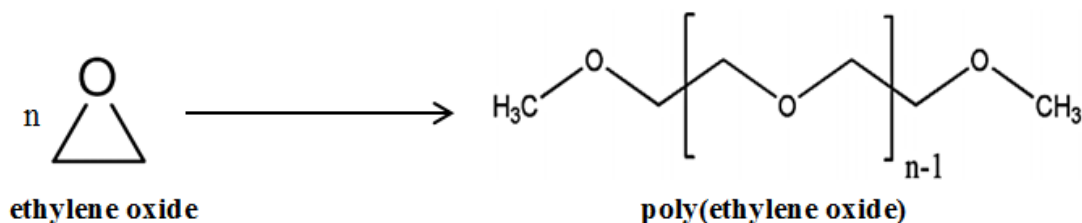

Figure 1. Poly(ethylene oxide) polymerization

Polymers can be divided in different ways. So we can talk about natural, semi - synthetic and synthetic polymers based on their origin. There are two main classes of polymerization reaction mechanisms: step-growth or condensation and chain-growth or addition, so there are two types of polymers as well. Considering constitutional units and number of different units type per macromolecule there are homopolymers, heteropolymers and copolymers. Classification of polymers based on the structure of the monomer chain different linear, branched – chain and cross-linked polymers. Based on molecular forces polymers are divided as elastomers, fibres, thermoplastics and thermosetting polymers.[9]

1.3. Polymerization

As mentioned before, polymers, if not naturally occurred, are generated synthetically trough addition or condensation polymerization.

In addition polymerization, monomers are added to each other by breaking the double bonds that exist between carbon atoms, allowing them to link to neighbouring carbon atoms to form long chains.[10] Figure 2 below shows one way that addition polymers can be made. This process has three stages: initiation, propagation, and termination. In the first stage, a substance is split into two identical parts, each with an unpaired electron. (Peroxides, which contain an O-O bond, are often used in this role.) A molecule with an unpaired electron is called a free radical. The free radical then initiates the reaction sequence by forming a bond to one of the carbon atoms in the

double bond of the monomer. One electron for this new bond comes from the free radical, and the second electron for the new bond comes from one of the two bonds between the carbon atoms. The remaining electron from the broken bond shifts to the carbon atom on the far side of the molecule, away from the newly formed bond, forming a new free radical. Each half-headed arrow indicates the shift of one electron.

The chain begins to grow "propagate" in stage two when the new free radical formed in the initiation stage reacts with another monomer to add two more carbon atoms. This process repeats over and over again to form chains containing thousands to millions carbon atoms. It can be terminated stage three when any two free radicals combine, thus pairing their unpaired electrons and forming a covalent bond that links two chains together. Figure 3 shows addition polymerization of polyethylene.
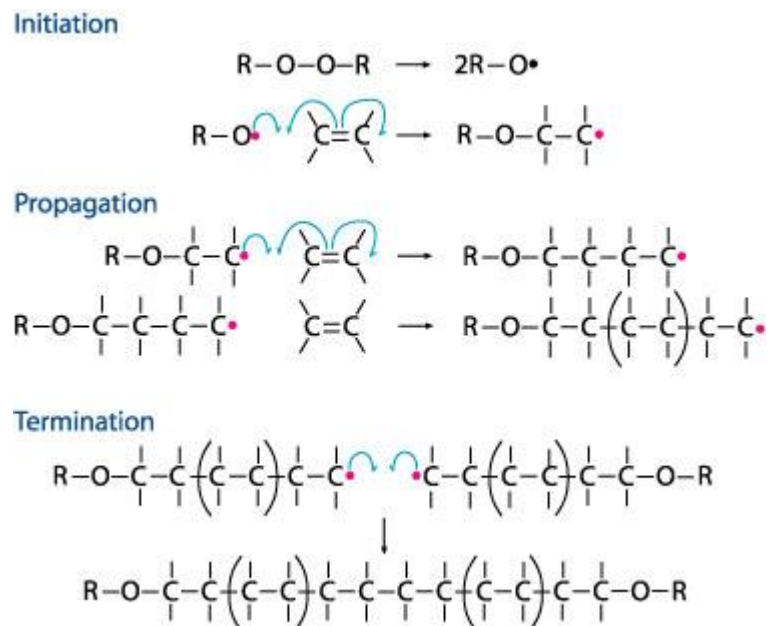
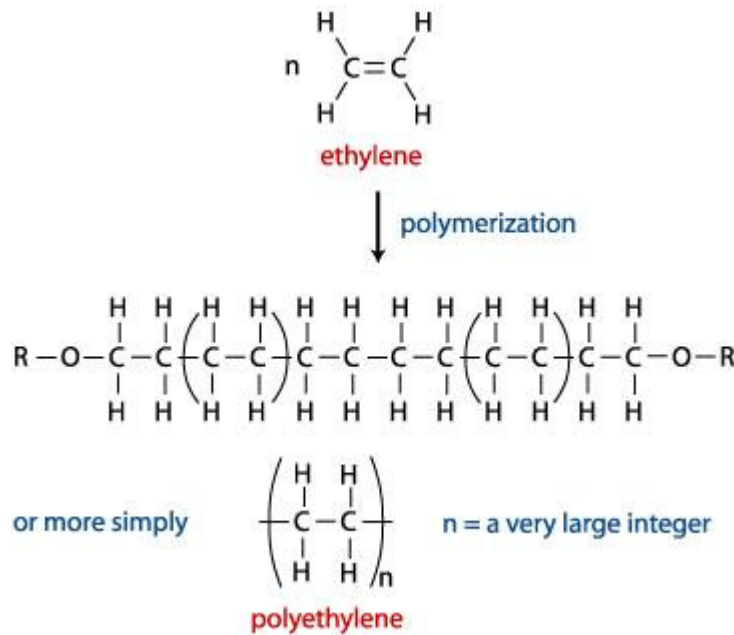**Figure 2.** Addition polymerization with three stages: initiation, propagation, and termination[11]

6

Figure 3. Addition polymerization of polyethylene simplified view[11]

Condensation polymerization or step-growth polymerization is a stepwise reaction between bi-functional or multi-functional monomers in which a high-molecular-weight polymer is formed after a large number of steps, Figure 4. Due to the nature of the polymerization mechanism, the reaction has to proceed for a long time to achieve high molecular weight polymers. Small molecules react with each other to form larger structural units while releasing smaller molecules as a by-product, such as water or methanol. A well-known example of a condensation reaction is the esterification of carboxylic acids with alcohols. If both monomers are difunctional, the condensation product is a linear polymer, and if at least one of the monomers is tri- or tetra-functional, the resulting polymer is a cross-linked polymer (i.e. a three-dimensional network). Adding monomers with only one reactive group will terminate a growing chain, and consequently lower the (average) molecular weight. Thus, the average molecular weight and the cross-link density will depend on the functionality of each monomer involved in the condensation polymerization and on its concentration in the mixture.[12]
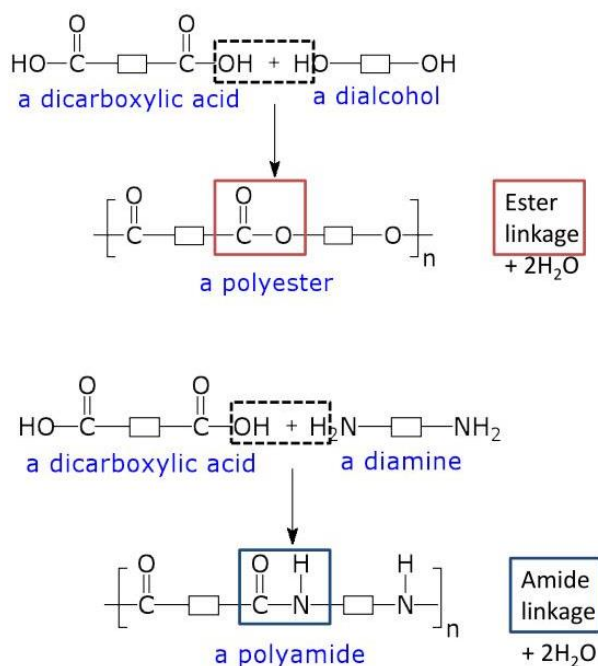
Figure 4. Condensation polymerization of polyamide[13]

1.3. Supermolecular structure of polymers

The properties of polymers are like those of ordinary substances to the extent that they depend on the structure and relative position of the molecules. Nevertheless, the idea long persisted that the ordering of polymeric macromolecules depends completely on their orientation and the formation of the space lattice during crystallization. The most important feature of the structure of solid polymers is the variety of supramolecular structures, i.e., complex structures consisting of bundles of macromolecules.[14]

Because of the comparatively low strength found in polymer components, it can be deduced that the forces holding a polymer component together do not come from -C-C-bonds but from intermolecular forces, or the so-called Van-der-Waals force. The energy that generates the inter-molecular attraction between two polymer molecules increases as the molecules come closer to each other. Thus, it becomes clear that as polymer sample is heated, the distance between the molecules increases as the vibration amplitude of the molecules increases. The vibration amplitude increase allows the molecules to move more freely, enabling the material to flow in the macroscopic level.[10]

Depending on factors such as the molecular shape, the nature of existing intermolecular forces, and the geometrical orientation of the atomic groups of each

8

molecule, a characteristic preferred orientation generally takes place which is temperature and density dependent. Considering all of these polymers could be in crystalline, semi-crystalline and amorphous state.

Crystal structures are three-dimensional in nature and exhibit a long range order. Crystalline polymers are obtained in process called crystallization. As an example, at room temperature natural rubber possess its characteristic elastomeric qualities of extensibility and recovery. On cooling to a suitable temperature, crystallization appear and the polymer becomes hard and relatively inelastic. Synthetic fibres are generally highly crystalline and strong, but if crystallinity is made to disappear, the physical properties of these polymers resemble very closely those of a viscous liquid.

In the classical concept, crystallinity is expressed by the presence in the polymer matrix of crystallites which can be from 5 to 95%. Only portions of the long chain molecules participate in a given crystallite, the remaining portion is part of amorphous phase. Such a polymer which contains crystalline and amorphous regions is generally termed as semi-crystalline, Figure 5. The crystallites are indicated by parallel array of portions of polymer chains. The ordered regions are randomly arranged relative to one another and are connected by portions of the chains passing through amorphous or other called disordered regions.[15] Crystallinity makes a polymer material strong, but it also makes it brittle, while amorphous regions creates a toughness, flexibility and material is able to bend without breaking. Depending on the purpose of the polymer material it is important to achive the right crystalline percentage of the polymer.
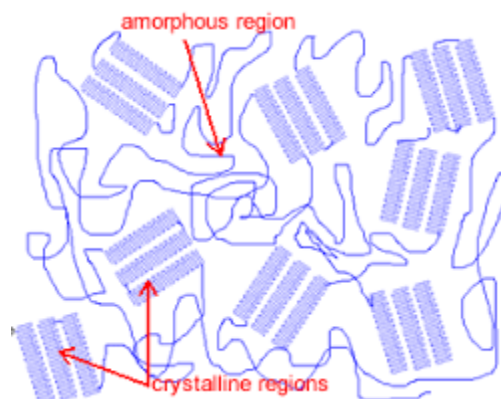

Figure 5. Semi-crystalline polymer[16]

1.5. Solid polymer electrolytes

High polymer material can be generally classified in the region between semiconductors and high quality insulation materials. The electrical properties of polymers are usefully assessed from behaviour at both low and very high electrical filed strenghts.[15]

Polymers with homopolar atomic bond, which leads to pairing of electrons, do not have free electrons and are not considered to be conductive. Conductive polymers in contrast, allow movement of electrons along the molecular cluster, since they are polymer salts.

Because of their structure, polymers can not be expected to conduct ions. However the extremely weak electric conductivity of polymers at room temperature and the fast decrease of conductivity with increasing temperatures is an indication that ions do move. They move because engineering polymers always contain a certain amount of added low molecular constituents which act as moveable charge carriers. This is a diffusion process which acts in filed direction and across the field. The ions „jump" from potential hole to potential hole as activated by higher temperatures. At the same time, the lower density speeds up this diffusion process.[10]

Experiments and detailed mechanistic studies clearly established in 1983 that ionic motion in salt-polymer complexes is not due to charges hopping from site to site. Rather it is a continuous motion occurring in the amorphous region of the polymeric material.[2]

Polymer electrolytes are defined as solid ion conductors formed by the dissolution of inorganic salts in suitable high molecular weight polymer solutions. Polymer electrolytes should be distinguished from polyelectrolytes and gel electrolytes. Polymer electrolytes are thus different and consist of a host polymer dissolved in solution and excess solvent is vapored. Thus, solid polymer electrolytes (SPE) are complex systems of suitable solvent and additionally an inorganic salt is added to the polymer.

To act as a successful host, the following conditions must be satisfied:

(i) The polymeric material or an active part of it must with sufficient electron donor capacity form coordinate bonds with cations or simple inorganic electrolytes;

(ii) The polymer chain must have repeat units which form segments having as far as possible free and sufficient rotation or motion within them;

(iii) The coordinating centers on the polymer chain should be suitably placed so that formation of multiple intrapolymeric ionic bonds can take place.[2]

A number of polymers satisfy this criterion, but PEO has been most widely studied. In the 1980s the PEO served as a prototype material for investing alternative models of ion transport, and for developing the concept of the film cell for solid batteries. However, from a practical standpoint the PEO was not itself an ideal electrolyte. Several manipulations were needed to prevent crystallization and to extend the domain of existence of elastomeric phase favourable to high ionic conductivity: plasticizing the matrix by addition of a low molecular weight polar molecule or forming block or comb copolymers. Peter V. Wright, a polymer chemist from Sheffield, first showed in 1975 that PEO can act as a host for sodium and potassium salt, thus producing a solid electrical conductor polymer/salt complex.[2]

Besides SPE based on modified PEO, there is also polycarbonate, polysiloxane, succinonitrile and organic-inorganic hybrid composite. But reason why SPEs gained much attention for promising materials in many electrochemical applications was because they offer outstanding advantages over conventional liquid electrolytes including no leakage of electrolytes, low flammability, good flexibility, safety and stable contact between the electrode and electrolyte. These properties make SPEs have strong adhesive function on the surface of electrodes and thus decrease the interface impedance between electrolytes and electrodes. Suitable SPEs are mainly aimed in the development of high safety, high energy and power density rechargeable batteries, which can be used in miniature electronic devices, energy conversion units, supercapacitors, electric vehicles and etc.[17]

1.6. Polyethylene oxide

Polyethylene oxides (PEOs) are nonionic, high molecular weight, hydrophilic (water-soluble), electrically and thermally stable, inert to many organic reagents and nontoxic polymers available in the form of white, free-flowing powders synthesized commercially through catalytic polymerization of ethylene oxide using various catalytic systems. Molecular weight ranges of 100,000–7,000,000. PEO is polyester, the general structure of PEO is $[-CH_2-CH_2-O-]_n$ where n is average number of oxyethylene groups. PEO structure is similar to that of polyethylene glycol (PEG), but has longer molecular chains, i.e., higher molecular weights. The ethylene oxide monomer is an epoxide ring and in the presence of a catalyst it forms a chain having the repeating unit $-CH_2-CH_2-O-$ (Figure 1). It is soluble in most solvents beside ethers, hot water,

aliphatic hydrocarbons. PEO polymers are safe and are not absorbed through the gastrointestinal tract. On hydration, PEO forms a gel and have high swelling capacity.[6,18]

PEO can be extruded at processing temperatures 20–30 °C higher than its melting point without significant degradation. Thermogravimetric analysis (TGA) data have indicated that PEO does not exhibit significant weight loss (degradation) until 350 °C. At temperatures far above the crystalline melting point, high molecular weight polymers of PEO still retain a very high degree of crystalline character.[18]

The use of PEO in such a wide range of applications is attributed to its physical, chemical as well as thermal stability, compressibility, hydrophilic nature, and high capacity to swell. Despite its high molecular weight, PEO is highly crystalline and has a melting point around 65 °C, above which, the polymer becomes thermoplastic. PEO having low melting point and good melt flow index may be considered as a suitable polymer for many uses such as in conductive composites with carbon black, cosmetology (skin creams, emulsions), gene therapy, pharmaceutical products, packaging material, and nowadays as very important part of SPE, etc.[18]

1.7. Sodium alginate

Alginates are known as natural polysaccharides extracted from brown seaweed. All commercial alginates are generated from marine algae including *Laminaria hyperborean*, *L. digitata*, *L. japonica*, *Lessonia nigerscence*, *Macrocystic pyrifera* and *Durvillea Antartica*.

Alginate can be extracted from raw seaweeds by a treatment with aqueous alkali solutions, typically NaOH, in which the natural alginate in various salt forms is converted into water-soluble sodium alginate (NaAlg). NaAlg has $(C_6H_7NaO_6)_n$ or $C_6H_9NaO_7$ molecular formula, IUPAC name sodium; 3,4,5,6-tetrahydroxyoxane-2-carboxylate. After filtration, the NaAlg in solution can be precipitated by the addition of calcium chloride. After further purification and conversion, water-soluble NaAlg power is produced. Alginates are the salts of alginic acids. Alginic acid is a naturally curing hydrophilic colloidal polysaccharide obtained from the various species of brown seaweeds (*Phaeophyceae*).

Chemically, alginate is a linear copolymer consisting mainly of residues of β-(1-4)-linked D-mannuronic acid and α-(1-4)-linked L-glucuronic acid units containing

carboxylic groups in their structures that define the adsorption capacity for metals, Figure 6. Alginate must be regarded as a collective term for a family of linear (1→4)-linked an L-guluronob D-mannuronans of widely varying composition and sequential structure.[19,20]

Figure 6. Molecular structure of β-D-manuuronic acid and α-L-guluronic acid

Algine has many useful properties and is very user-friendly and consumer friendly because it is renewable, biodegradable, and vegetable, not animal, in origin. It has been widely used in food, fabric and medical fields because of its remarkable gelation properties, and application in hemostatic materials. Alginate has been utilized to develop biodegradable or edible films due to its unique colloidal properties, such as thickening, stabilizing, suspending, film forming, gel producing, and emulsion stabilizing properties. Algae also contain almost all vitamins and amino acids. NaAlg, a polyelectrolyte having a rigid molecular chain, forms strong films and has been extensively investigated for biomedical applications as a drug carrier and in hemostatic materials.[19,20]

Sodium alginate forms gels with interconnected pores by ionotropic gellation in the presence of bi- or trivalent cations such as calcium, barium, zinc, copper, among others. The bivalent calcium cation has the ability to fit into the guluronate structures (G-blocks) like eggs in an egg-box. Furthermore, the increase of ions concentration promotes a co-operative binding mechanism among egg-boxes sequentially leading to gelling of the solution (Figure 7).[21,22]

As soon as sodium alginate is added to a solution of calcium chloride, a gel forms as the sodium ions (Na^+) are exchanged with calcium ions (Ca^{2+}) and the polymers become crosslinked (Figure 8).

The calcium ions are able to cross-link the alginate polymers because they can form two bonds, as opposed to monovalent ions such as sodium, which can only form one bond. The longer the alginate is in contact with the calcium chloride solution, the more

rigid the gel will become, as more crosslinks are formed. Also, depending on the concentration of calcium ions, the gels are either thermoreversible (low concentrations) or not (high concentrations).[23]
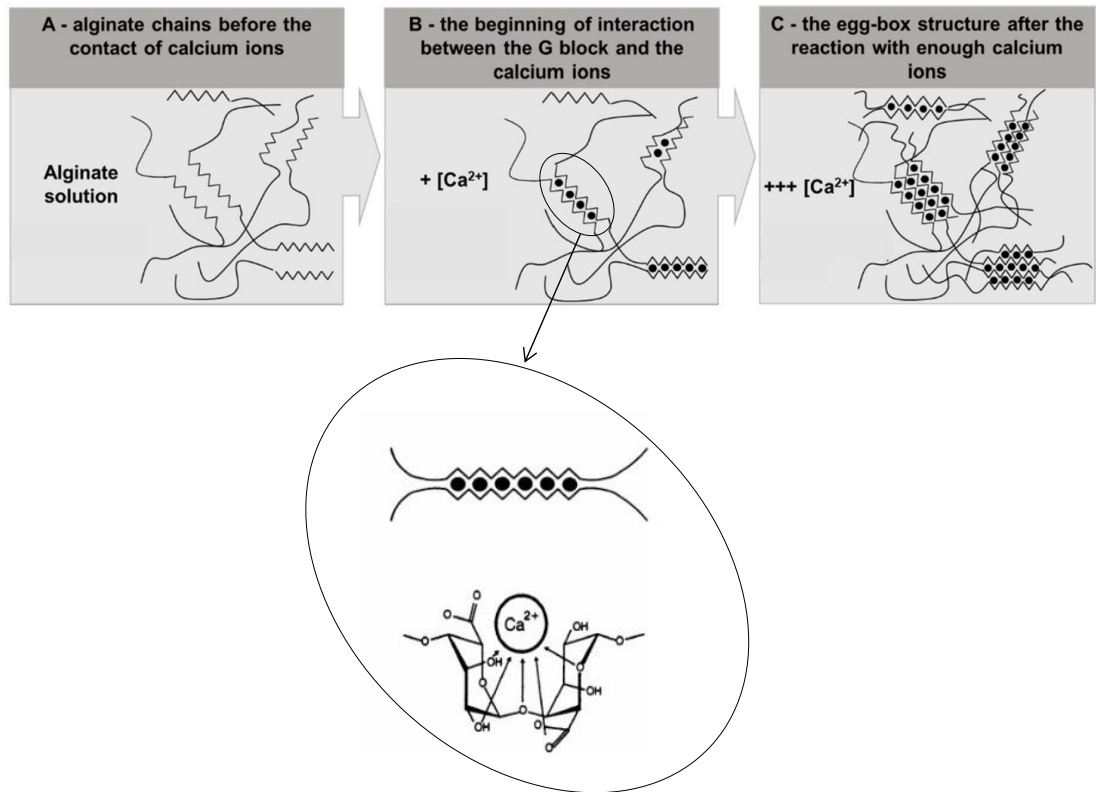

Figure 7. Schematic representation of the three steps of egg-box formation: A) alginate chains before the contact of calcium ions; B) the beginning of interaction between the G block and the calcium ions; C) the egg-box structure after the reaction with enough calcium ions.
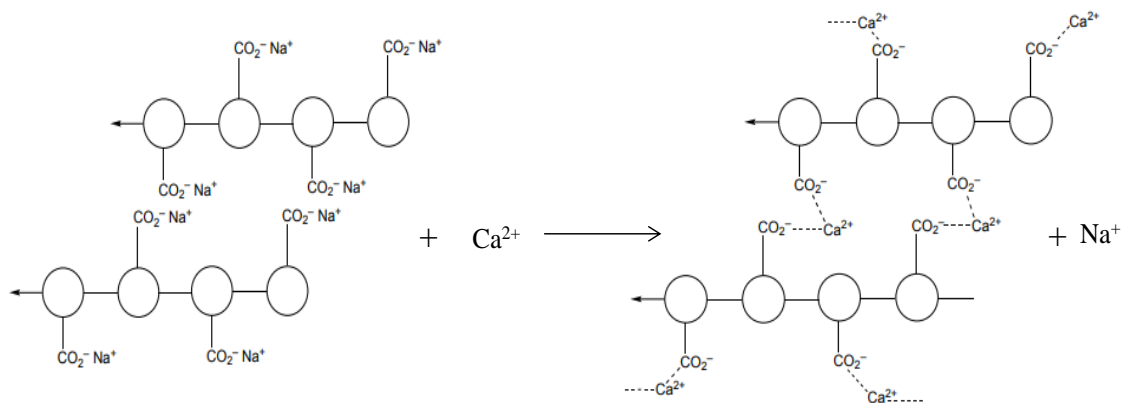

Figure 8. Cross-linking of sodium alginate with calcium ions [23]

1.8. Polymer blends

Besides many polymers that were developed in past which had their unique properties and applications, during the period of 1940-1960s, the polymer industry and academia have realized the requirement of new polymers. But the cost of bringing a new polymer to market and its commercial production seemed unviable. The polymer industry and academia both focused on developing a polymer material of novel and valuable properties. Therefore, it was suggested to develop new techniques for the modification of already existing polymers which would be economically viable. A new polymers modification process, based on a simple mechanical mixture of two polymers first appeared when Thomas Hancock (founder of British rubber industry) developed one mixture of natural rubber with Gutta-percha. This process generated a brand new polymer class called polymer blend.

Polymers which can produce better polymer electrolytes are generally semicrystalline at room temperature and those are amorphous, do not possess criteria for polymer electrolyte i.e., they should have properties like high molecular weight, low glass transition temperature, low cohesive energy density and high flexibility.

In this way, polymer blends became key components of current polymer research and technology. Mixing of two or more polymers at their matrix level is termed as polymer blends.[24] It is a physical mixture of two or more polymers which are not linked by covalent bond. When two or more polymers are completely miscible down to the segmental level, they form a single homogeneous phase. Their properties are generally proportional to the ratio of the polymers in the blend, and the polymer blend is called homogeneous blends. Polymer blend provides a new desirable polymeric material for a variety of applications. It has many advantages such as simple to prepare, easier to control of physical properties by compositional changes and possession of better properties compared to individual polymer component. Commercially, it can be used in industries as it enhances the processability of high temperature or heat-sensitive thermoplastic to improve the impact resistance. It also reduces the cost of an expensive engineering thermoplastic. The properties of polymer blends depend on the physical and chemical properties of the participating polymers, and, on the state of the phase, whether it is in homogenous or heterogeneous phase. If two different polymers are able to be dissolved successfully in a common solvent, this polymer blends or intermixing of

the dissolved polymers will occur due to the fast establishment of the thermodynamic equilibrium. Polymer blending is one of the effective methods to reduce the crystalline content and to enhance the amorphous content. When blend-based polymer electrolytes, especially the ones with PEO, are formed through the interaction between two or more kinds of molecular chains of polymer, the regularity of the molecular chain arrangement of PEO is destroyed which affects crystallization and obtains amorphous structure.[17] Polymer blends often exhibit properties that are superior to the individual component polymers.

In recent years, polymer blends have drawn considerable interest in most rapidly growing areas in polymer material science. Other objectives of blending are to dilute polymers through addition of low cost commodity polymers and to recycle industrial plastic waste. Application of polymer blends in numerous fields such as adhesion, colloidal stability, and design of composite and biocompatible materials requires fundamental understanding of the structure, phase state and composition of blends in the vicinity of interacting surfaces. As polymeric materials are rarely used in their pure form, and, are usually filled with additives that improve their processability and properties, including creating some new ones. For these purposes, particulate disperse fillers and fibrous fillers are widely used. Polymer blends may be considered as composite materials. These can be considered as heterogeneous systems with developed phase boundaries between constituent components or phases. At the polymer–polymer interface, interphase layers are formed whose structure and properties depend on the thermodynamic interactions between two components or phases. Due to thermodynamic and kinetic reasons, polymer blends are usually characterized by two-phase structure arising as a result of thermodynamic immiscibility of initial components. The processes that occur during their formation lead to development of a complex structure because of incomplete phase separation. Though extensive research has been carried out, very few polymer blend electrolytes have been found to show significant comprehensive properties which can fulfil the practical requirements.[25,26]

PEO is found to be suitable for Na-alginate blends, as the hydroxyl (-OH) groups on Na-alginate can interact through the hydrogen bond with the ether oxygen in PEO just as the primary -OH group on cellulose/methylcelluloses forms hydrogen bond with ether oxygen in PEO. *F. Zia et al* [27]. and *J.-W. Rhim*[28] preparaed blended and pure alginate films by solution casting method, respectively. *J.-W. Rhim* [28] did further modification of the films (pure NaAlg) by 'immersion film' where the preformed

alginate blend films were immeresed for 5 min in different concentrations of CaCl$_2$ solutions. Reason of further modification was to obtain water resistant alginate films through inducing cross-linking with ionic calcium.

1.9. Methods of polymer film preparation

Polymer film preparation can be classified as chemical and physical. The solid polymer electrolytes are easy to fabricate as soft films of only a few microns and their flexibility permits interfaces with solid electrodes, which remain intact, when the device is in use. This makes the application and development of all electrochemical devices possible. In the present study, our interest is in the preparation of polymer films. As per the literature available, there are various methods to prepare good quality polymer films in this work solution-casting method was choosen amoung the others. The possible preparation methods are:

a. Solution – casting method (Figure 9)

b. Hot pressing method

c. Film blowing

d. Thermal evaporation method

e. Laser evaporation method

f. Flash evaporation method

g. Polymerization of monomer

h. Gaseous discharge

i. Sputtering

j. Photolytic Process

k. Pyrolysis.[29-32]
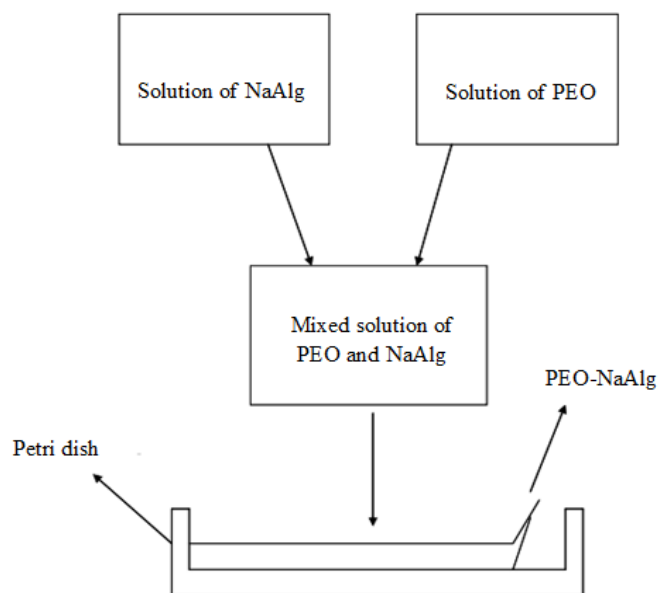
Figure 9. Schematic illustration of the preparation procedure of polymer electrolyte film by solution casting method

1.9.1. Solution casting method

Solution casting method is one of the easiest traditional methods for the preparation of polymer electrolytes. In this method, the polymer is dissolved in the compatible solvent at room temperature followed by adding the required amount of non-aqueous salt in the polymer matrix. After complete dissolution of polymer and salt a homogenous mixture is obtained. Then the nanofiller/plasticizer is dispersed in the mixture and further stirring is done till a homogenous solution is obtained. Then the resulting solution is casted on well cleaned petri-dishes (glass/poly propylene) in a controlled atmosphere and dried under room temperature for few days. Further the film can be dried in a vacuum oven at appropriate temperature for complete removal of the solvent. Finally, a free standing mechanical stable polymer film with flexibility is obtained and kept in a vacuum desiccator to avoid from moisture absorption for further characterization.[33]

2. EXPERIMENTAL PART

2.1. Materials

For preparation of polymer blend following chemicals where used:

- poly(ethylene oxide) ($\bar{M}_V$ = 100 000 g mol^{-1} (PEO1)), Sigma-Aldrich, Inc., St. Louis, SAD

- sodium alginate (SA)($\bar{M}_V$ = 10 000 - 600 000 g mol^{-1}), PanReac AppliChem ITW Reagents, (Spain, Italy, Germany)

- calcium chloride (CaCl$_2$) ($\bar{M}_V$ = 110.99 g mol^{-1}), Gram − mol d.o.o., Zagreb, Croatia

Solvents:

- distilled water

- methanol (CH$_3$OH) ($\bar{M}_V$ = 32.04 g mol^{-1}), BDH PROLABO, United Kingdom

2.2. Preparation of polymer films

At first, two separated 1.5% w/v solutions were prepared by dissolving PEO and NaAlg in distilled water, solutions were stirred for one hour using magnetic stirrer by 400 rpm. After that 50 mL of 80 wt% PEO and 20 wt% NaAlg solution was prepared by mixing 40 mL of PEO and 10 mL of NaAlg. The solution was stirred with magnetic stirrer for 24 hours by 300 rpm (Figure 10). The wt% ratio of PEO and NaAlg in the film was chosen according to *A. Sesar*[34] investigation of the thermal properties of NaAlg and PEO blend films with different wt% ratios. It was concluded that 80%PEO/20%NaAlg had the lowest degree of crystallinity and the best prepositions for future work in SPE field. Twenty one aqueous solutions of mixed polymers and one solution of pure PEO were prepared to make twenty two polymer films.

Prepared 80%PEO/20%NaAlg aqueous solutions were poured into Petri dish and dried in oven for five days to get the polymer films by evaporation of the solvent. First 24 hours they were dried at temperature of 25 °C while next 24 hours at 35 °C (Figures 11 and 12). Additional 72 hours drying was in vacuum oven at 40 °C and at pressure of -0,1 MPa. After drying, the films were removed from Petri dish and cut to same shape and size to insure same predisposition for further steps (Figure 13).

Solutions of CaCl$_2$ in methanol were prepared with concentrations of 1, 2.5, 5, 7.5 and 10% w/v. Methanol was used as a solvent for CaCl$_2$ since it was matching

nonsolvent for both polymers (PEO and NaAlg) so the films stayed unchanged (Figure 14). 80%PEO/20%NaAlg films were immersed in the solutions of $CaCl_2$ during exposure time of 10, 30, 60 and 180 minutes to induce ion exchange of Na^+ ions with Ca^{2+} ions to get cross-linking of the blend films (Figure 15). After cross-linkage procedure the wet films were rinsed in methanol to remove residue of $CaCl_2$ and sodium chloride (NaCl) as a product of ion exchange. Two series of the samples were made, one series was rinsed once while second series two times. After rinsing the films were placed on the glass plate and dried in vacuum oven for 4 days at 40 °C and -0,1 MPa (Figure 16).

Samples were stored in PE bags separately one from another and kept in dark and dry place before measurements were performed.

Figure 10. Stirring of PEO/NaAlg liquid mixture on the magnetic stirrer

Figure 11. Beginning of the drying process in oven

Figure 12. Polymer films after 48 hours of drying in oven

Figure 13. 80%PEO/20%NaAlg film after five days of drying and after cutting in wanted shape

Figure 14. Different solutions of $CaCl_2$ in methanol

Figure 15. Immersion of 80%PEO/20%NaAlg films in CaCl$_2$ solutions

Figure 16. The blend films after cross-linkage and rinsing with methanol

2.3. Methods of characterization

2.3.1. Fourier-transform infrared spectroscopy

Fourier transform infrared (FT-IR) spectra of pure PEO, pure NaAlg and 80%PEO/20%NaAlg film before and after cross-linkage procedure were recorded on FT-IR Spectrum One spectrometer (Perkin-Elmer, USA) by the Horizontal Attenuated Total Reflectance (HATR) technique between 4000-650 cm^{-1} with 4 cm^{-1} resolution in 10 scans at 25 °C. The internal reflection crystal, made of zinc selenide, had a 45˚ angle. The aim was to investigate the efficiency of cross-linkage with Ca^{2+} ions.

2.3.2. Differential scanning calorimetry

For thermal characterization of pure PEO, pure NaAlg and 80%PEO/20%NaAlg film before and after cross-linkage procedure differential scanning calorimetry (Mettler Toledo DSC 823^e) was used. The calibration of the instrument was performed with

indium (T_m =156.6 °C, ΔH_m = 28.45 J g^{-1}). Before the beginning of the measurement the instrument was stabilized for around one hour. The samples of approximately 10 mg were pressed in aluminum pans with a hole in the lid, the measurement was made in the nitrogen atmosphere (30 cm^3 min^{-1}) and with customized method for these samples. The first step was cooling the sample from 25 °C to -90 °C with the cooling rate of 20 °C min^{-1} (first cooling scan), kept at -90 °C for 10 min and then heated from -90 to 110 °C with the heating rate of 20 °C min^{-1} (first heating scan). After heating the sample was kept at 110 °C for 5 min and then cooled from 110 to -90 °C with the cooling rate of 20 °C min^{-1} (second cooling scan), kept at -90 °C for 10 min and finally heated from -90 to 110 °C with the heating rate of 20 °C min^{-1} (second heating scan).

These values can be obtained from DSC curve of the first heating scan:
- temperature, T/°C: the cold crystallization (T_{cc}), the premelting crystallization (T_{pmc}), melting (T_m)
- enthalpy, ΔH/J g^{-1}: the cold crystallization (H_{cc}), the premelting crystallization (H_{pmc}), melting (H_m).

From DSC cooling curve next values can be obtained:
- the melt crystallization temperature, T_{mc}/°C
- the enthalpy of the melt crystallization, H_{mc}/J g^{-1}.

DSC curve of the second heating scan gives the same features as the curve of the first heating scan with addition of the values of glass transition:
- the glass transition temperature, T_g/°C
- the change of the specific heat capacity at glass transition, Δc_p / J g^{-1} °C^{-1}.

According to Croatian standard HRN EN ISO 11357-3:2009 for determination of the thermal transitions using DSC, in case of crystallization and melting, two temperatures are determined (because of the huge amount of data in this thesis) although according to the standard three temperatures should be specified:
- the extrapolated onset transition temperature, T_{ei}/°C (e.g. T_{eim}-the extrapolated onset melting temperature)
- the peak temperature, T_p/°C.

According to Croatian standard HRN ISO 11357-2:2009 two temperatures are determined for glass transition:

- the extrapolated onset transition temperature, $T_{ei}/°C$
- the temperature at which the change in specific heat capacity is equal to half of its maximum value (the midpoint glass transition temperature), $T_{mg}/°C$.

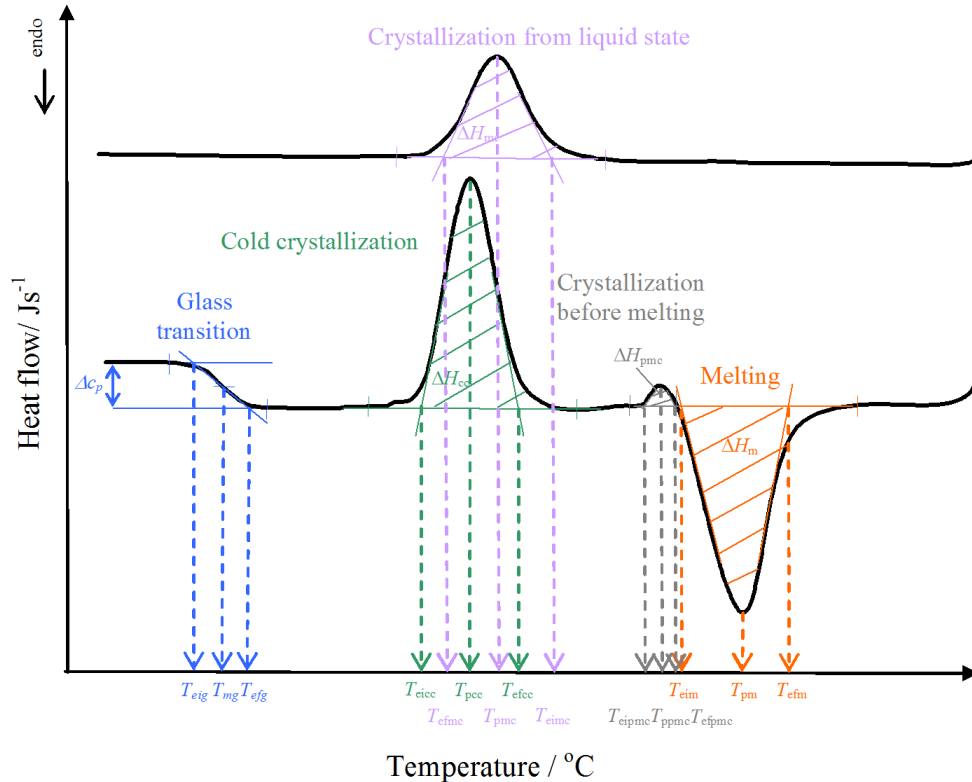Determination of the thermal characteristics of all transitions is shown in Figure 17.

Figure 17. Determination of the thermal characteristics[34]

Degree of crystallinity (X_c) of PEO was calculated according to Eq. (1) :

$$X_c(\%) = \frac{\Delta H_m}{\Delta H_{100\%} \times w_{PEO}} \times 100 \qquad (1)$$

Where ΔH_m is the melting enthalpy of the sample, $\Delta H_{100\%}$ is the melting enthalpy of 100% crystalline PEO (188,1 J g^{-1}) and w is the mass fraction of PEO in the sample.[35]

2.3.3. Non-isothermal thermogravimetry

The thermal degradation of pure PEO, pure NaAlg and 80%PEO/20%NaAlg film before and after cross-linkage procedure was investigated thermogravimetrically (Pyris 1 TGA, Perkin-Elmer, USA). Sample weight was 10.0 ± 0.1 mg. TG analysis was carried out in the temperature range 50-500 °C under nitrogen atmosphere (flow rate was 20 cm^3 min^{-1}) at the heating rate of 10 °C min^{-1}.

The results of non-isothermal thermogravimetry are thermogravimetric (TG) and derivative thermogravimetric (DTG) curve. TG curve (Figure 18 red curve) represents change (loss) of sample mass (residual mass) in dependence of temperature, while DTG curve (Figure 18 blue curve) represents rate of mass loss with temperature. Thermal degradation can take place in one or more degradation stages what can be seen on TG curve as mass change, while on DTG curve as one or more peaks (Figure 18).
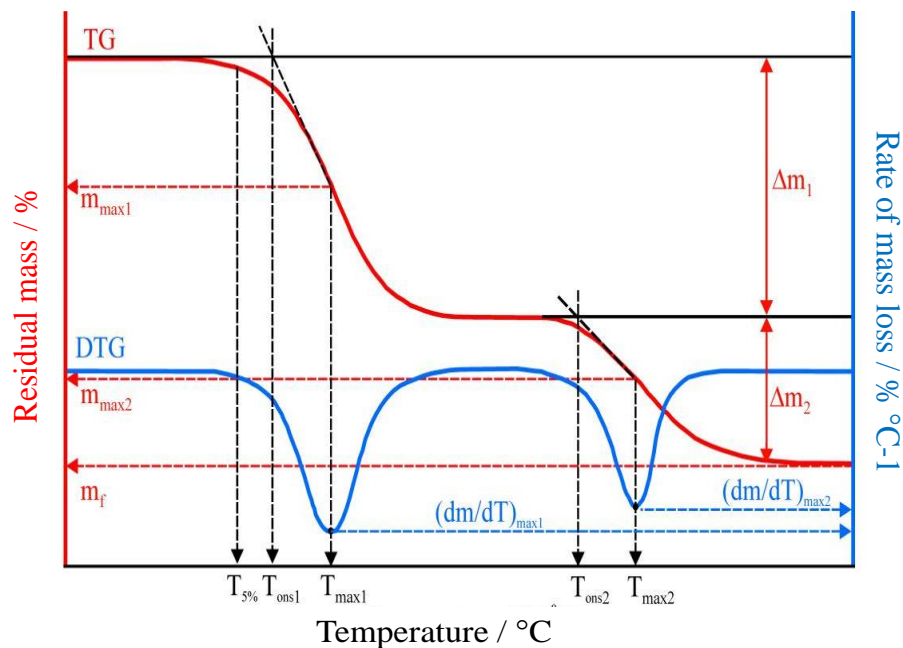
Figure 18. Determination of TG and DTG thermal characteristics[34]

Thermal characteristics that can be determined from TG and DTG curves according to HRN EN ISO 11358-1:2014 standard are:

- the temperature at 5% mass loss, $T_{5\%}$/°C
- the onset temperature, T_{onset}/°C, (crossing of the base line, flat part of TG curve, and tangent line made on the lowering part of TG curve at the inflection point)

- temperature at the maximum degradation rate, T_{max}/°C, which equals to minimum of DTG curve

  - the residual mass at the onset, m_{onset}/g or %

  - the residual mass at the maximum degradation, m_{max}/g or %

  - the residual mass at the end of degradation, m_f/g or %

  - the mass loss at a degradation stage, Δm/g or %

  - the maximum degradation rate, $(dm/dT)_{max}$/% °C^{-1}.

Thermal stability of polymers and their materials is mostly defined as the onset temperature, T_{ons1}.

3. RESULTS AND DISCUSSION

The results of all measurement are shown in two forms, graphical and numerical, for each method. The graphical results are shown in the Figures by changing the immersion or exposure time at the same concentration of $CaCl_2$ solution in methanol, while numerical results are lined up in the Tables by changing the concentration of $CaCl_2$ solutions in methanol at the same immersion of exposure time. Different display of the results, graphs vs. tables, is given with the aim to observe much easier possible changes depending on all parameters. Results are divided in two groups depending on the number of rinsing with methanol (single rinse (A), double (B)).

3.1. Fourier-transform infrared spectroscopy

Fourier transform infrared (FT-IR) analysis was carried out in order to detect any peak shift that could be attributed to the interactions between PEO and NaAlg in the blend film (hydrogen bonds) and to detect structural changes of NaAlg in the blend film due to the influence of different concentration of $CaCl_2$ solution (complexation). The variation of time during which the film was immersed in the solutions and the influence of the rinsing with methanol is also investigated.

FT-IR spectra of pure NaAlg, PEO and its blend 80%PEO/20%NaAlg were recorded and compared (Figure 19).

The spectrum of NaAlg showed important absorption bands regarding hydroxyl and carboxylic functional groups. Stretching vibrations of the hydroxyl groups (O–H bonds) of alginate appeared at 3208 cm^{-1}. Observed bands at 1591 and 1402 cm^{-1} are attributed to the asymmetric and symmetric stretching vibrations of carboxylate ion (COO^-), respectively. These bands are very significant for characterization of NaAlg structure under the influence of Ca^{2+} cross-linked with $CaCl_2$ solutions that will produce calcium alginate (CaAlg). The tendency of NaAlg chains to create complex structures with Ca^{2+} ions is due to COO^- group.[36]

The spectrum of PEO shows its characteristic bands but the most important ones for the detections of polymers miscibility are the triplet at 1145, 1090 and 1057 cm^{-1} which confirms the crystalline PEO phase by the presence of C–O–C stretching vibration and two peaks at 959 and 840 cm^{-1} which confirms the characteristic in supporting Gauche conformation of –CH_2–CH_2– group.[37]

The FT-IR spectra of the referent film (80%PEO/20%NaAlg blend) shows spectral features similar to those for the pure polymers, but some vibrational bands are shifted to higher wave numbers. The triplet of C–O–C stretching vibrations in the film 80%PEO/20%NaAlg occurs at 1146, 1105 and 1059 cm^{-1} and only the wave number at 1090 cm^{-1} of pure PEO moves towards higher wave number (1105 cm^{-1}) by adding 20% w/v of NaAlg (Table 2). The other two wave numbers didn't change significantly. *G. Patel et al.*[38] investigated the miscibility between PEO and poly(acrylamide) and they noticed only the change in one triplet wave number, i.e. the middle wave number at 1106 cm^{-1}. The observed shift of the mentioned wave number indicated the existence of intermolecular interactions between the polymers in the blend, i.e. the establishment of a hydrogen bond. The wave numbers of Gauche conformation didn't change with addition of NaAlg (Table 2). Stretching vibrations of O–H bonds of alginate shifted to higher wave number (3389 cm^{-1}) in blend 80%PEO/20%NaAlg film (Table 2). Asymmetric and symmetric stretching vibrations of COO$^-$ of NaAlg moved to lower wave numbers (1579 and 1396 cm^{-1}) in the blend (Figure 19 and Table 2). This change also indicates the established interactions between two polymers confirming their miscibility via hydrogen bonds. These results are in good agreement with previous investigation.[39]
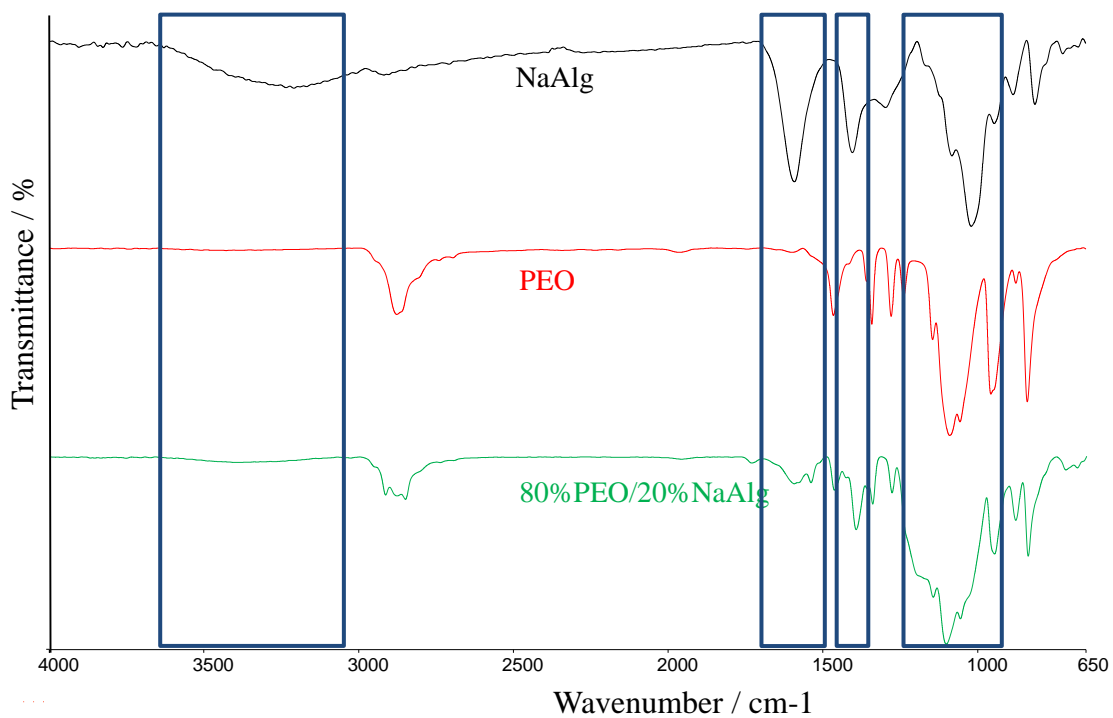
Figure 19. FT-IR spectra of pure NaAlg, pure PEO and referent blend 80%PEO/20%NaAlg film
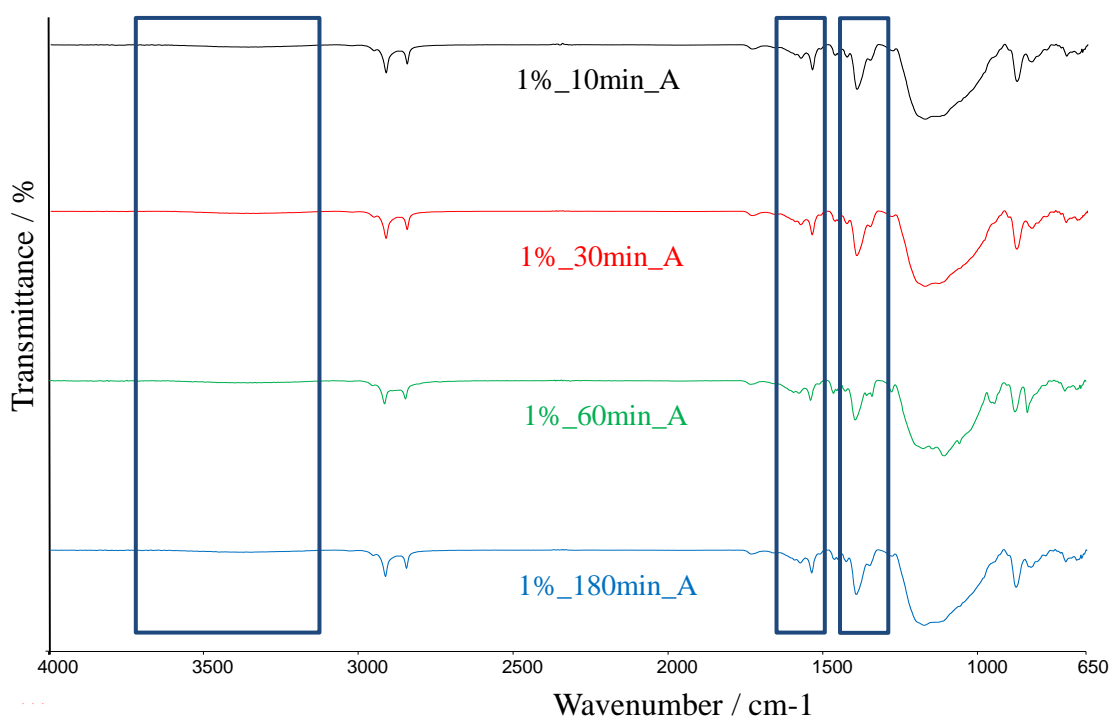
Figure 20. FT-IR spectra of the films after immersion in 1% w/v $CaCl_2$ solution for 10, 30, 60 and 180 min with single rinse (A)
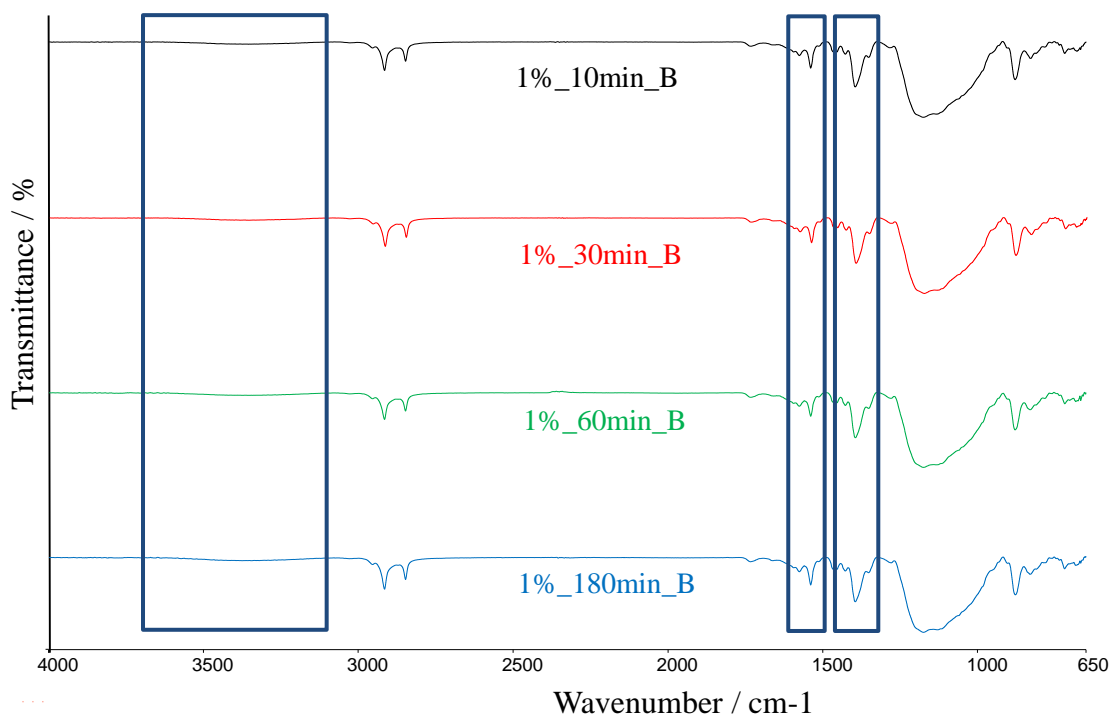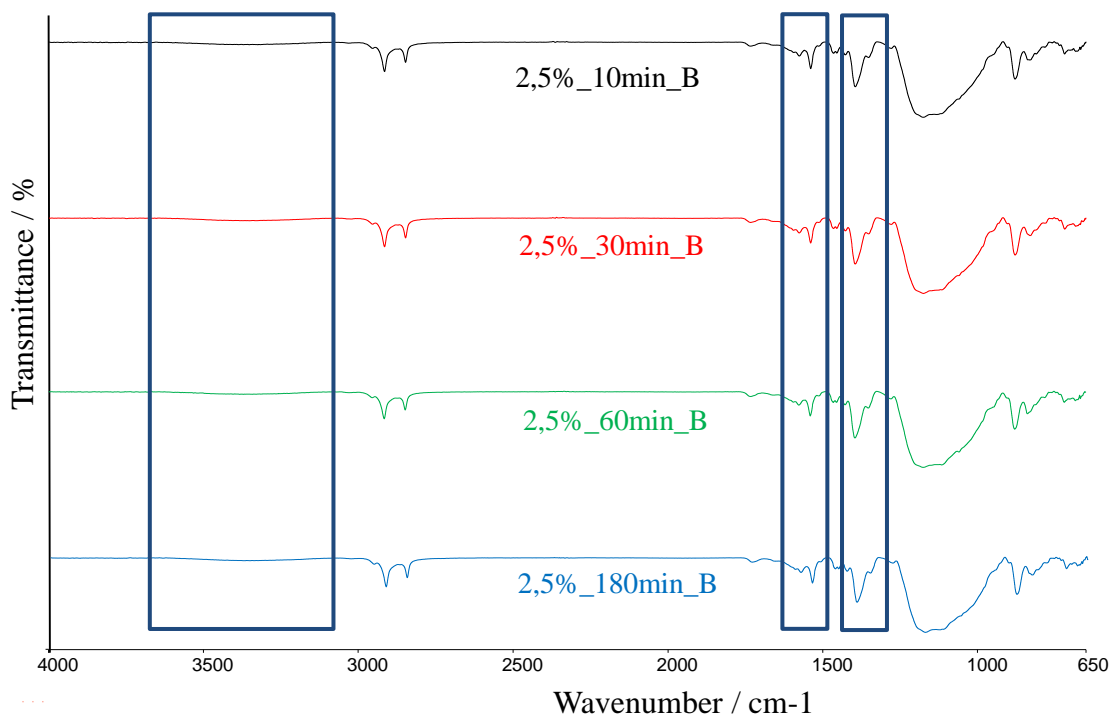
Figure 21. FT-IR spectra of the films after immersion in 1% w/v CaCl$_2$ solution for 10, 30, 60 and 180 min with double rinse (B)
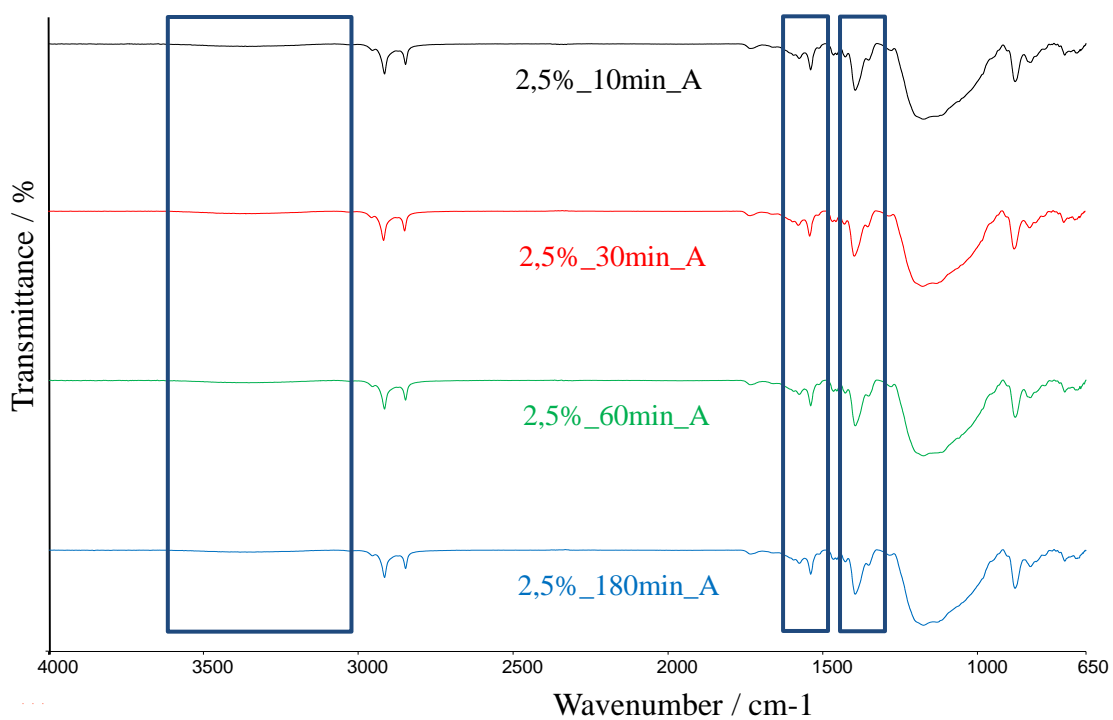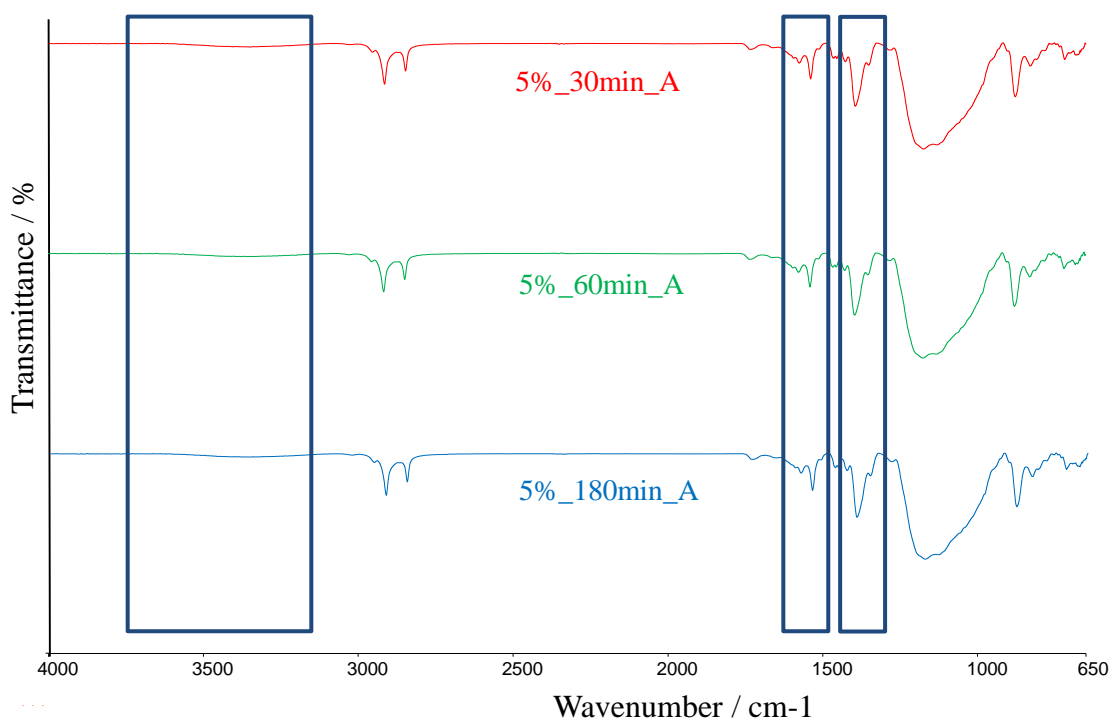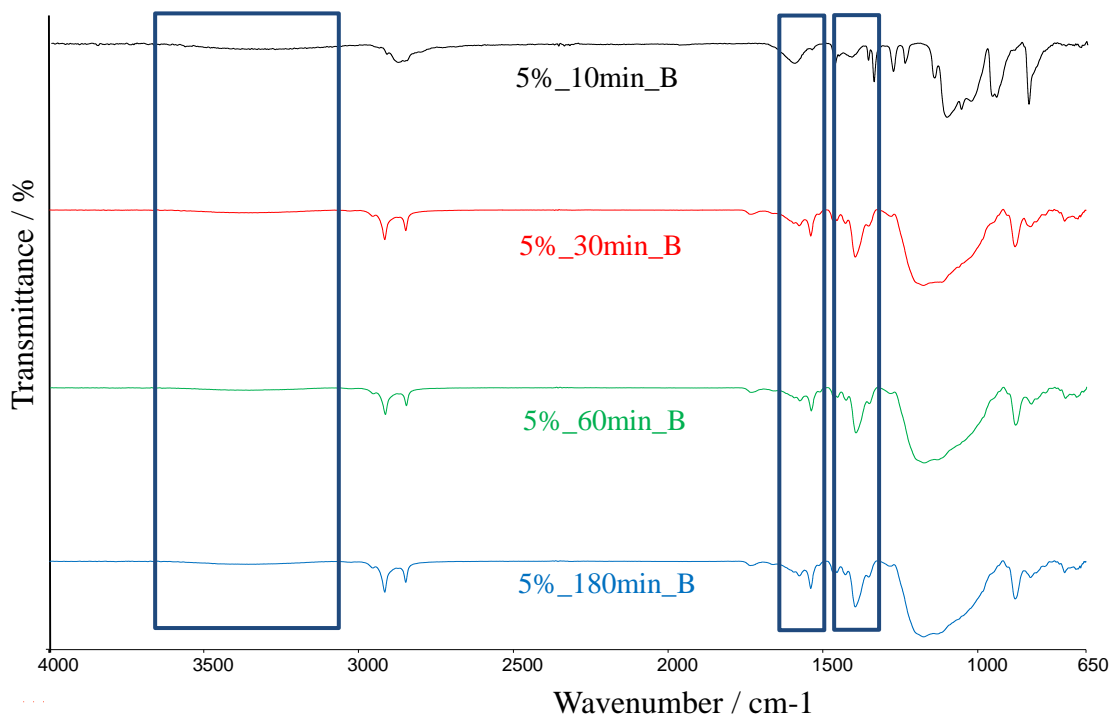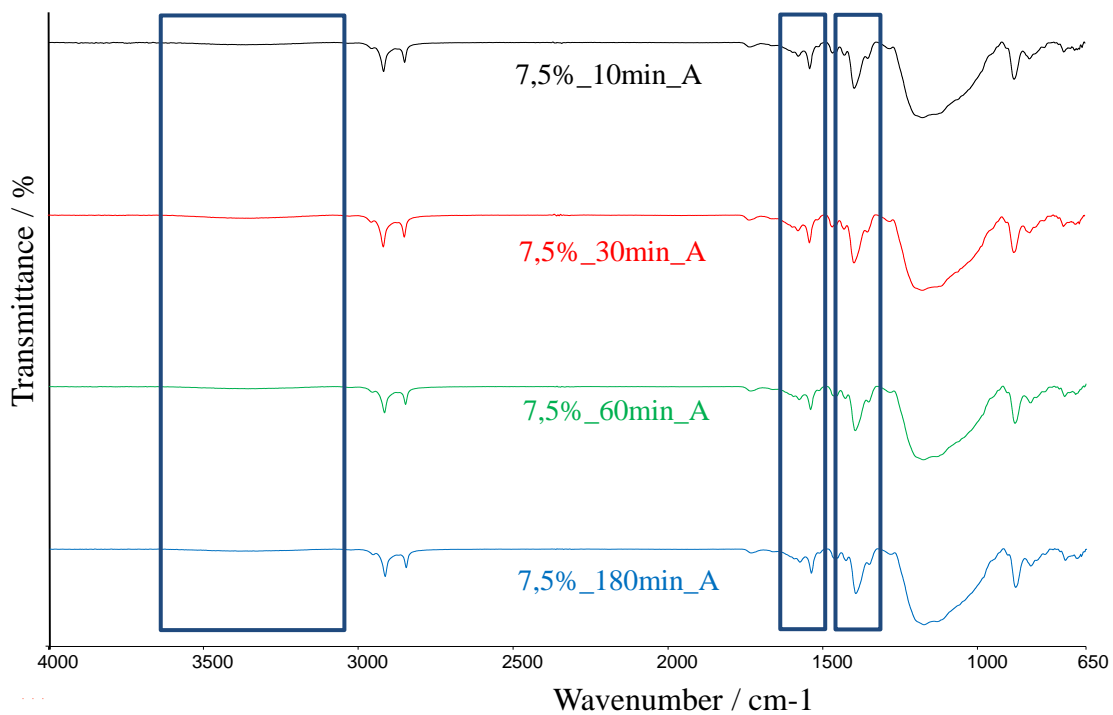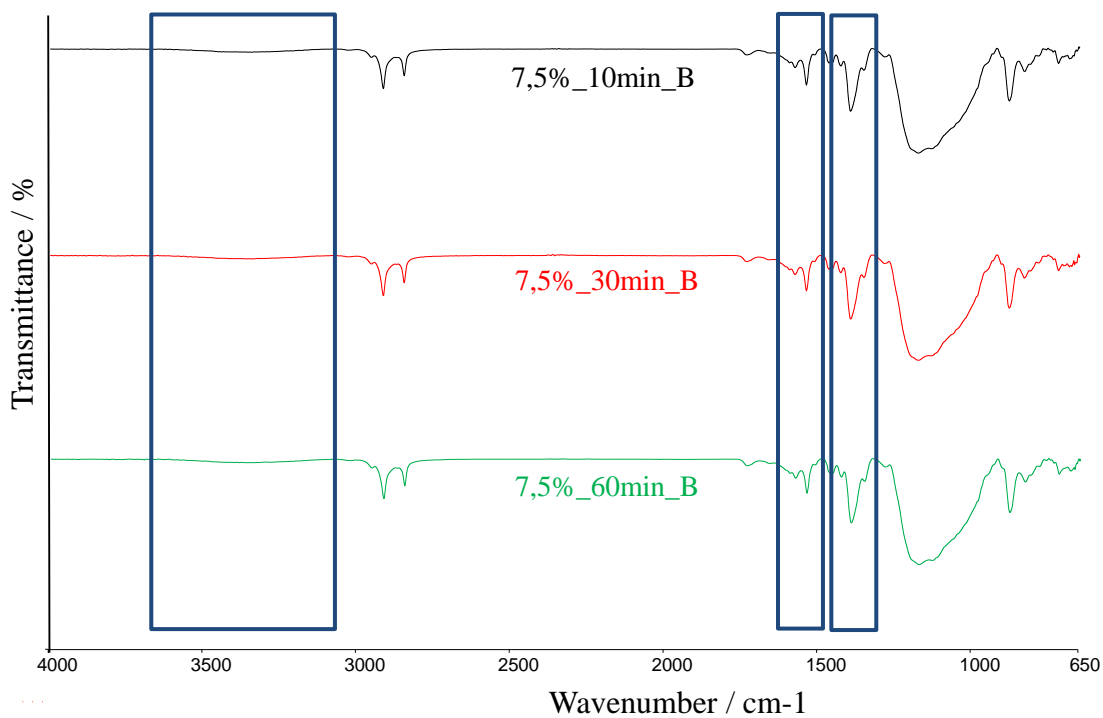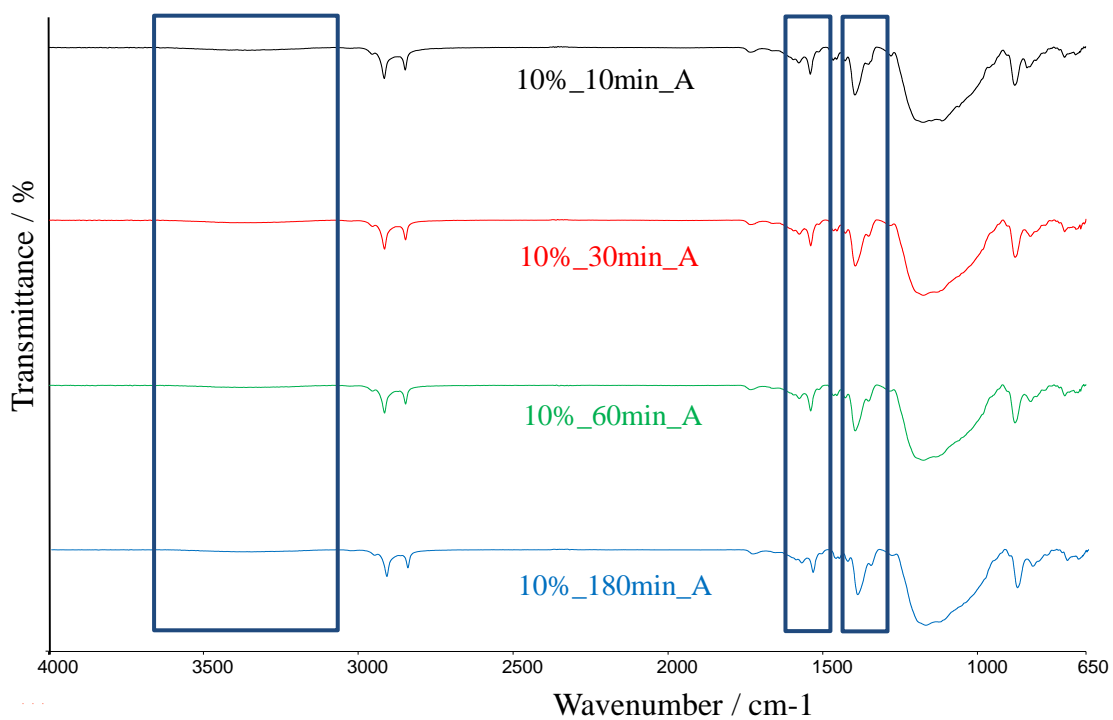

Figure 22. FT-IR spectra of the films after immersion in 2.5% w/v CaCl$_2$ solution for 10, 30, 60 and 180 min with single rinse (A)
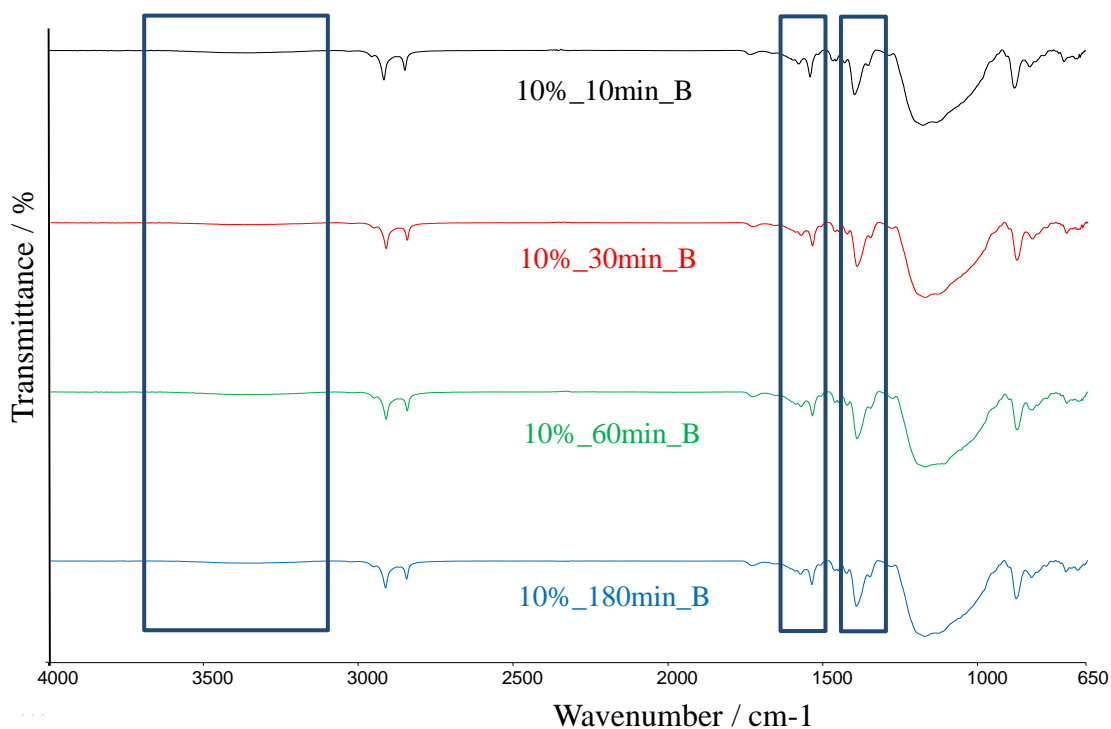
Figure 23. FT-IR spectra of the films after immersion in 2.5% w/v CaCl$_2$ solution for 10, 30, 60 and 180 min with double rinse (B)

Figure 24. FT-IR spectra of the films after immersion in 5% w/v CaCl$_2$ solution for 30, 60 and 180 min with single rinse (A)

Figure 25. FT-IR spectra of the films after immersion in 5% w/v $CaCl_2$ solution for 10, 30, 60 and 180 min with double rinse (B)

Figure 26. FT-IR spectra of the films after immersion in 7.5% w/v $CaCl_2$ solution for 10, 30, 60 and 180 min with single rinse (A)

Figure 27. FT-IR spectra of the films after immersion in 7.5% w/v $CaCl_2$ solution for 10, 30 and 60 min with double rinse (B)

Figure 28. FT-IR spectra of the films after immersion in 10% w/v $CaCl_2$ solution for 10, 30, 60 and 180 min with single rinse (A)

Figure 29. FT-IR spectrum of the films after immersion in 10% w/v CaCl$_2$ solution for 10, 30, 60 and 180 min with double rinse (B)

Figures 20, 22, 24, 26 and 28 show FT-IR spectra of 80%PEO/20%NaAlg films treated with different concentrations of CaCl$_2$ solution during different time after single rinse with methanol to remove lagged CaCl$_2$ and produced sodium chloride (NaCl) on the film surface after ion exchange procedure, if they were deposited on the film surface. The significant vibration bands for detection of cross-linked with Ca^{2+} ions are marked on FT-IR spectra and the corresponding wave numbers of the minimum vibration bands are given in Tables 3 and 4.

Figures 21, 23, 25, 27 and 29 present FT-IR spectra of the same films after double rinse with methanol while in Tables 3 and 4 are given the corresponding wave numbers with the same aim as before.

Any changes from cross-linked with Ca^{2+} that can be reflected on the triplet of C–O–C stretching vibrations can't be analysed because the triplet peaks are not visible as before cross-linking. Region of the triplet absorption is changed in a manner of wide absorption region with one or max two peaks, strong overlapping.

After evaluations of all FT-IR spectra for structural changes of NaAlg only significant change in the stretching vibrations of O–H bonds of alginate was noticed. This change can be attributed to the cross-linking with Ca^{2+} ions. In the literature[36-43]

34

the important change is expected with the stretching vibration of O–H bonds, asymmetric and symmetric stretching vibrations of COO⁻ group. The main explanation is based on the participation of hydroxyl and carboxylate groups of alginate to the calcium ion in order to form chelating structure.

The bands of COO⁻ groups didn't change with the variation of CaCl$_2$ solution concentration, the variation of time during which the films were immersed in the solutions as well as with the variation of the number of rinses with methanol. The reason can lie in the fact that the film is composed from two polymers that have lot of absorption vibration in this absorption region and additional cross-linked with Ca^{2+} ions makes it even more complex. Hence the influence of cross-linked can be overlapped with before mentioned stronger absorptions, because there is no information on how much of the ion exchange was conducted.

This isn't the case with the stretching vibration of O–H bonds which has no interference with absorptions from PEO. In the future investigation it is necessary to include additional structural analysis like X-ray diffraction and X-ray micro Computed tomography to additionally confirm structural change of the alginate, to detect the percentage of this change and where it is accomplished (through the sample mass or just on the surface).

In even simple samples like pure NaAlg or NaAlg with some additives this cross-linked is not simple to detect. Some researchers reported that the absorption region of stretching vibrations of O–H bonds in CaAlg appears narrower than in NaAlg[39,40], stretching vibrations of O–H bonds shifted to a higher wave numbers[22], the asymmetric stretching vibration of COO⁻ group are slightly shifted to lower wave numbers[39,41], asymmetric and symmetric stretching vibration of COO⁻ group are slightly shifted to lower wave numbers[36,22], asymmetric stretching vibration of COO⁻ group are slightly shifted to a lower wave numbers while at the same time symmetric stretching vibration of COO⁻ group are shifted to a higher wave numbers[42], an intensity decrease in the region of stretching vibration of COO⁻ group.[43]

It is evident that different changes can be observed but they are all the indication of NaAlg cross-linked with Ca^{2+} ions. All wave numbers of the stretching vibrations of O–H bonds after treatment with CaCl$_2$ solutions have lower values comparing to referent untreated film 80%PEO/20%NaAlg. The change of the stretching vibrations of O–H bonds with the increase of concentration of CaCl$_2$ solution at the same immersion time

is irregular, but it is evident that the highest values are obtained in 50% cases at highest concentration (10% w/v), (Tables 3 and 4).

The increase of immersion time at the same concentration of CaCl$_2$ solutions decreases the wave number at all investigated concentrations (Tables 3 and 4). The values of wave numbers are not the same but the change is.

Difference between the single and double rinse is noticed in a lower wave numbers after double rinse, (Tables 3 and 4).

All this observed changes of the stretching vibrations of O–H bonds indicate successfull establishment of cross-linking with Ca^{2+} ions.

Table. 2. Wave numbers of the characteristic vibrations of pure NaAlg, pure PEO and referent blend 80%PEO/20%NaAlg film

Sample	O-H stretching / cm^{-1}	Asimetric COO- stretching / cm^{-1}	Simetric COO- stretching / cm^{-1}	Asymmetric stretching of C-O-C, (triplet) / cm^{-1}	Scissorig vibration of C-O-C / cm^{-1}
NaAlg	3208	1591	1402	-	-
PEO	-	-	-	1145/1090/1057	959/840
80%PEO/20%NaAg	3389	1579	1396	1146/1105/1059	955/840

Table 3. Wave numbers of the characteristic vibrations of the blend 80%PEO/20%NaAlg films modified by immersion in CaCl$_2$ solutions of different concentrations for 10 and 30 min, with single (A) and double rinse (B)

	Sample	O-H stretching / cm^{-1}	Asimetric COO- stretching / cm^{-1}	Simetric COO$^-$ stretching / cm^{-1}		Sample	O-H stretching / cm^{-1}	Asimetric COO- stretching / cm^{-1}	Simetric COO$^-$ stretching / cm^{-1}
Samples after single rinse (A)	1%_10min_A	3363	1577	1396	**Samples after double rinse (B)**	1%_10min_B	3360	1577	1396
	2.5%_10min_A	3360	1577	1396		2.5%_10min_B	3354	1576	1396
	-	-	-	-		5%_10min_B	3277	1579	1399
	7.5%_10min_A	3363	1577	1396		7.5%_10min_B	3355	1577	1396
	10%_10min_A	3375	1577	1396		10%_10min_B	3361	1576	1396
	1%_30min_A	3360	1577	1396		1%_30min_B	3359	1576	1396
	2.5%_30min_A	3360	1577	1396		2.5%_30min_B	3353	1577	1396
	5%_30min_A	3358	1577	1396		5%_30min_B	3358	1577	1396
	7.5%_30min_A	3336	1577	1396		7.5%_30min_B	3347	1577	1396
	10%_30min_A	3372	1577	1395		10%_30min_B	3348	1577	1395

Table 4. Wave numbers of the characteristic vibrations of the blend 80%PEO/20%NaAlg films modified by immersion in CaCl$_2$ solutions of different concentrations for 60 and 180 min, with single (A) and double rinse (B)

	Sample	O-H stretching / cm^{-1}	Asimetric COO- stretching / cm^{-1}	Simetric COO$^-$ stretching / cm^{-1}		Sample	O-H stretching / cm^{-1}	Asimetric COO- stretching / cm^{-1}	Simetric COO$^-$ stretching / cm^{-1}
Samples after single rinse(A)	1%_60min_A	3358	1578	1396	Samples after double rinse (B)	1%_60min_B	3353	1577	1395
	2.5%_60min_A	3356	1576	1396		2.5%_60min_B	3353	1577	1395
	5%_60min_A	3358	1577	1396		5%_60min_B	3357	1577	1396
	7.5%_60min_A	3358	1577	1396		7.5%_60min_B	3338	1577	1396
	10%_60min_A	3365	1577	1396		10%_60min_B	3346	1577	1396
	1%_180min_A	3348	1576	1396		1%_180min_B	3346	1576	1396
	2.5%_180min_A	3343	1576	1396		2.5%_180min_B	3357	1577	1396
	5%_180min_A	3353	1577	1396		5%_180min_B	3351	1576	1396
	7.5%_180min_A	3363	1576	1396	-	-	-	-	-
	10%_180min_A	3353	1576	1396		10%_180min_B	3345	1577	1396

3.2. Differential scanning calorimetry

Differential scanning calorimetry (DSC) method was applied to analyse the thermal properties and crystallinity of pure NaAlg, PEO and their blend 80%PEO/20%NaAlg film before and after modification with different concentration of $CaCl_2$ solutions (complexation). The influence of immersion time or exposure time to Ca^{2+} ions and the rinse with methanol after the treatment with Ca^{2+} ions was also investigated. The first heating scan curve represents the influence of the thermal history of the sample together with the influence of the cross-linkage with Ca^{2+} ions, while the second heating scan curve is reflection only of the cross-linkage because with the first scan the thermal history is removed. The cooling scan curve presents the crystallization from the melt of the samples after the thermal history was removed. Figures 30, 36 and 42 show curves of the first heating scan, cooling scan and second heating scan, respectively, for pure NaAlg and PEO and the referent blend 80%PEO/20%NaAlg film. The values of numeric data of thermal characteristic for each thermal transition are shown in Table 5.

Pure NaAlg does not have any thermal transitions in the temperature interval of investigated DSC measurement according to the literature.[44] The extrapolated onset melting temperature (T_{eim1}) for pure PEO is 60 °C, while for the referent 80%PEO/20%NaAlg film is 55 °C (Table 5). This lower value indicates that interactions between PEO and NaAlg led to miscible blend. When a polymer blend is a mixture of semicrystalline and amorphous polymers, decrease of the melting temperature is a proof of established interactions between two polymers that leads to miscibility.[45] The peak melting temperature (T_{pm1}) is 69 °C for pure PEO, while for the referent 80%PEO/20%NaAlg film are 63 °C and 73 °C (Table 5). The reason of these two values is visible in Figure 30 in the form of main endothermic peak and smaller peak or shoulder on the main peak (grey number in Table 5). This is the result of the presence of smaller and larger crystals of PEO, the smaller crystals and less regular melts at lower temperatures, while a larger and more regular crystals melt at higher melting temperature.[46] The melting enthalpy (ΔH_{m1}) of pure PEO is 166.7 J g^{-1} while for the referent 80%PEO/20%NaAlg film is 115.3 J g^{-1} (Table 5). Degree of crystallinity (X_{c1}) of pure PEO is 89% and for the referent 80%PEO/20%NaAlg film is 77% (Table 5). Decrease of these thermal characteristics of PEO in the presence of NaAlg reflects from NaAlg interference with the crystallization process of PEO. From all analysed

thermal characteristic, it can be concluded that miscibility of the polymers in the referent 80%PEO/20%NaAlg film is established.

The crystallization from the melt occurs for pure PEO as well as for the referent 80%PEO/20%NaAlg film. The extrapolated onset crystallization temperature (T_{eimc}), the peak crystallization temperature (T_{pmc}) and the crystallization enthalpy (ΔH_{mc}) values of pure PEO are 41 °C, 38 °C and 121.9 J g^{-1}, respectively (Table 5). The values of T_{eimc}, T_{pmc} and ΔH_{mc} of the referent 80%PEO/20%NaAlg film are 44 °C, 34 °C (40 °C is the value at the shoulder on the main peak) and 99.9 J g^{-1}, respectively (Table 5). The appearance of exothermic shoulder on the main crystallization peak (Figure 36) is pointed out in Table 5 with grey numbers. The reason for this shoulder is due to the crystals changes during crystal formation.[47] According to all these thermal characteristics the same conclusion is drawn as before, noticed decrement is the effect of NaAlg in the blend film and its function as the barrier for the crystallization of PEO. After the thermal history of PEO and the referent film was removed, the change of the thermal characteristics is almost the same as before, Table 5, and points out to the similar conclusions. Two endothermic peaks or peak and shoulder are still present. The extrapolated onset glass transition temperature (T_{eig}) and the midpoint glass transition temperature (T_{mg}) are slightly lower for the referent 80%PEO/20%NaAlg film (-59 and -53 °C, respectively) comparing to the values of pure PEO (-55 and -51 °C, respectively), Table 5. Although change in the glass transition temperatures is small it is clear sign that NaAlg and PEO are miscible. *S. Kuo*[48] in his investigation showed how the influence of hydrogen bonds affects polymers miscibility. He pointed out that decrease of glass transition was due to polymers miscibility that frequently occurs at solid polymer electrolytes like PEO. The change of the specific heat capacity at glass transition (Δc_p) of pure PEO comparing to the referent 80%PEO/20%NaAlg film is from 0,15 J g^{-1} °C^{-1} to 0,06 J g^{-1} °C^{-1}, Table 5. The values of T_{eim2}, T_{pm2}, ΔH_{m2} and X_{c2} for pure PEO are 57 °C, 64 °C, 127.5 J g^{-1} and 68%, respectively. The values of the same thermal characteristics for the referent 80%PEO/20%NaAlg film are 56 °C, 74 °C (64 °C is the value at the shoulder on the main peak), 100.7 J g^{-1} and 67%, respectively. This confirms conclusions made for the first heating scan that decrease of thermal characteristics of PEO in the presence of NaAlg reflects from NaAlg interference with the crystallization process of PEO and that miscibility in blend is established.

The DSC curves of blend 80%PEO/20%NaAlg films after cross-linkage procedure with Ca^{2+} ions are shown in Figure 31-35; 37-41; 43-47. The values of the thermal characteristics obtained from DSC curves are presented in Tables 6-13. It is important to emphasize that NaAlg and CaAlg does not have any thermal transitions in the temperature interval of investigated DSC measurement according to the literature.[44] Hence obtained data is attributed to PEO and how cross-linkage of NaAlg with Ca^{2+} ions affects its thermal properties. The main difference between the referent film and cross-linked films is in the crystallization process that influences the shape of the phase transitions and the appearance of small endothermic peaks or shoulders at the main melting peak and small exothermic peak or shoulder at the main crystallization peak (crystallization from the melt). This is probably due to the melting and crystallization of PEO crystals of different sizes and thermal stability. Even after removal of the thermal history of the treated films with Ca^{2+} ions the same pattern is observed. The smaller and imperfect crystals will melt at lower temperatures, unlike the larger and perfect crystals.[46] This also can be due to the formation of the crystals that changes during the crystallization because of thickening or thinning of the crystals.[47] All investigated thermal characteristics are under the influence of different concentration of $CaCl_2$ solutions, different immersion time and the rinse procedure but there is irregular change that can't be connected to any variations of this parameters. After detail analysis of all thermal characteristics presented in Tables 6-13 it can be concluded that the change is evident, but all these results are comparable to the results of the referent films, there is no major change that is recorded, with some exceptions that confirms the previous conclusions. The appearance of the shoulders at the main endothermic and exothermic transition has a large influence on the values of all temperature parameters which serves for evaluation of the influence of cross-linkage with Ca^{2+} on thermal properties of 80%PEO/20%NaAlg films. Only degree of crystallinity (X_c) is subjected to significant change, but the same irregular change is noticed with the influence of different concentration of $CaCl_2$ solutions and the rinse procedure, Table 6-13. The ability of NaAlg to cross-link with Ca^{2+} interferes the crystallization of PEO. When the influence of immersion time was analysed it can be noticed that X_c has tendency to be smaller upon 180 min treatment, Table 12-13. After the first heating scan 25 samples of total 38 samples have X_c value under the value of referent sample film (77%), while 13 of them have X_c value above the value of referent sample film. The second heating scan produced 27 samples of total 38 samples that have X_c value under the value of referent

sample film (67%), while 11 of them have X_c value above the value of referent sample film. The values of X_c goes from 40 to 100%, but these higher values are in majority closer to values of referent film. It can be generally concluded that X_c value of PEO depends on the proportion of cross-linkage in the films and that the largest exchange of Na^+ with Ca^{2+} is achieved with longer exposure time to $CaCl_2$ solutions. Hence, this immersion time or exposure time showed the greatest potential for the preparation of solid polymer electrolyte. The aim of this work was to reduce the amount of the crystalline phase of PEO in the blend film in order to achieve a better conductivity of PEO when a lithium salt is added in order to produce a solid polymer electrolyte for a lithium batteries. Finally, in the future investigations cross-linkage of NaAlg with Ca^{2+} ions in 80%PEO/20%NaAlg will be carried out only at 180 min.
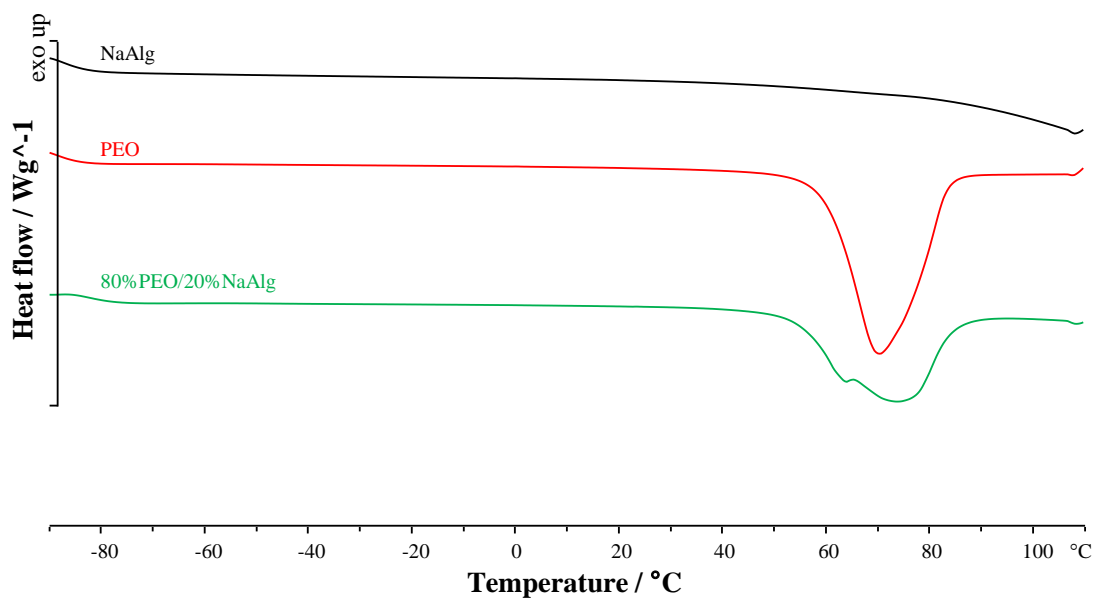
Figure 30. DSC curves of the first heating scan for pure NaAlg, pure PEO and referent blend 80%PEO/20%NaAlg film
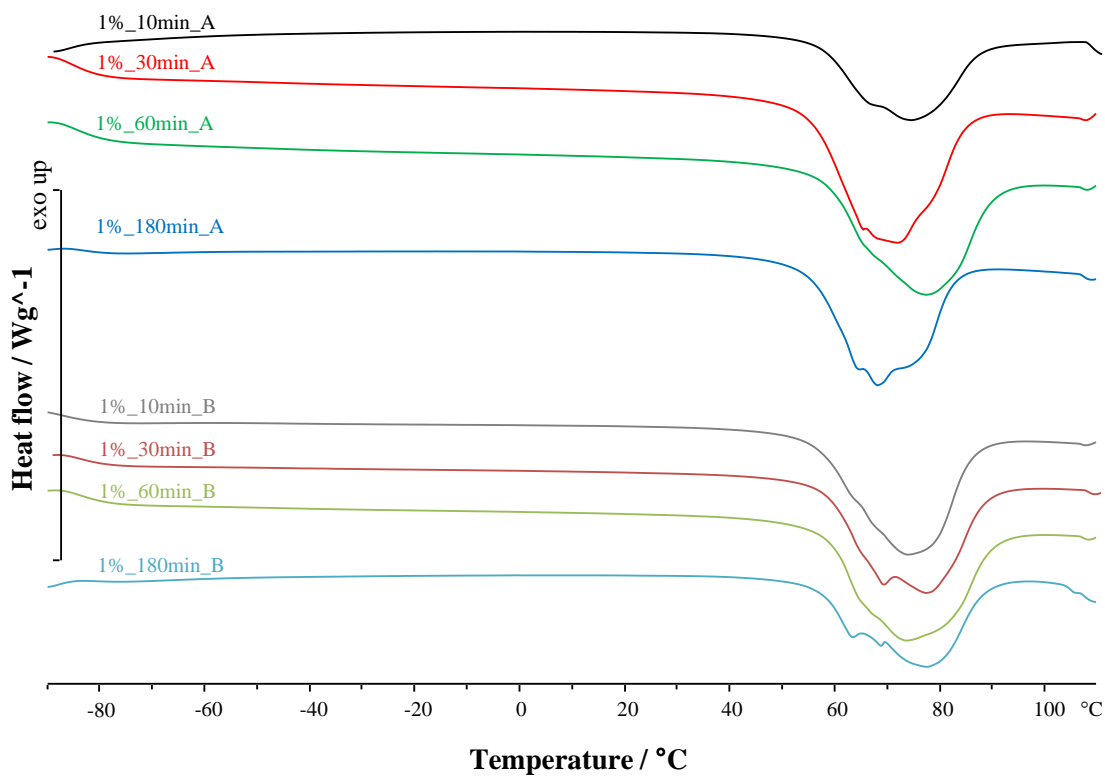
Figure 31. DSC curves of the first heating scan for the films after immersion in 1% w/v CaCl$_2$ solution for 10, 30, 60 and 180 min, with single (A) and double rinse (B)
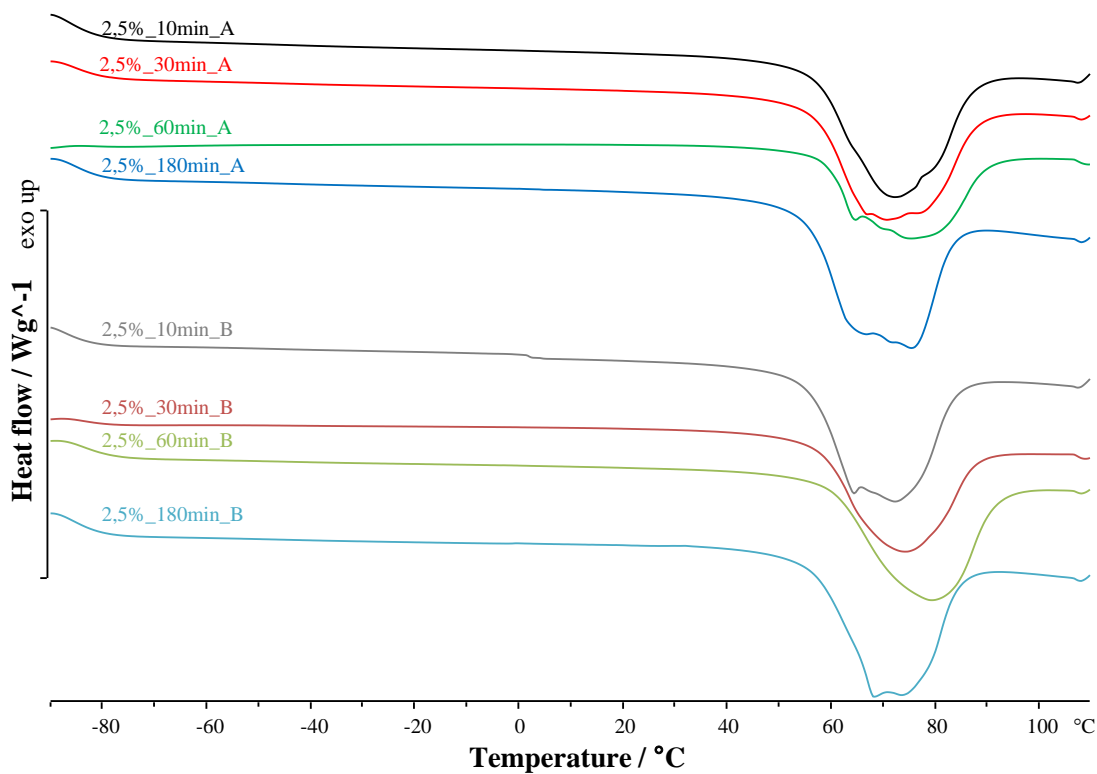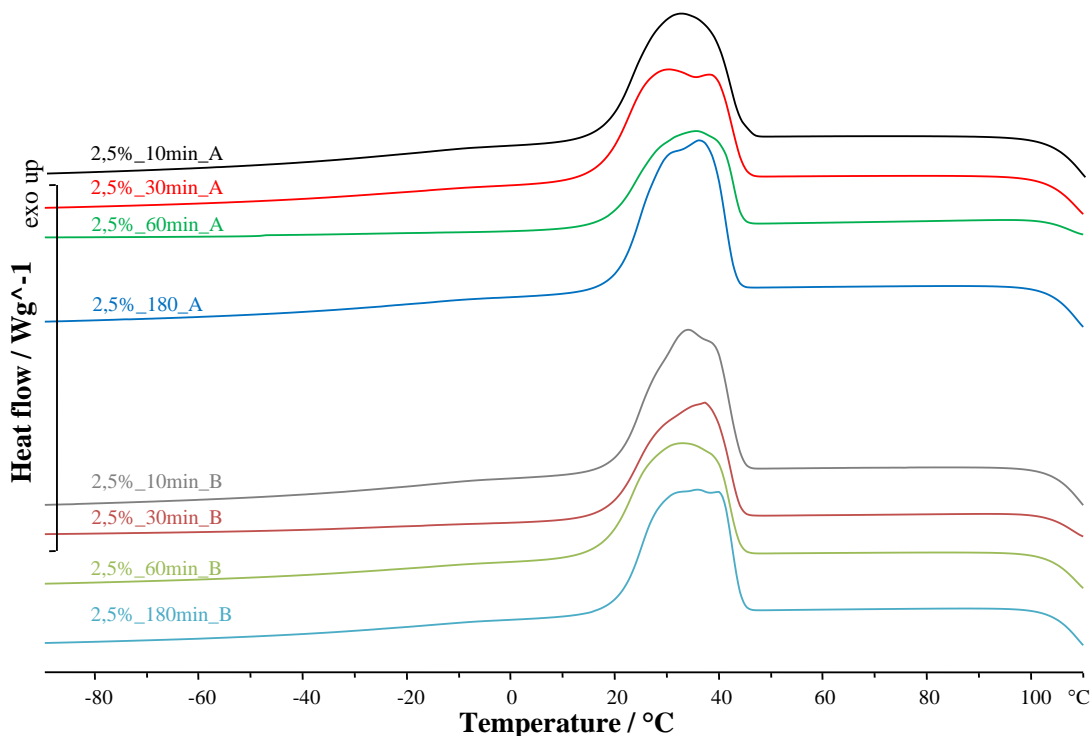

Figure 32. DSC curves of the first heating scan for the films after immersion in 2.5% w/v CaCl$_2$ solution for 10, 30, 60 and 180 min, with single (A) and double rinse (B)
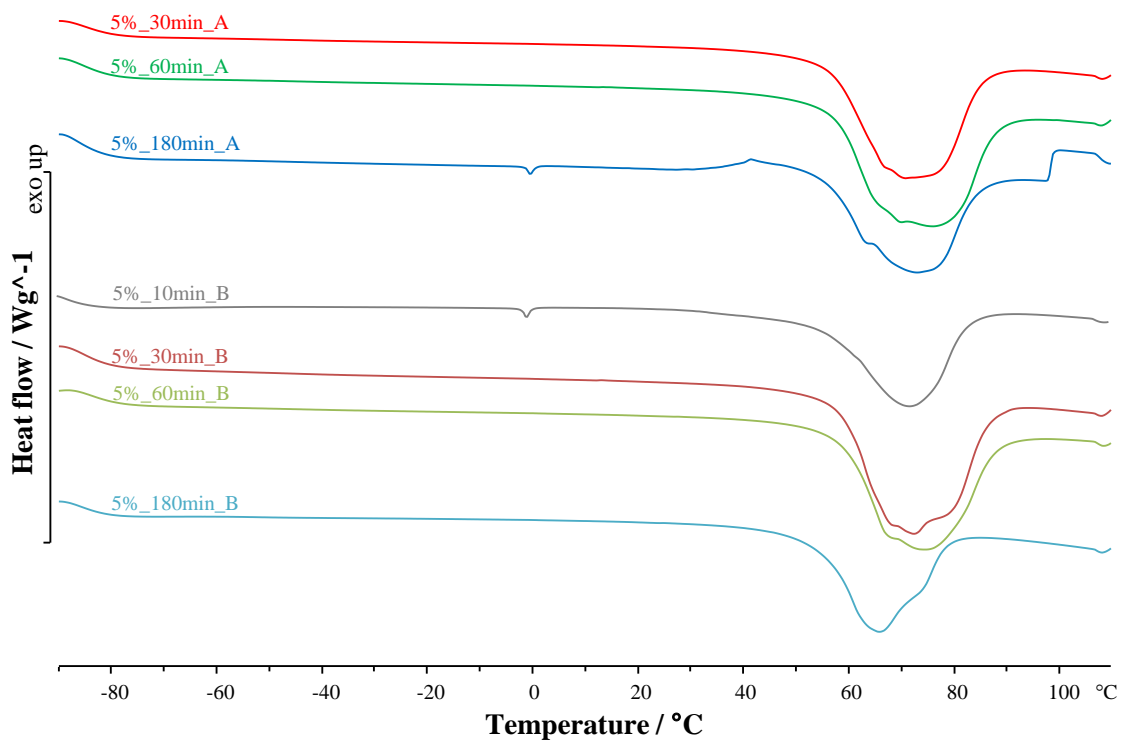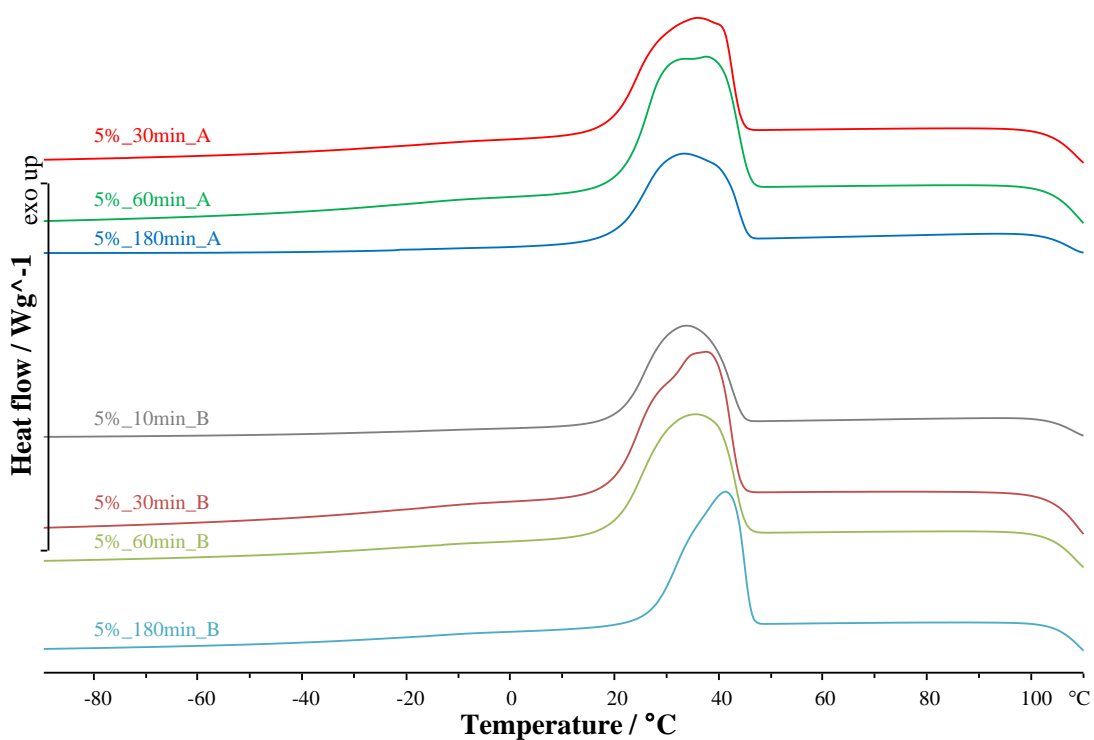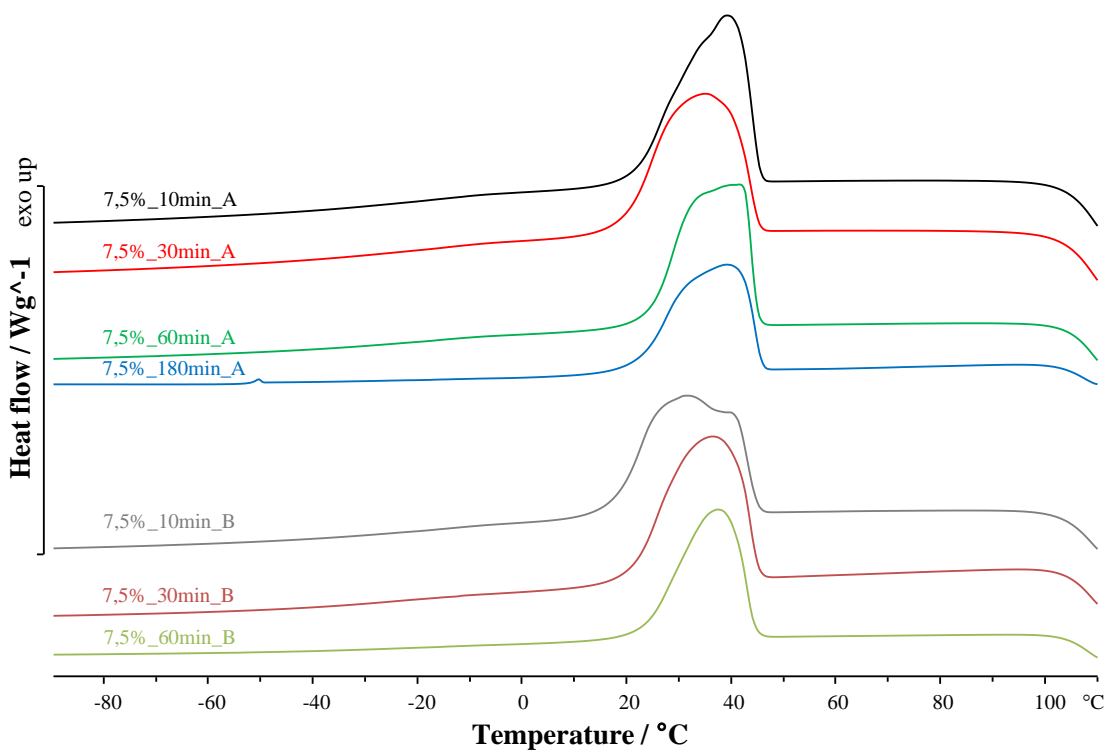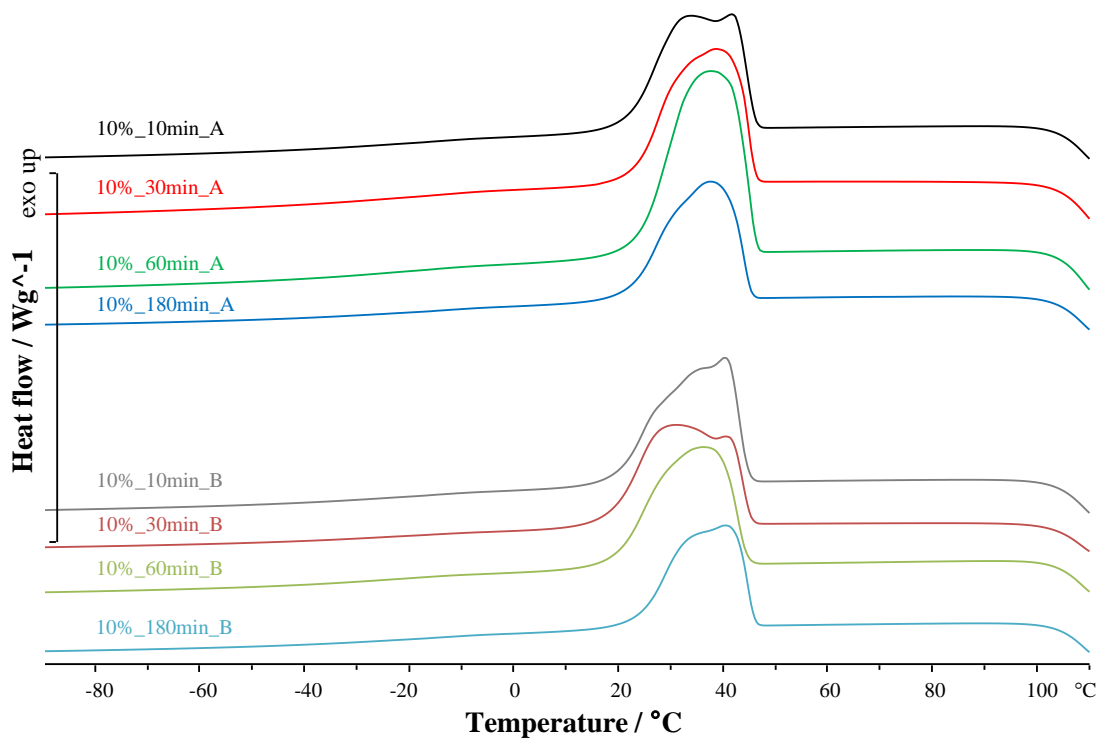
Figure 33. DSC curves of the first heating sacn for the films after immersion in 5% w/v CaCl$_2$ solution for 10, 30, 60 and 180 min, with single (A) and double rinse (B)
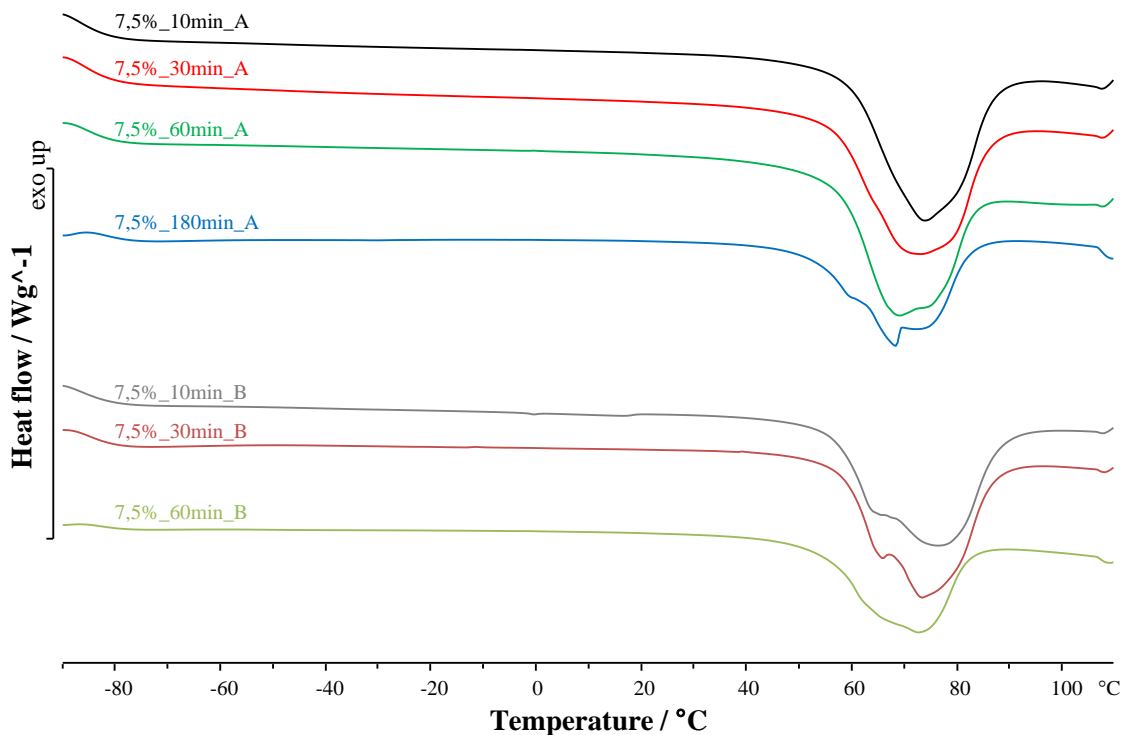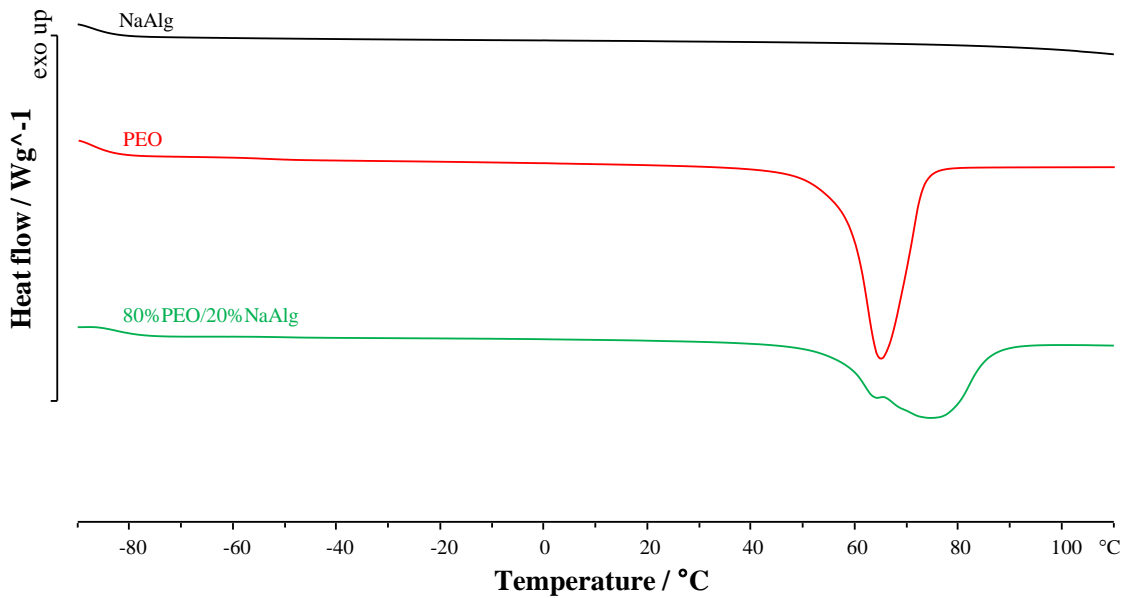

Figure 34. DSC curves of the first heating scan for the films after immersion in 7.5% w/v CaCl$_2$ solution for 10, 30, 60 and 180 min, with single (A) and double rinse (B)
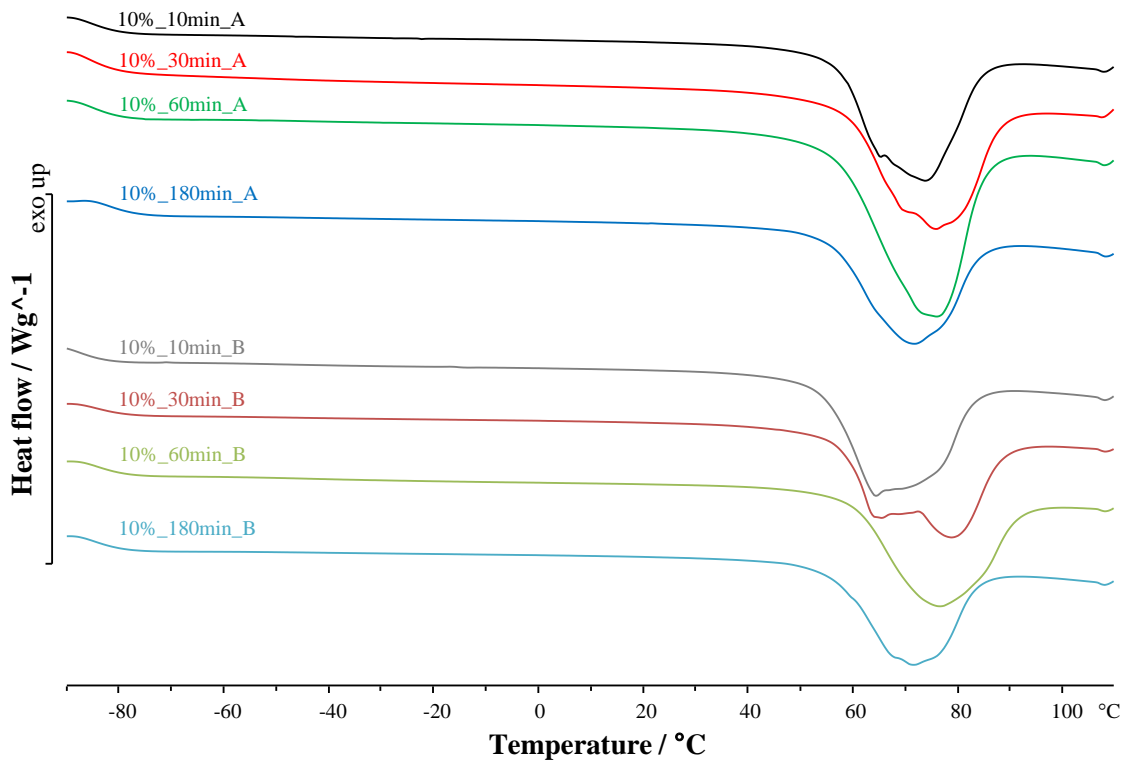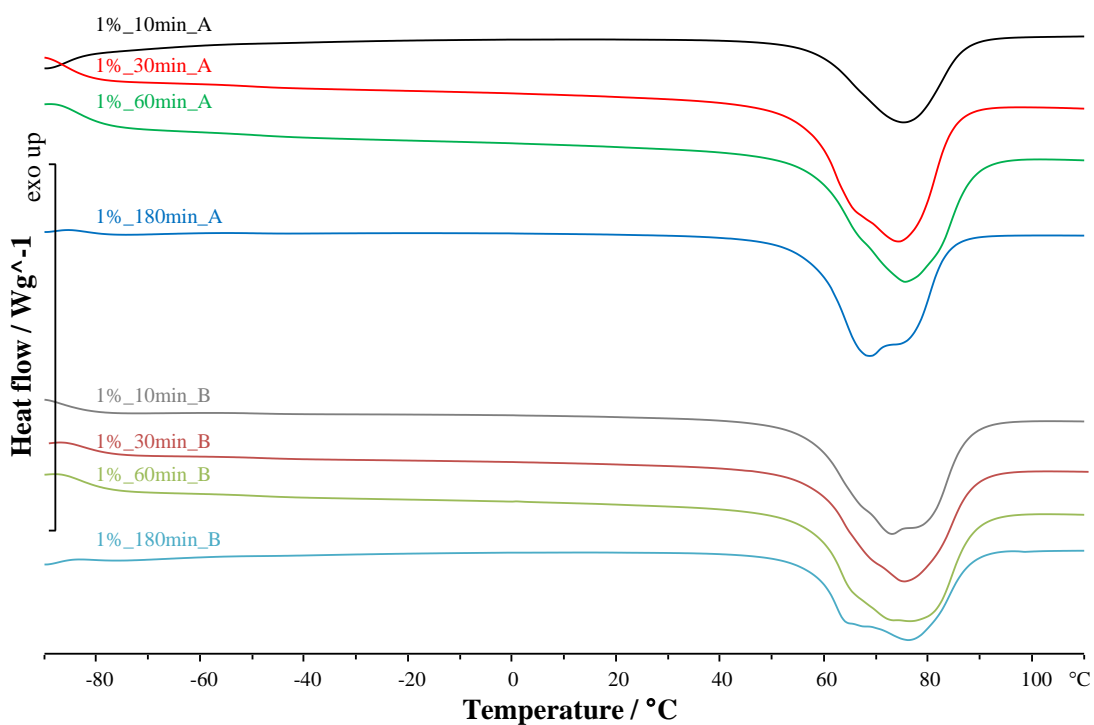
Figure 35. DSC curves of the first heating scan for the films after immersion in 10% w/v CaCl₂ solution for 10, 30, 60 and 180 min, with single (A) and double rinse (B)
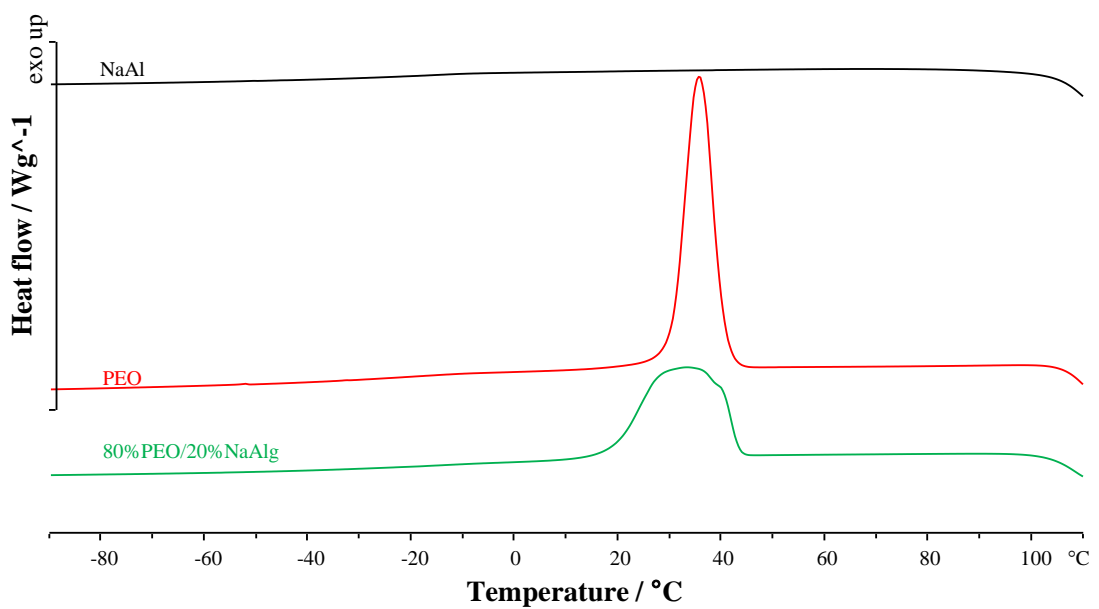
Figure 36. DSC curves of the second cooling scan for the pure NaAlg, pure PEO and referent blend 80%PEO/20%NaAlg film

45
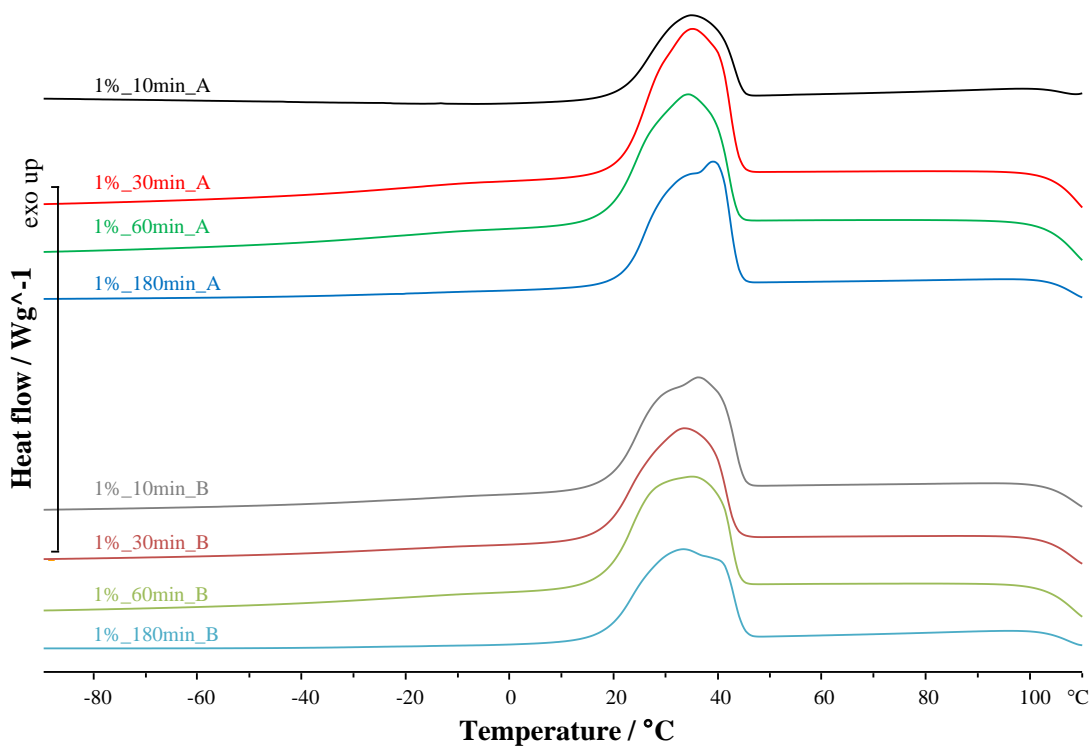
Figure 37. DSC curves of the second cooling scan for the films after immersion in 1% w/v CaCl$_2$ solution for 10, 30, 60 and 180 min, with single (A) and double rinse (B)
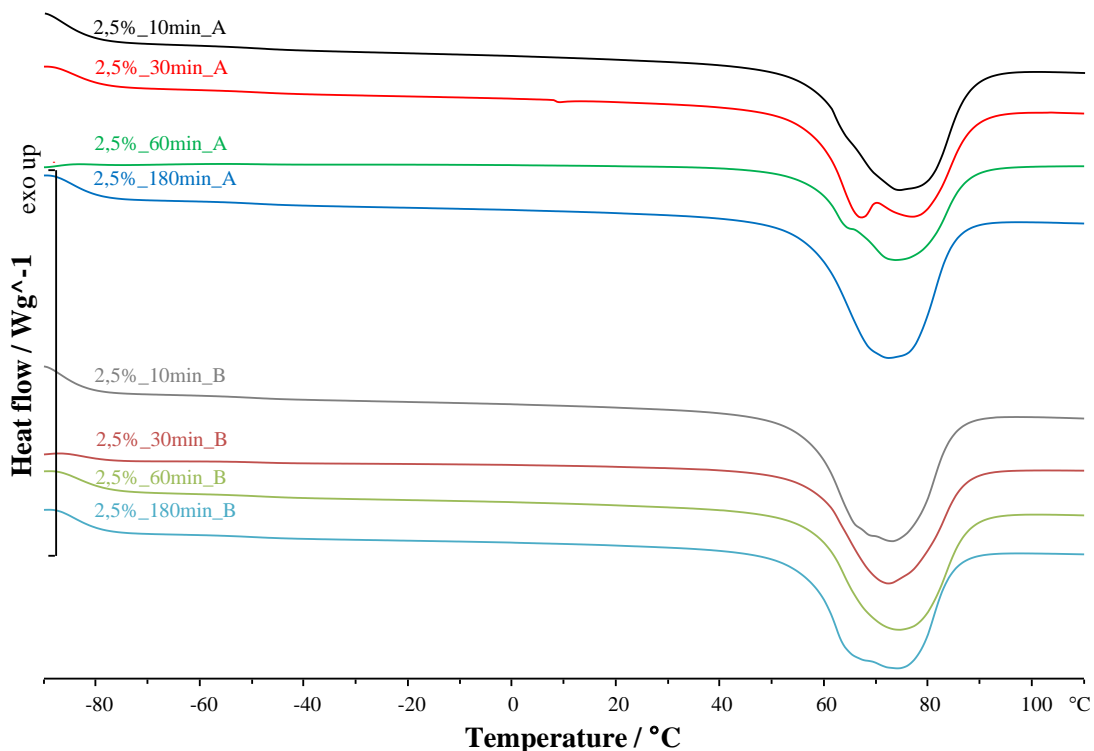

Figure 38. DSC curves of the second cooling scan for the films after immersion in 2.5% w/v CaCl$_2$ solution for 10, 30, 60 and 180 min, with single (A) and double rinse (B)
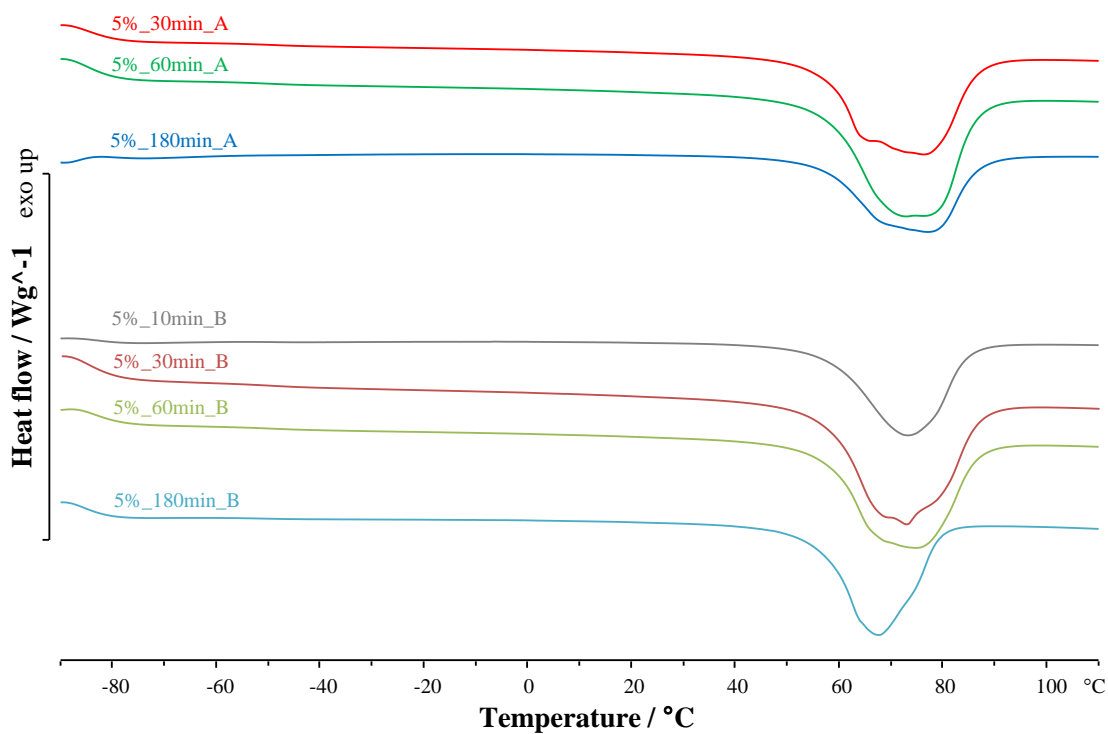
Figure 39. DSC curves of the second cooling scan for the films after immersion in 5% w/v $CaCl_2$ solution for 10, 30, 60 and 180 min, with single (A) and double rinse (B)
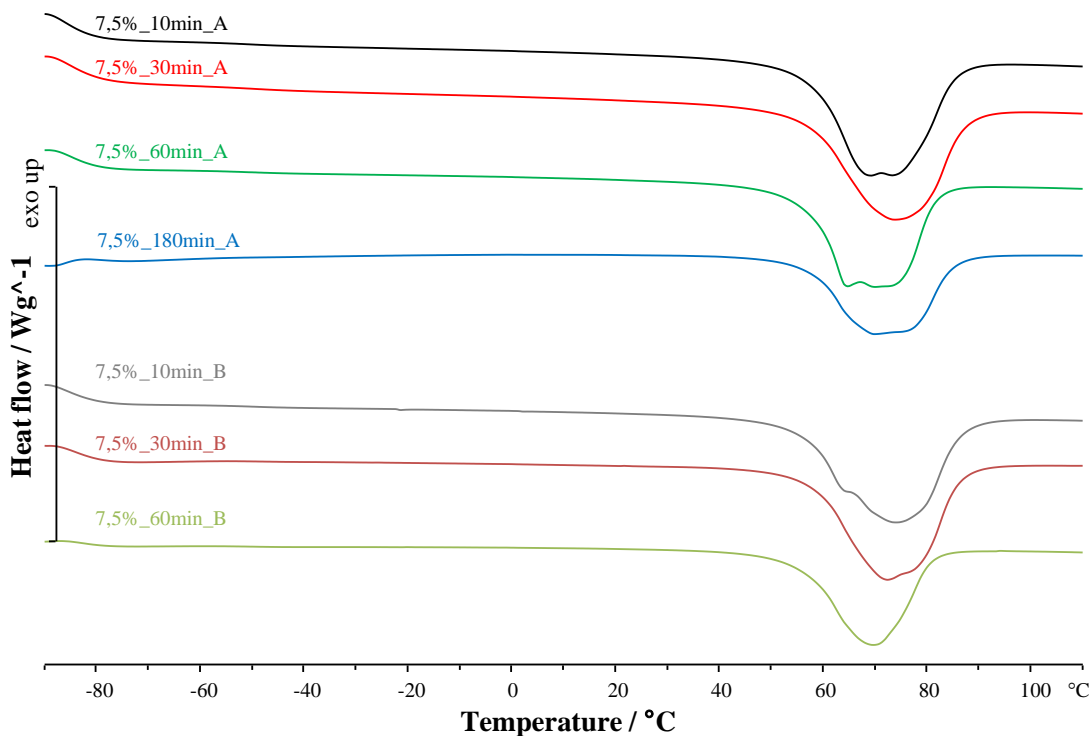

Figure 40. DSC curves of the second cooling scan for the films after immersion in 7.5% w/v $CaCl_2$ solution for 10, 30, 60 and 180 min, with single (A) and double rinse (B)
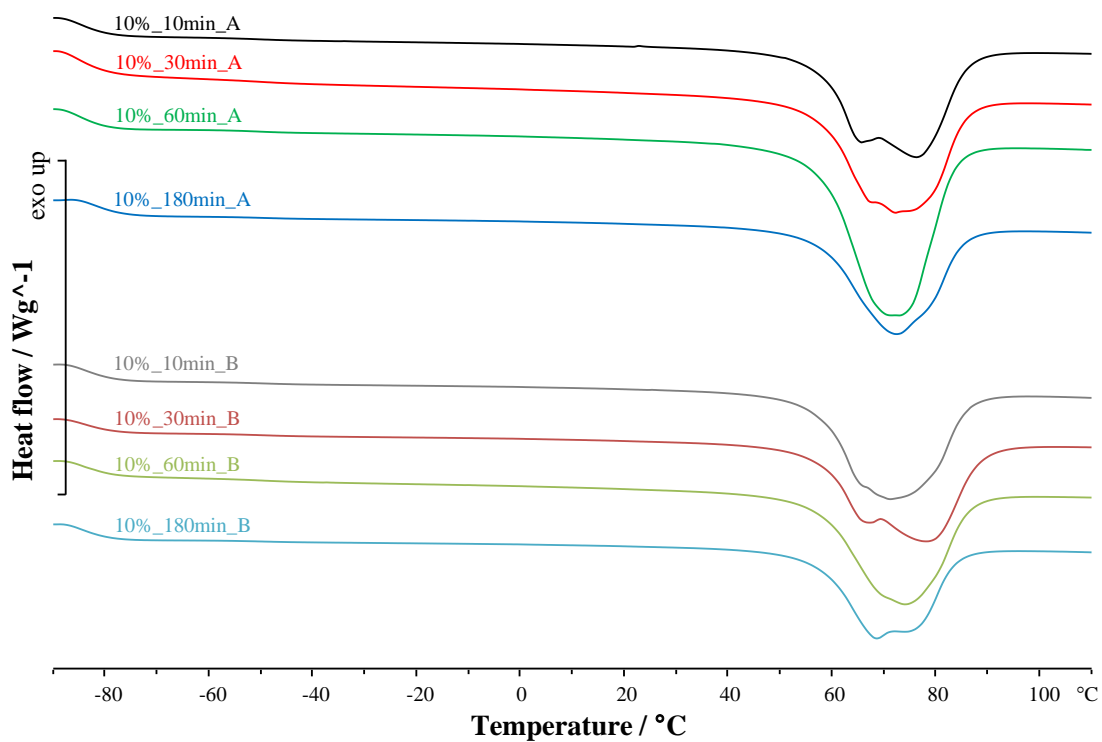
Figure 41. DSC curves of the second cooling scan for the films after immersion in 10% w/v CaCl$_2$ solution for 10, 30, 60 and 180 min, with single (A) and double rinse (B)

Figure 42. DSC curves of the second heating scan for pure NaAlg, pure PEO and referent blend 80%PEO/20%NaAlg film

Figure 43. DSC curves of the second heating scan for the films after immersion in 1% w/v $CaCl_2$ solution for 10, 30, 60 and 180 min, with single (A) and double rinse (B)

Figure 44. DSC curves of the second heating scan for the films after immersion in 2.5% w/v $CaCl_2$ solution for 10, 30, 60 and 180 min, with single (A) and double rinse (B)

Figure 45. DSC curves of the second heating scan for the films after immersion in 5% w/v CaCl$_2$ solution for 10, 30, 60 and 180 min, with single (A) and double rinse (B)

Figure 46. DSC curves of the second heating scan for the films after immersion in 7.5% w/v CaCl$_2$ solution for 10, 30, 60 and 180 min, with single (A) and double rinse (B)

Figure 47. DSC curves of the second heating scan for the films after immersion in 10% w/v CaCl$_2$ solution for 10, 30, 60 and 180 min, with single (A) and double rinse (B)

Table 5. DSC characteristics of the first heating, cooling and second heating curves of pure NaAlg, pure PEO and referent blend 80%PEO/20%NaAlg film

Sample	1st Heating				Cooling			2nd Heating						
	T_{eim1} / °C	T_{pm1} / °C	$-\Delta H_{m1}$ / J g^{-1}	X_{c1} / %	T_{eimc} / °C	T_{pmc} / °C	ΔH_{mc} / J g^{-1}	T_{eig} / °C	T_{mg} / °C	Δc_p / J g^{-1} °C^{-1}	T_{eim2} / °C	T_{pm2} / °C	$-\Delta H_{m2}$ / J g^{-1}	X_{c2} / %
NaAlg	-	-	-	-	-	-	-	-	-	-	-	-	-	-
PEO	60	69	166.7	89	41	38	121.9	-59	-53	0.15	57	64	127.5	68
80%PEO/20%NaAlg	55	63 / 73	115.3	77	44	34 / 40	99.9	-55	-51	0.06	56	64 / 74	100.7	67

Table 6. DSC characteristics of the first heating, cooling and second heating curves of the films after immersion in 1, 2.5, 7.5 and 10% w/v $CaCl_2$ solutions for 10 min with single rinse (A)

Sample	1st Heating				Cooling			2nd Heating						
	T_{eim1} / °C	T_{pm1} / °C	$-\Delta H_{m1}$ / J g^{-1}	X_{c1} / %	T_{eimc} / °C	T_{pmc} / °C	ΔH_{mc} / J g^{-1}	T_{eig} / °C	T_{mg} / °C	Δc_p / J g^{-1} °C^{-1}	T_{eim2} / °C	T_{pm2} / °C	$-\Delta H_{m2}$ / J g^{-1}	X_{c2} / %
1%_10min_A	56	66 / 73	81.9	54	45	35	61.0	-	-	-	58	75	62.2	41
2.5%_10min_A	56	71 / 77	119.5	79	45	33	101.9	-54	-48	0.13	57	73	102.7	68
7.5%_10min_A	59	72	114.9	76	46	40	97.4	-56	-50	0.12	66	68 / 72	98.5	66
10%_10min_A	57	64 / 73	117.8	78	46	35 / 42	99.6	-56	-49	0.11	43	65 / 76	100.9	67

Table 7. DSC characteristics of the first heating, cooling and second heating curves of the films after immersion in 1, 2.5, 5, 7.5 and 10% w/v CaCl$_2$ solutions for 10 min with double rinse (B)

Sample	1st Heating				Cooling			2nd Heating						
	T_{eim1} /°C	T_{pm1} /°C	$-\Delta H_{m1}$ /J g^{-1}	X_{c1} /%	T_{eimc} /°C	T_{pmc} /°C	ΔH_{mc} /J g^{-1}	T_{eig} /°C	T_{mg} /°C	Δc_p /J g^{-1} °C^{-1}	T_{eim2} /°C	T_{pm2} /°C	$-\Delta H_{m2}$ /J g^{-1}	X_{c2} /%
1%_10min_B	56	73	109.6	73	45	37 / 32	93.3	-54	-50	0.05	56	72 / 77	94.9	63
2.5%_10min_B	68	63 / 71	119.0	79	45	35 / 39	100.8	-56	-50	0.12	56	72	102.1	68
5%_10min_B	55	71	79.8	53	45	34	64.8	-52	-49	0.01	58	73	66.0	44
7.5%_10min_B	57	65 / 75	114.1	76	45	32 / 40	94.6	-56	-50	0.09	56	64 / 73	96.9	64
10%_10min_B	54	63 / 68	114.4	76	45	38 / 41	98.3	-56	-50	0.09	57	65 / 71	100.0	66

Table 8. DSC characteristics of the first heating, cooling and second heating curves of the films after immersion in 1, 2.5, 5, 7.5 and 10% w/v $CaCl_2$ solutions for 30 min with single rinse (A)

Sample	1st Heating				Cooling			2nd Heating						
	T_{eim1} / °C	T_{pm1} / °C	$-\Delta H_{m1}$ / J g^{-1}	X_{c1} / %	T_{eimc} / °C	T_{pmc} / °C	ΔH_{mc} / J g^{-1}	T_{eig} / °C	T_{mg} / °C	Δc_p / J g^{-1} °C^{-1}	T_{eim2} / °C	T_{pm2} / °C	$-\Delta H_{m2}$ / J g^{-1}	X_{c2} / %
1%_30min_A	55	64 / 70	127.8	85	45	36	106.9	-56	-49	0.12	56	65 / 73	107.3	71
2.5%_30min_A	57	66 / 70 / 75	118.6	79	34	31 / 39	100.1	-55	-48	0.12	41	66 / 76	101.9	68
5%_30min_A	56	66 / 70	101.9	68	45	36 / 41	86.1	-56	-49	0.10	57	66 / 76	87.2	58
7.5%_30min_A	56	71	114.8	76	46	36	98.3	-54	-47	0.14	56	73	99.6	66
10%_30min_A	59	69 / 75	126.3	84	47	40	104.8	-55	-47	0.15	57	67 / 71	106.2	71

Table 9. DSC characteristics of the first heating, cooling and second heating curves of the films after immersion in 1, 2.5, 5, 7.5 and 10% w/v $CaCl_2$ solutions for 30 min with double rinse (B)

Sample	1st Heating				Cooling			2nd Heating						
	T_{eim1} /°C	T_{pm1} /°C	$-\Delta H_{m1}$ / J g^{-1}	X_{c1} / %	T_{eimc} /°C	T_{pmc} /°C	ΔH_{mc} / J g^{-1}	T_{eig} /°C	T_{mg} /°C	Δc_p / J g^{-1} °C^{-1}	T_{eim2} /°C	T_{pm2} /°C	$-\Delta H_{m2}$ / J g^{-1}	X_{c2} / %
1%_30min_B	42	67 / 75	108.2	72	44	34	90.5	-55	-49	0.08	57	74	92.3	61
2.5%_30min_B	58	73	99.9	66	44	38	85.7	-55	-49	0.07	57	72	88.4	59
5%_30min_B	58	67 / 71 / 78	116.8	78	44	38	98.5	-55	-48	0.13	57	68 / 72	99.8	66
7.5%_30min_B	58	65 / 73	111.6	74	45	37	92.7	-52	-49	0.03	57	72	94.5	63
10%_30min_B	60	65 / 78	111.8	74	37	31 / 41	97.1	-56	-49	0.09	50	67 / 77	98.5	65

Table 10. DSC characteristics of the first heating, cooling and second heating curves of the films after immersion in 1, 2.5, 5, 7.5 and 10% w/v $CaCl_2$ solutions for 60 min with single rinse (A)

Sample	1st Heating				Cooling			2nd Heating						
	T_{eim1} / °C	T_{pm1} / °C	$-\Delta H_{m1}$ / J g^{-1}	X_{c1} / %	T_{eimc} / °C	T_{pmc} / °C	ΔH_{mc} / J g^{-1}	T_{eig} / °C	T_{mg} / °C	Δc_p / J g^{-1} °C^{-1}	T_{eim2} / °C	T_{pm2} / °C	$-\Delta H_{m2}$ / J g^{-1}	X_{c2} / %
1%_60min_A	58	76	118.7	79	44	35	101.2	-53	-45	0.13	57	75	101.6	68
2.5%_60min_A	59	64 / 74	91.0	61	45	36	75.6	-53	-49	0.03	57	64 / 73	78.6	52
5%_60min_A	57	69 / 74	115.8	77	46	35 / 38	100.5	-56	-50	0.10	57	72 / 75	101.8	68
7.5%_60min_A	58	68 / 72	96.9	64	45	37 / 42	84.9	-57	-51	0.09	69	64 / 69	87.5	58
10%_60min_A	57	74	151.0	100	47	39	135.2	-57	-52	0.11	57	70	137.9	92

Table 11. DSC characteristics of the first heating, cooling and second heating curves of the films after immersion in 1, 2.5, 5, 7.5 and 10% w/v $CaCl_2$ solutions for 60 min with double rinse (B)

Sample	1st Heating				Cooling			2nd Heating						
	T_{eim1} / °C	T_{pm1} / °C	$-\Delta H_{m1}$ / J g^{-1}	X_{c1} / %	T_{eimc} / °C	T_{pmc} / °C	ΔH_{mc} / J g^{-1}	T_{eig} / °C	T_{mg} / °C	Δc_p / J g^{-1} °C^{-1}	T_{eim2} / °C	T_{pm2} / °C	$-\Delta H_{m2}$ / J g^{-1}	X_{c2} / %
1%_60min_B	58	72	117.9	78	44	36	99.1	-54	-48	0.10	57	75	103.0	69
2.5%_60min_B	60	78	115.4	77	44	33	94.7	-54	-48	0.11	58	73	97.9	65
5%_60min_B	59	73	106.8	71	45	36	88.0	-55	-48	0.11	58	74	89.7	60
7.5%_60min_B	55	72	70.6	47	45	38	68.1	-55	-50	0.03	56	69	69.7	46
10%_60min_B	60	75	113.5	75	45	37	96.6	-55	-49	0.12	57	73	99.6	66

Table 12. DSC characteristics of the first heating, cooling and second heating curves of the films after immersion in 1, 2.5, 5, 7.5 and 10% w/v CaCl$_2$ solutions for 180 min with single rinse (A)

Sample	1st Heating				Cooling			2nd Heating						
	T_{eim1} / °C	T_{pm1} / °C	$-\Delta H_{m1}$ / J g^{-1}	X_{c1} / %	T_{eimc} / °C	T_{pmc} / °C	ΔH_{mc} / J g^{-1}	T_{eig} / °C	T_{mg} / °C	Δc_p / J g^{-1} °C^{-1}	T_{eim2} / °C	T_{pm2} / °C	$-\Delta H_{m2}$ / J g^{-1}	X_{c2} / %
1%_180min_A	56	64 / 67 / 73	105.1	70	44	36 / 40	88.0	-53	-50	0.02	58	68 / 74	90.1	60
2.5%_180min_A	55	66 / 71 / 74	121.3	81	44	32 / 37	10.9	-55	-49	0.12	57	72	106.2	71
5%_180min_A	56	63 / 72	87.5	58	46	34	64.5	-	-	-	56	69 / 77	65.3	43
7.5%_180min_A	56	59 / 68 / 72	84.8	56	46	39	68.7	-	-	-	57	70 / 75	69.5	46
10%_180min_A	56	70	99.8	66	46	38	86.7	-55	-50	0.07	57	72	87.4	58

Table 13. DSC characteristics of the first heating, cooling and second heating curves of the films after immersion in 1, 2.5, 5 and 10% w/v $CaCl_2$ solutions for 180 min with double rinse (B)

Sample	1st Heating				Cooling			2nd Heating						
	T_{eim1} / °C	T_{pm1} / °C	$-\Delta H_{m1}$ / J g^{-1}	X_{c1} / %	T_{eimc} / °C	T_{pmc} / °C	ΔH_{mc} / J g^{-1}	T_{eig} / °C	T_{mg} / °C	Δc_p / J g^{-1} °C^{-1}	T_{eim2} / °C	T_{pm2} / °C	$-\Delta H_{m2}$ / J g^{-1}	X_{c2} / %
1%_180min_B	57	63 68 77	88.5	59	45	34 39	80.2	-	-	-	57	64 76	79.4	53
2.5%_180min_B	66	67 72	117.5	78	45	36 41	98.4	-56	-50	0.11	56	67 73	99.4	66
5%_180min_B	55	65 73	69.2	46	47	42	69.0	-57	-51	0.05	57	67	70.0	47
10%_180min_B	56	70	88.8	59	46	36 41	75.5	-56	-54	0.07	57	68 73	75.9	50

3.3 Non-isothermal thermogravimetry

Thermal stability is very important property of solid-state polymers and their blends. If they are going to be used as a solid polymer electrolyte, scientists must have in mind that the condition of minimum thermal stability must be at 150 °C.[38] Nonisothermal TG method was applied to analyse the thermal stability of pure NaAlg, PEO and their blend 80%PEO/20%NaAlg film before and after modification with different concentration of $CaCl_2$ solutions (complexation). The influence of immersion time or exposure time to Ca^{2+} ions and the rinse with methanol after the treatment with Ca^{2+} ions were also investigated. The obtained results are TG and DTG curves presented in Figures 48–69, while the thermal characteristics derived from TG and DTG curves are given in Tables 14-22.

Thermal degradation of pure NaAlg occurs through two degradation stages, Figure 48 and 59. The temperature at 5% mass loss ($T_{5\%}$) is 37 °C. The onset temperature (T_{onst}) and the temperature at maximum degradation rate (T_{max}) for the first degradation stage are 66 °C and 86 °C, respectively (Table 14). This degradation stage is usually attributed to the loss of water due to the hydrophilic nature of the alginate.[49,50] The residual mass at the onset (m_{onset}), the residual mass at the maximum degradation rate (m_{max}) and the maximum degradation rate (($dm/dT)_{max}$) for the first degradation stage are 98.7%, 95.3% and 1.8 % $°C^{-1}$, respectively. The second degradation stage has a major mass loss with T_{onst} and T_{max} at 239 and 247 °C, respectively (Table 14). This degradation stage represents the degradation of NaAlg polymeric structure into more simple forms like Na_2CO_3, NaOH and eventually Na_2O.[21,49,50] The second degradation stage has m_{onset}, m_{max} and (($dm/dT)_{max}$ 86.6 %, 68.3 C% and -23.3% $°C^{-1}$, respectively. The residual mass at the end of degradation process (m_f) is 38.6%, Table 14. Degradation of PEO is fast and almost complete (m_f is 3.9%), Figures 48 (TG) and 59 (DTG). It is carried through one degradation stage with $T_{5\%}$, T_{onset}, T_{max}, m_{onset}, m_{max} and (($dm/dT)_{max}$ are at 366 °C, 380 °C, 404 °C, 100.0%, 40.4% and -26.0 % $°C^{-1}$ (Table 14). If the degradation process of pure initial polymers are compared, it is visible that NaAlg degrades at lower temperature, around 140 °C lower than PEO and that m_f of NaAlg is much higher due to higher amount of inorganic substances that are released during degradation of NaAlg in the temperature interval of TG measurement.

The TG and DTG curves of blend 80%PEO/20%NaAlg film (referent film) before cross-linkage procedure with Ca^{2+} ions are shown in Figures 48 and 59. The values of

the thermal characteristics obtained from TG and DTG curves are presented in Table 14. The referent film has three degradation stages. The first stage occurs due to water loss, the second stage represents degradation of NaAlg and the third one is attributed to the degradation of PEO. The values of $T_{5\%}$ of the referent film is 234 °C. The values of T_{onset}, T_{max}, m_{onset}, m_{max} and $(dm/dT)_{max}$ of the first, the second and the third degradation stages are 64 °C, 85 °C, 99.9%, 98.5% and 0.8 % °C^{-1}; 234 °C, 250 °C, 96.4%, 91.8% and 2.6 % °C^{-1}; 398 °C, 416 °C, 85.7%, 39.6% and 25.9 % °C^{-1}, respectively (Table 14). The addition of NaAlg to PEO affected the degradation of the referent film which occured at lower temperatures comparing to pure PEO, i.e. the blend films has inferior thermal stability due to addition of NaAlg, Figure 48 and 59. It has to be emphasized that the thermal stability of PEO in the blend film was improved, T_{onset} is higher for 18 °C while T_{max} for 12 °C which could indicate the miscibility of this two polymers. Thermal stability of NaAlg is improved for just a few degrees.
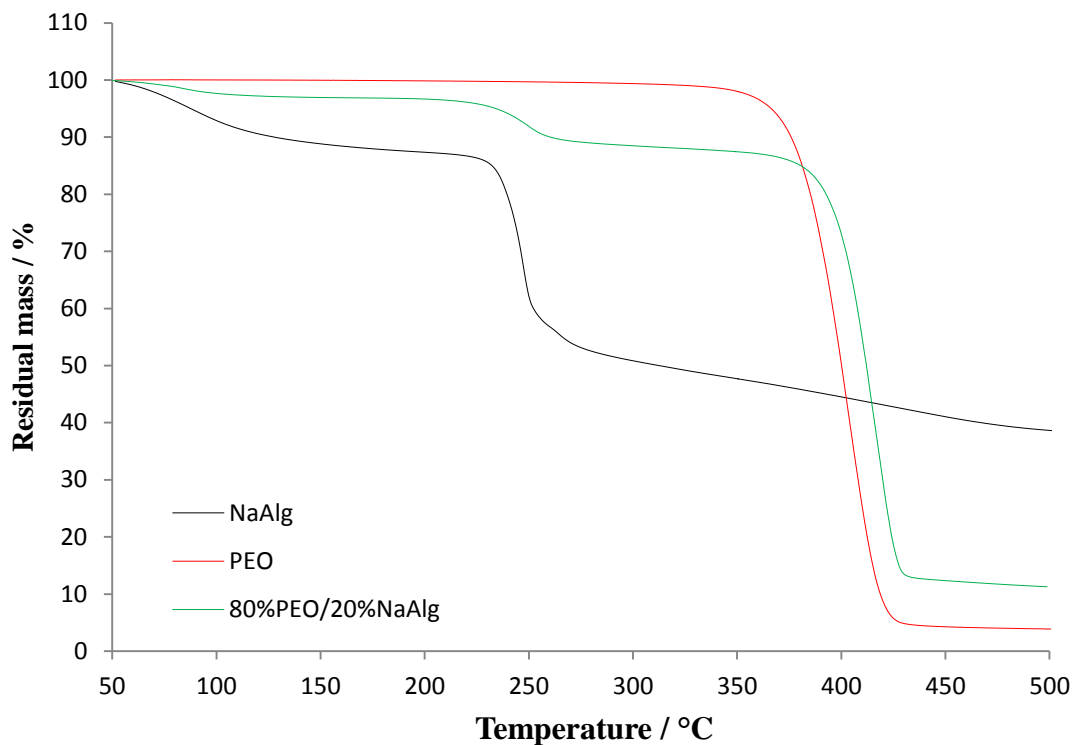

Figure 48. TG curves of the the nonisothermal degradation for pure NaAlg, pure PEO and referent blend 80%PEO/20%NaAlg film
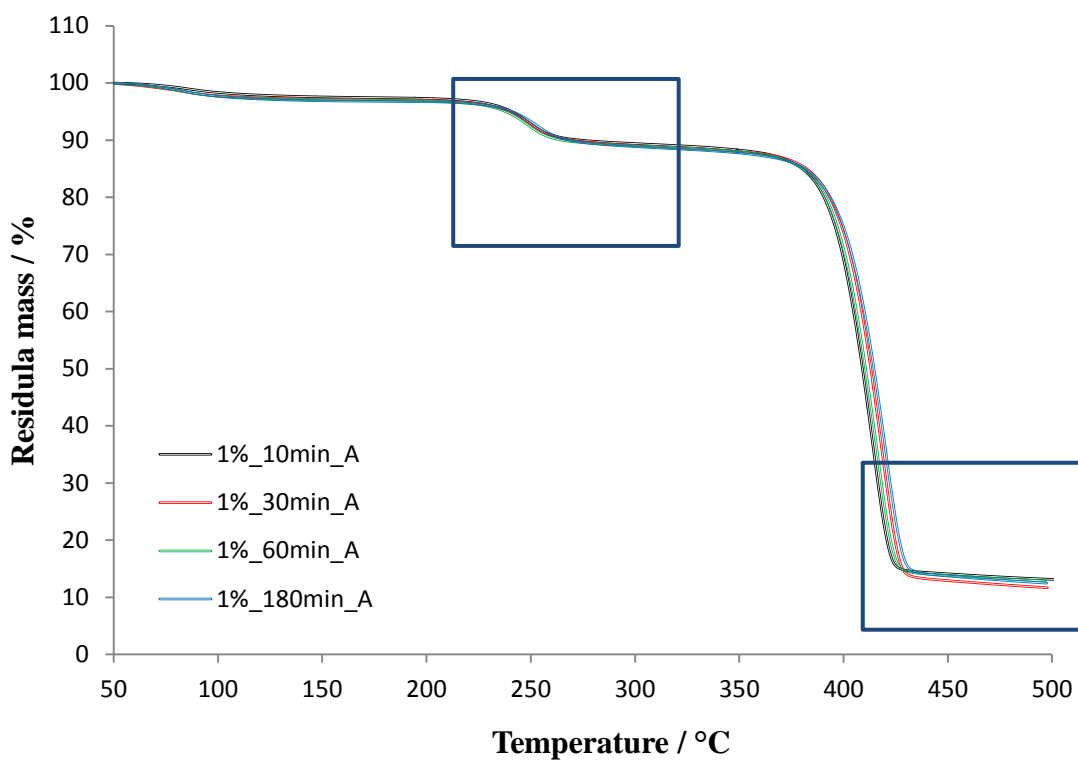
Figure 49. TG curves of the nonisothermal degradation for the films after immersion in 1% w/v CaCl$_2$ solution for 10, 30, 60 and 180 min with single rinse (A)
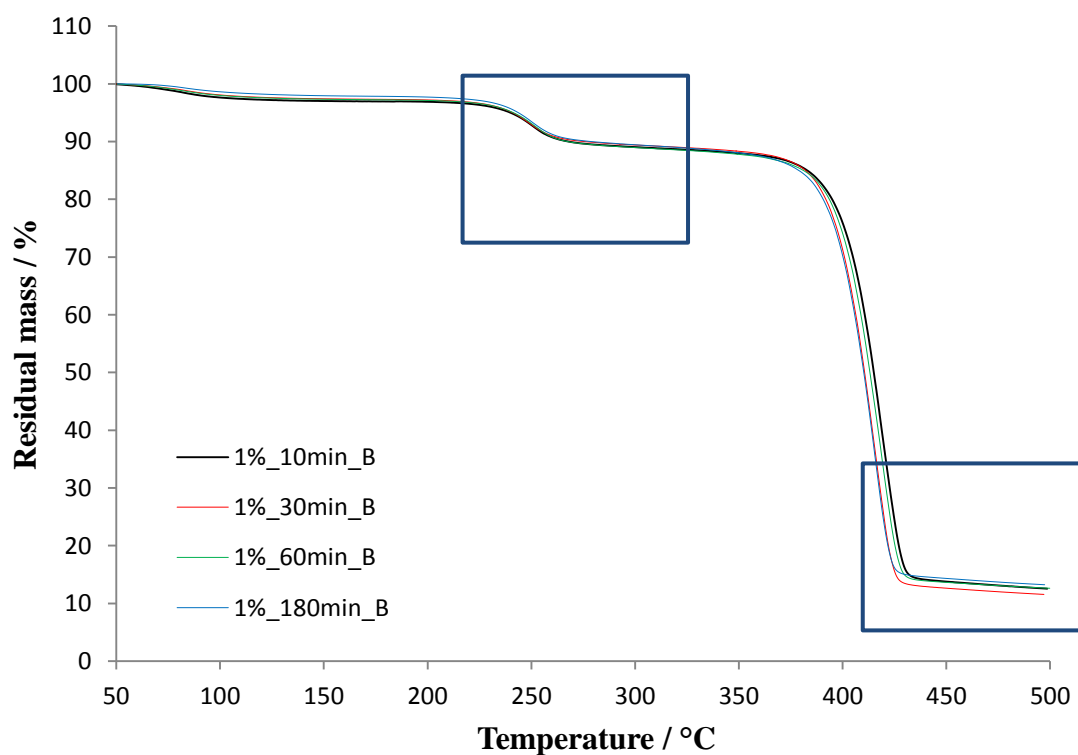

Figure 50. TG curves of the nonisothermal degradation for the films after immersion in 1% w/v CaCl$_2$ solution for 10, 30, 60 and 180 min with double rinse (B)
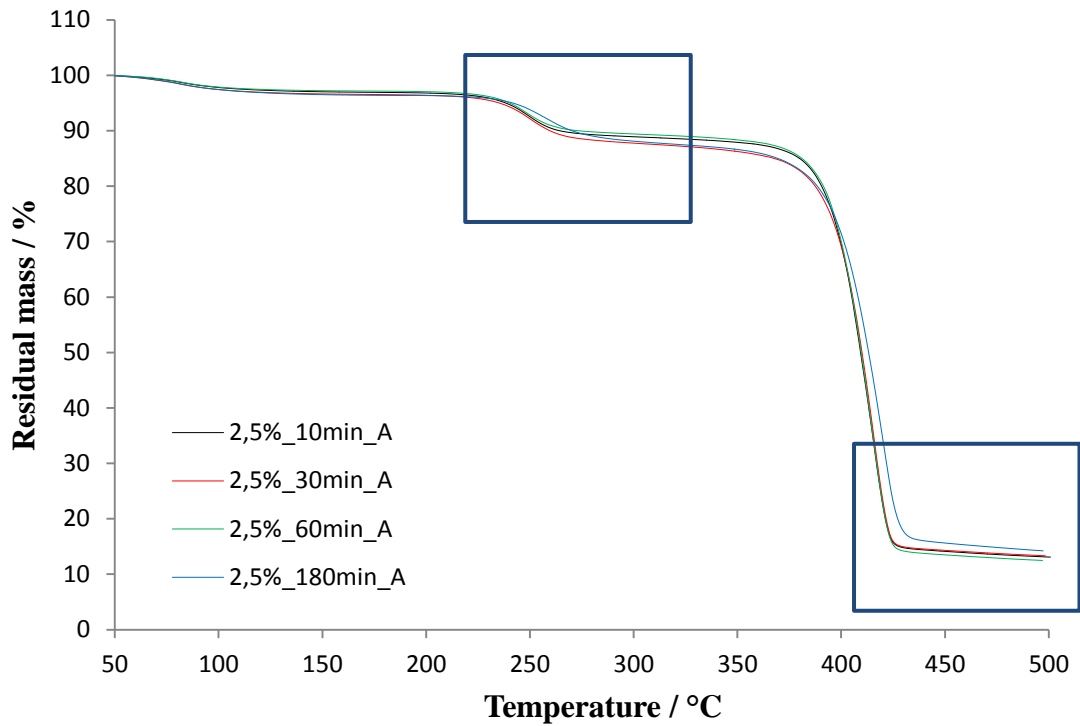
Figure 51. TG curves of the nonisothermal degradation for the films after immersion in 2.5% w/v CaCl$_2$ solution for 10, 30, 60 and 180 min with single rinse (A)
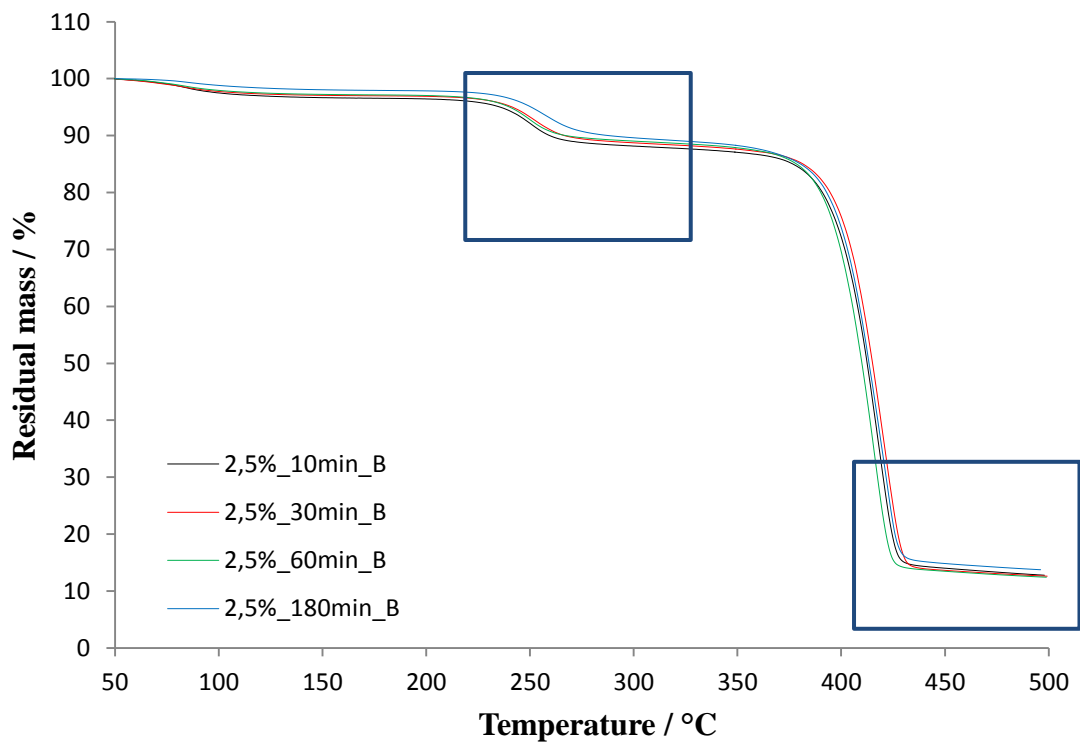

Figure 52. TG curves of the nonisothermal degradation for the films after immersion in 2.5% w/v CaCl$_2$ solution for 10, 30, 60 and 180 min with double rinse (B)

Figure 53. TG curves of the nonisothermal degradation for the films after immersion in 5% w/v CaCl$_2$ solution for 30, 60 and 180 min with single rinse (A)

Figure 54. TG curves of the nonisothermal degradation for the films after immersion in 5% w/v CaCl$_2$ solution for 10, 30, 60 and 180 min with double rinse (B)
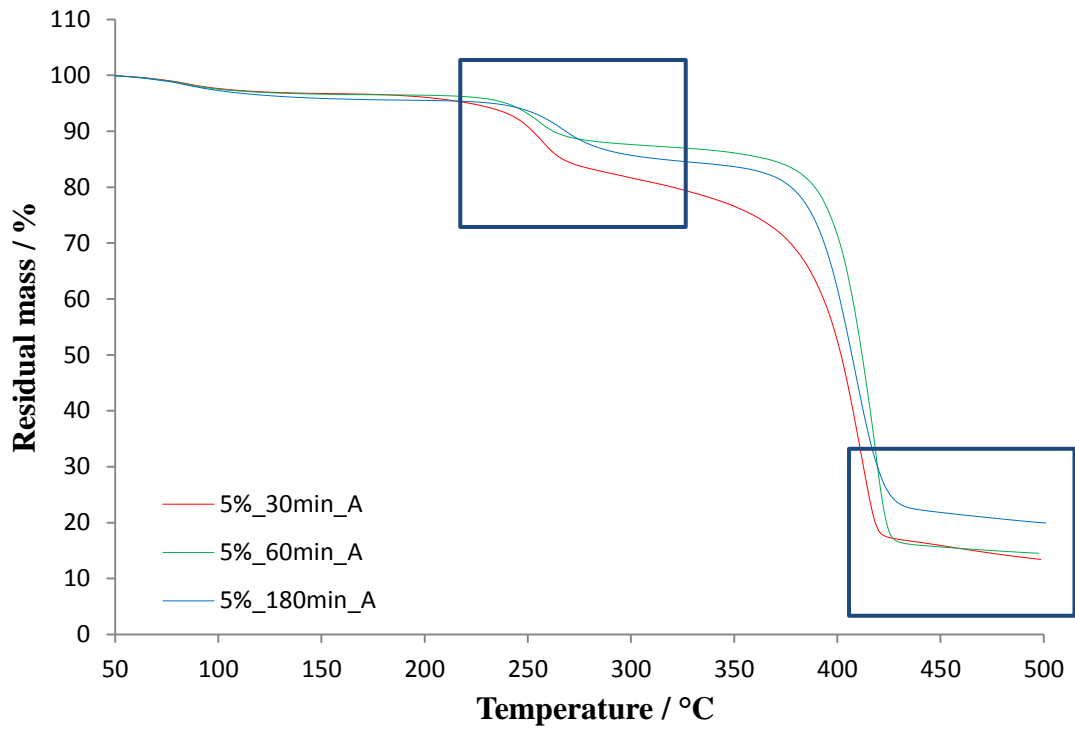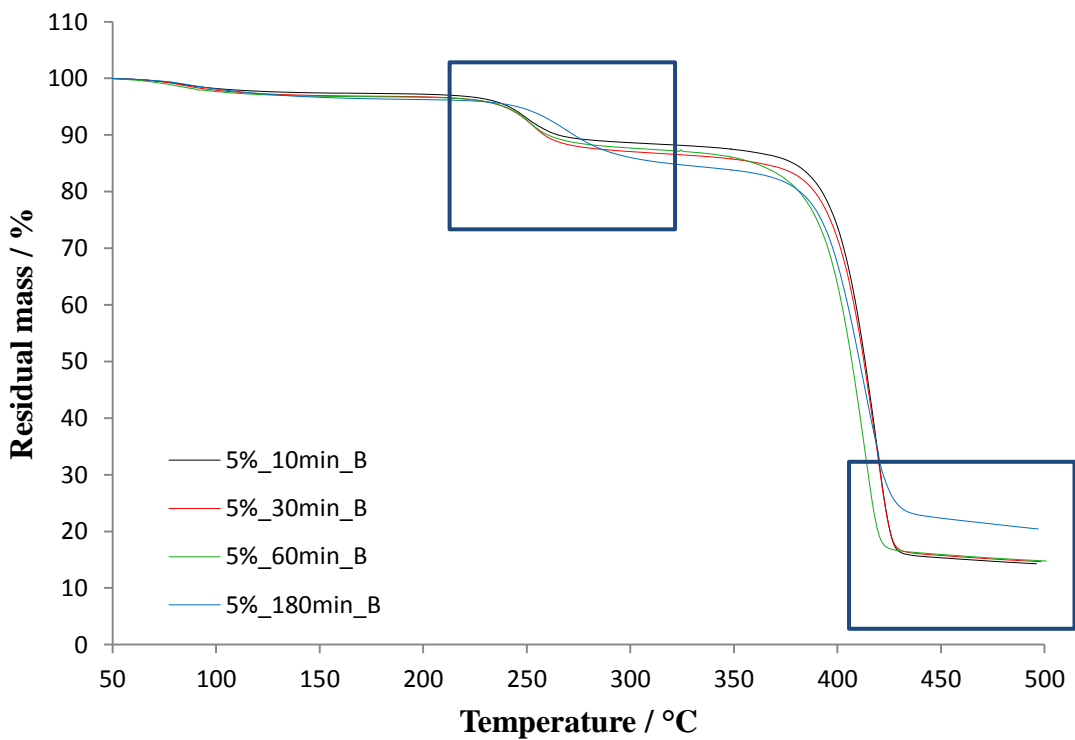
Figure 55. TG curves of the nonisothermal degradation for the films after immersion in 7.5% w/v CaCl$_2$ solution for 10, 30, 60 and 180 min with single rinse (A)

Figure 56. TG curves of the nonisothermal degradation for the films after immersion in 7.5% w/v CaCl$_2$ solution for 10, 30, and 60 min with double rinse (B)
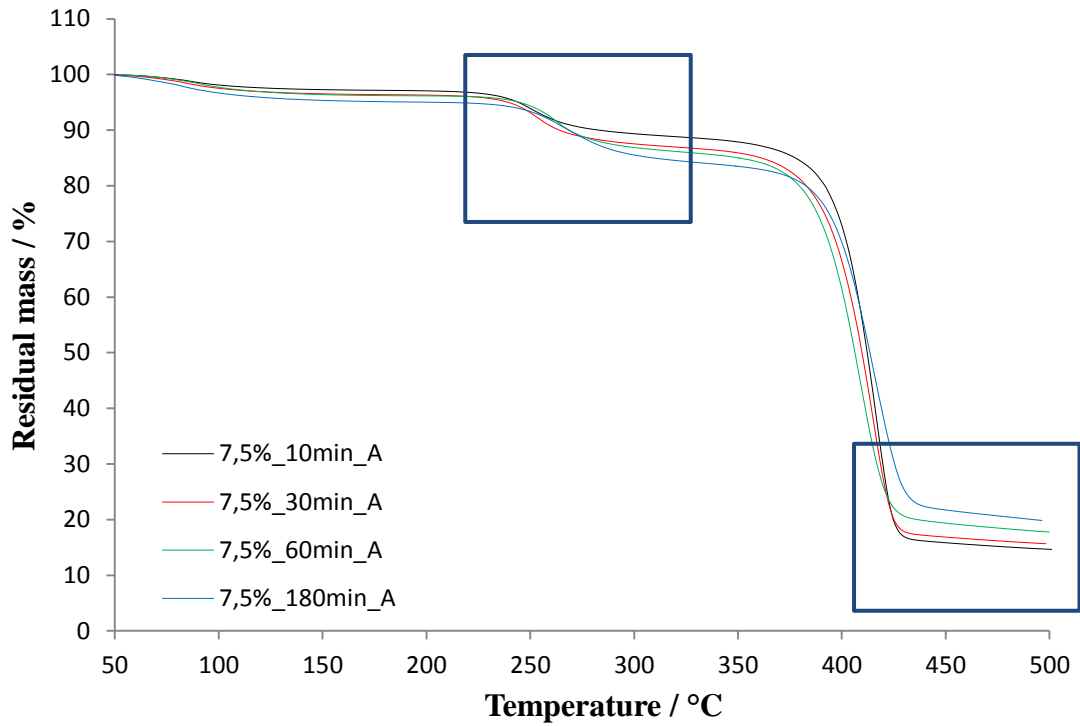
Figure 57. TG curves of the nonisothermal degradation for the films after immersion in 10% w/v CaCl$_2$ solution for 10, 30, 60 and 180 min with single rinse (A)

Figure 58. TG curves of the nonisothermal degradation for the films after immersion in 10% w/v CaCl$_2$ solution for 10, 30, 60 and 180 min with double rinse (B)

Figure 59. DTG curves of the nonisothermal degradation for pure NaAlg, pure PEO and referent blend 80%PEO/20%NaAlg film

Figure 60. DTG curves of the nonisothermal degradation for the films after immersion in 1% w/v $CaCl_2$ solution for 10, 30, 60 and 180 min with single rinse (A)
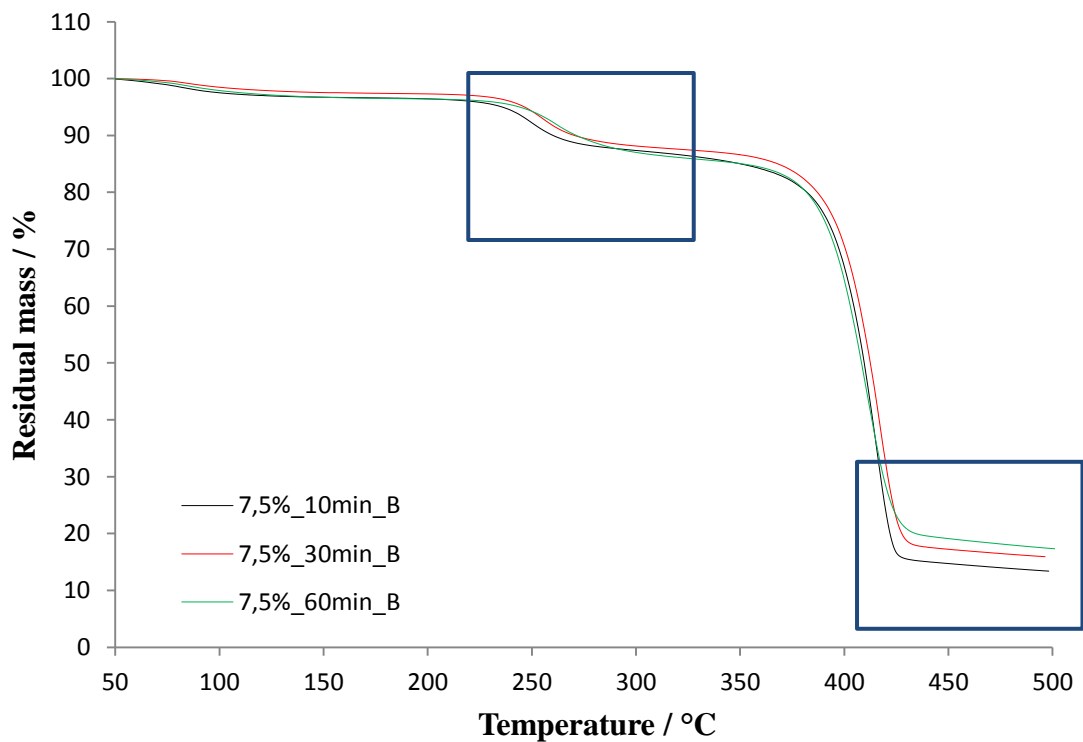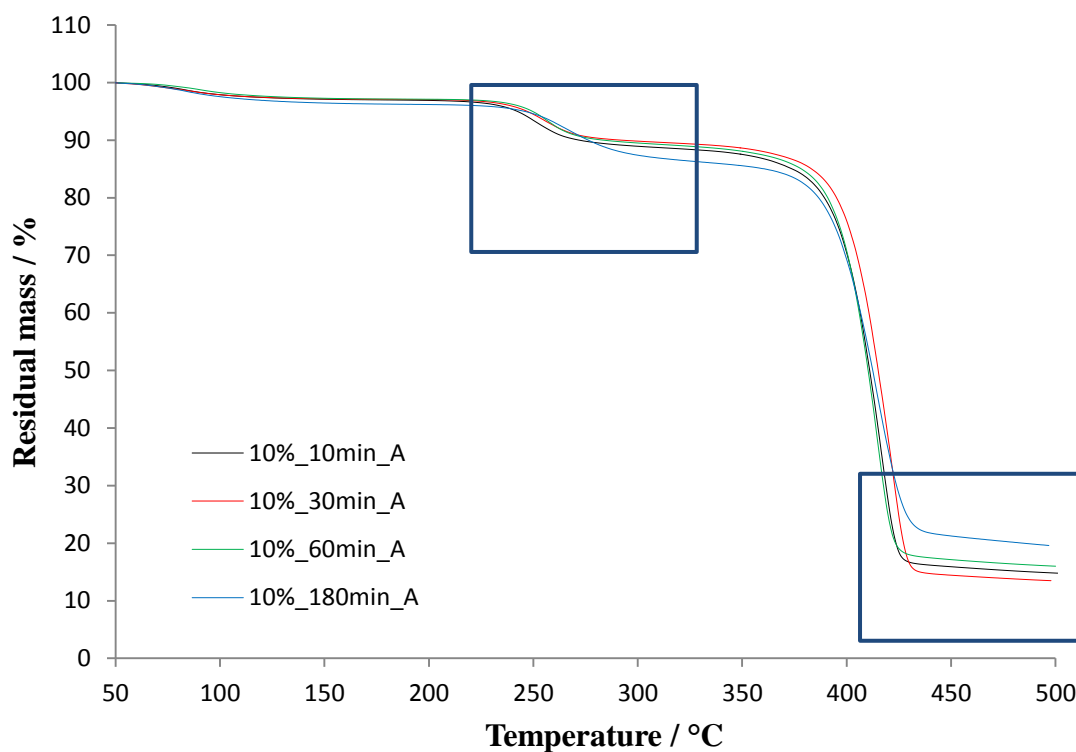
Figure 61. DTG curves of the nonisothermal degradation for the films after immersion in 1% w/v CaCl$_2$ solution for 10, 30, 60 and 180 min with double rinse (B)
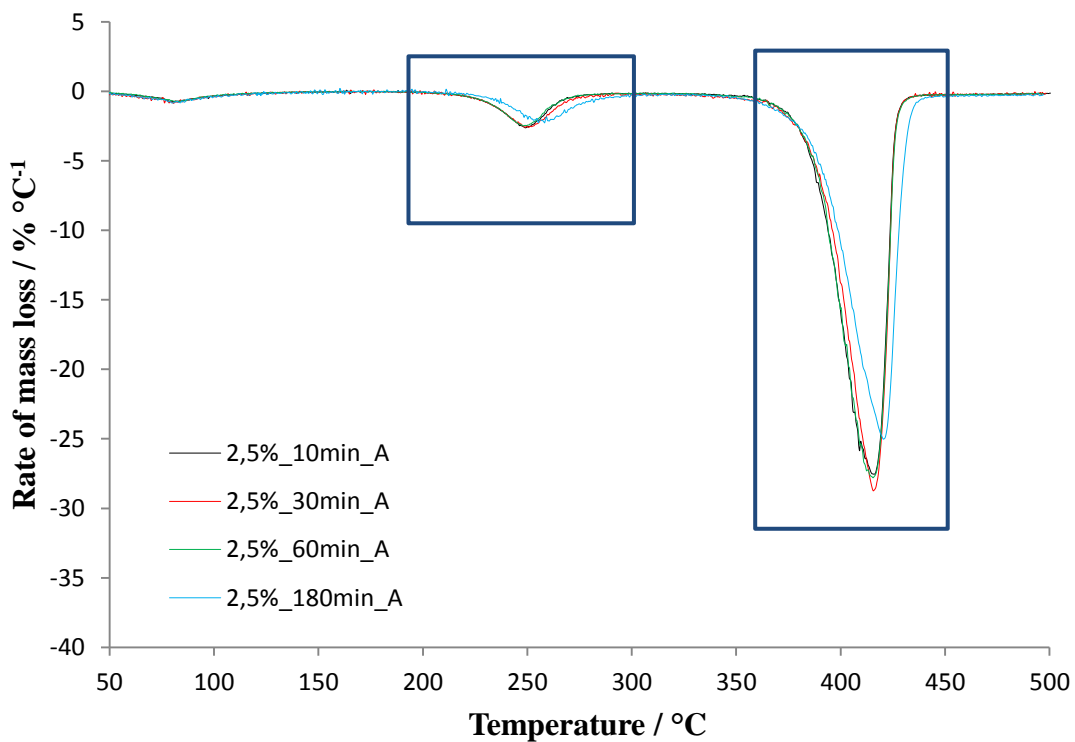
Figure 62. DTG curves of the nonisothermal degradation for the films after immersion in 2.5% w/v CaCl$_2$ solution for 10, 30, 60 and 180 min with single rinse (A)
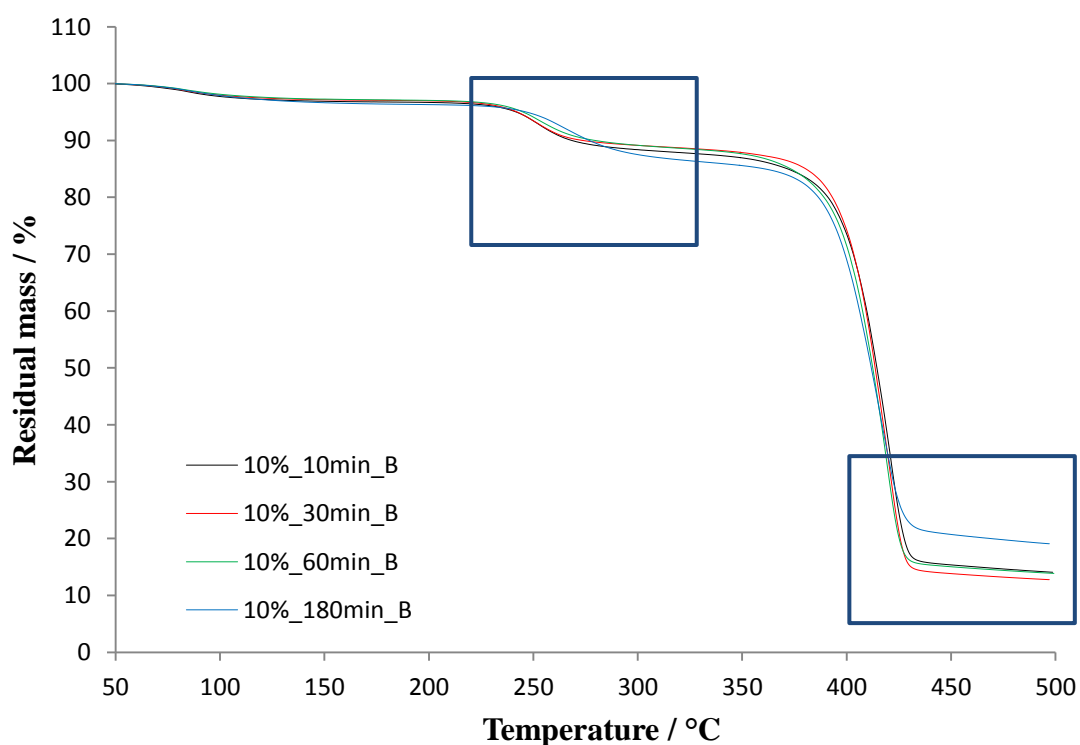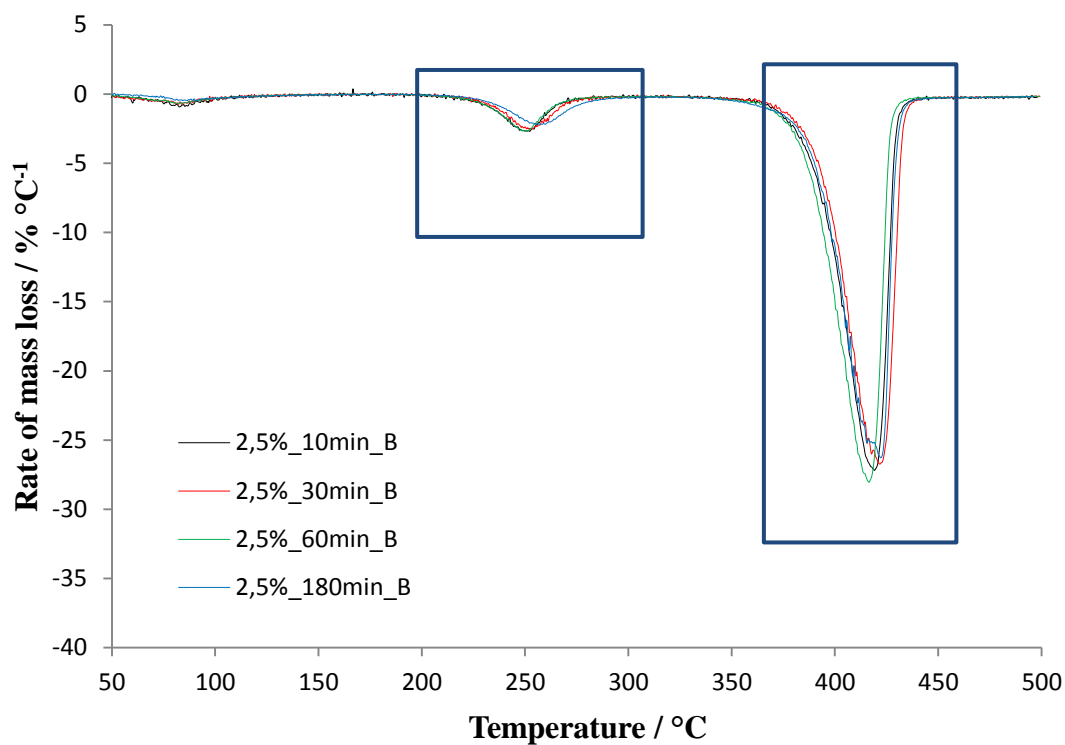
Figure 63. DTG curves of the nonisothermal degradation for the films after immersion in 2.5% w/v CaCl$_2$ solution for 10, 30, 60 and 180 min with double rinse (B)
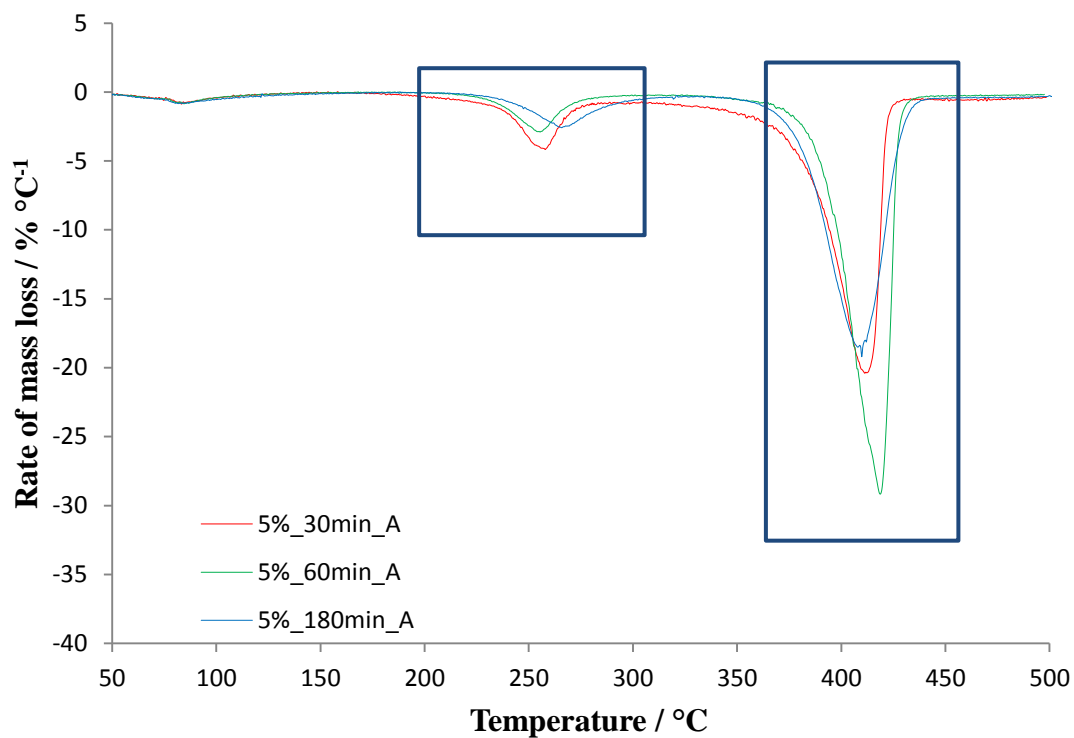
Figure 64. DTG curves of the nonisothermal degradation for the films after immersion in 5% w/v CaCl$_2$ solution for 30, 60 and 180 min with single rinse (A)
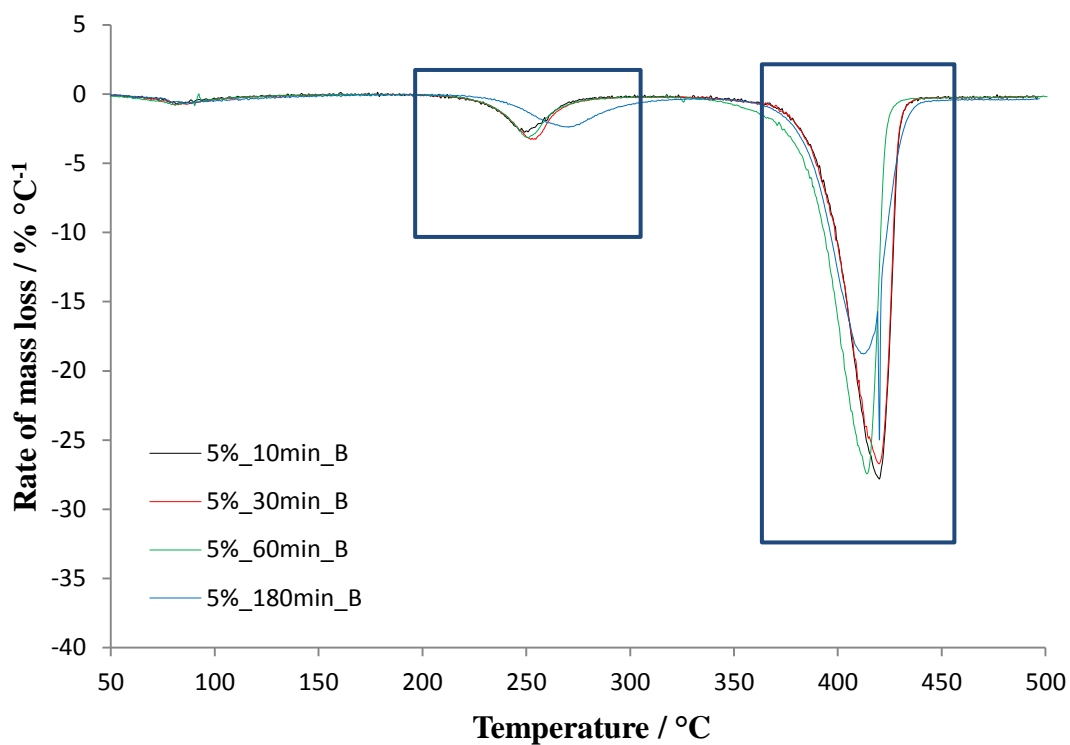
Figure 65. DTG curves of the nonisothermal degradation for the films after immersion in 5% w/v CaCl$_2$ solution for 10, 30, 60 and 180 min with double rinse (B)
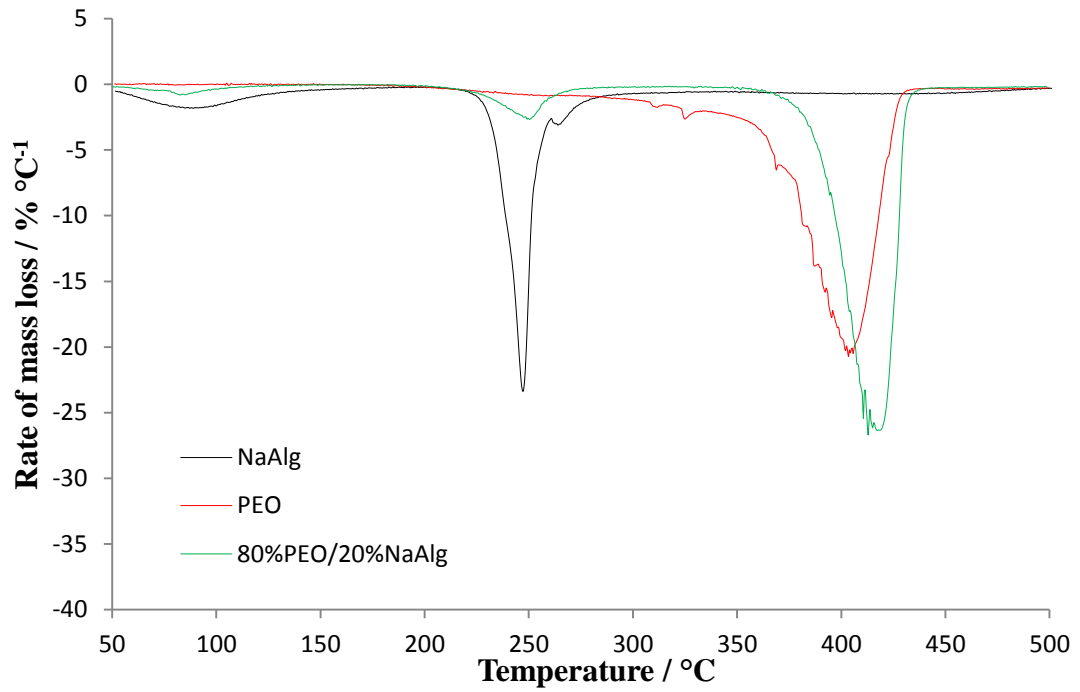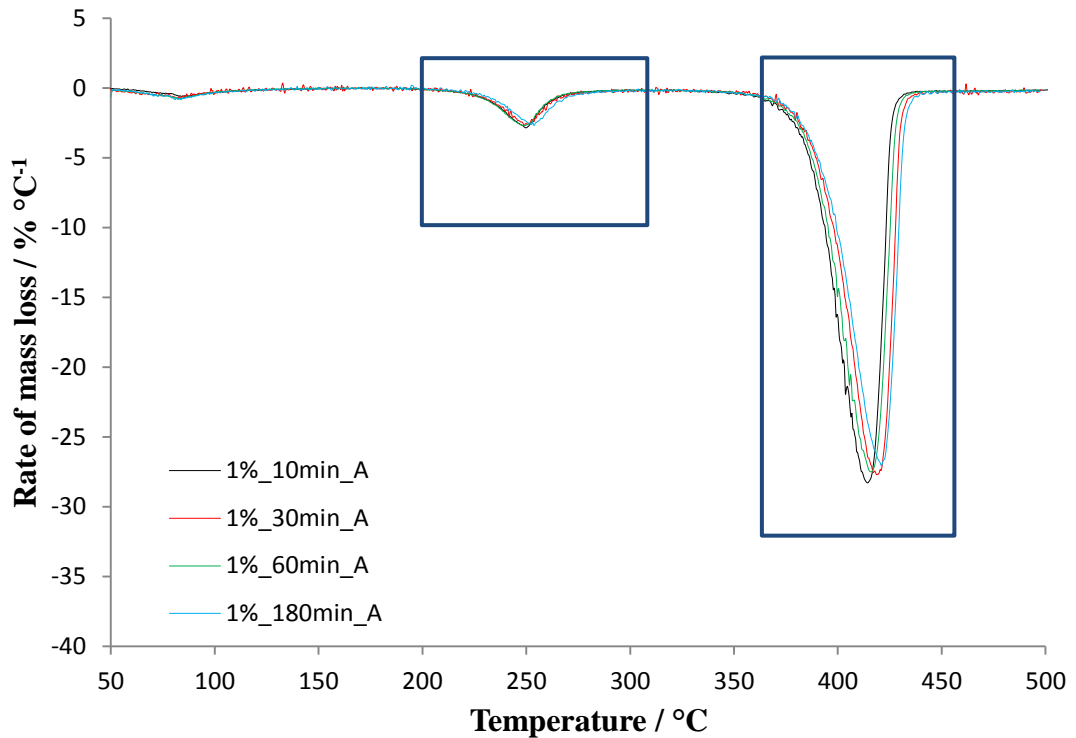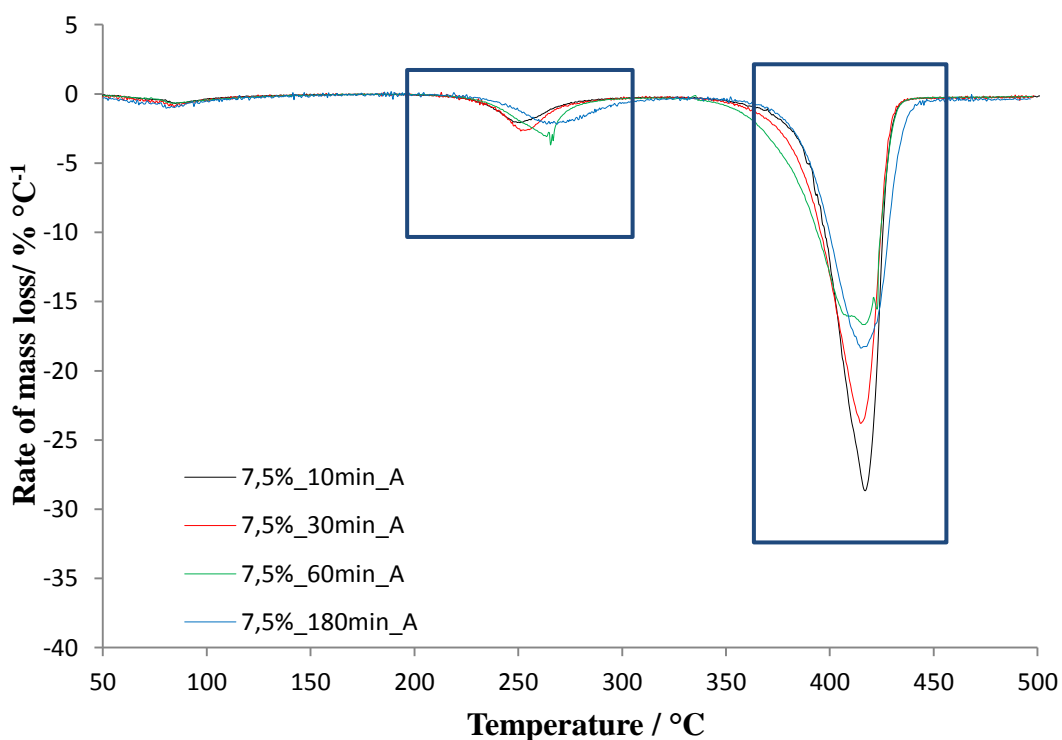

Figure 66. DTG curves of the nonisothermal degradation for the films after immersion in 7.5% w/v CaCl$_2$ solution for 10, 30, 60 and 180 min with single rinse (A)

Figure 67. DTG curves of the nonisothermal degradation for the films after immersion in 1% w/v CaCl$_2$ solution for 10, 30, and 60 min with double rinse (B)
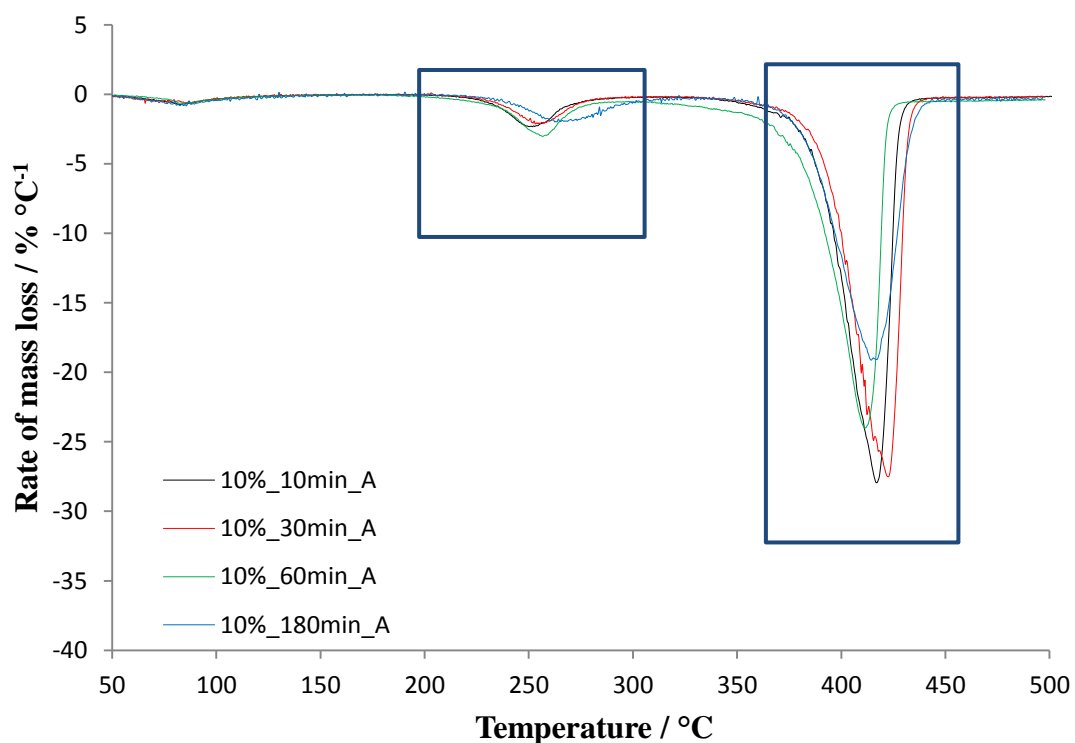
Figure 68. DTG curves of the nonisothermal degradation for the films after immersion in 10% w/v CaCl$_2$ solution for 10, 30, 60 and 180 min with single rinse (A)
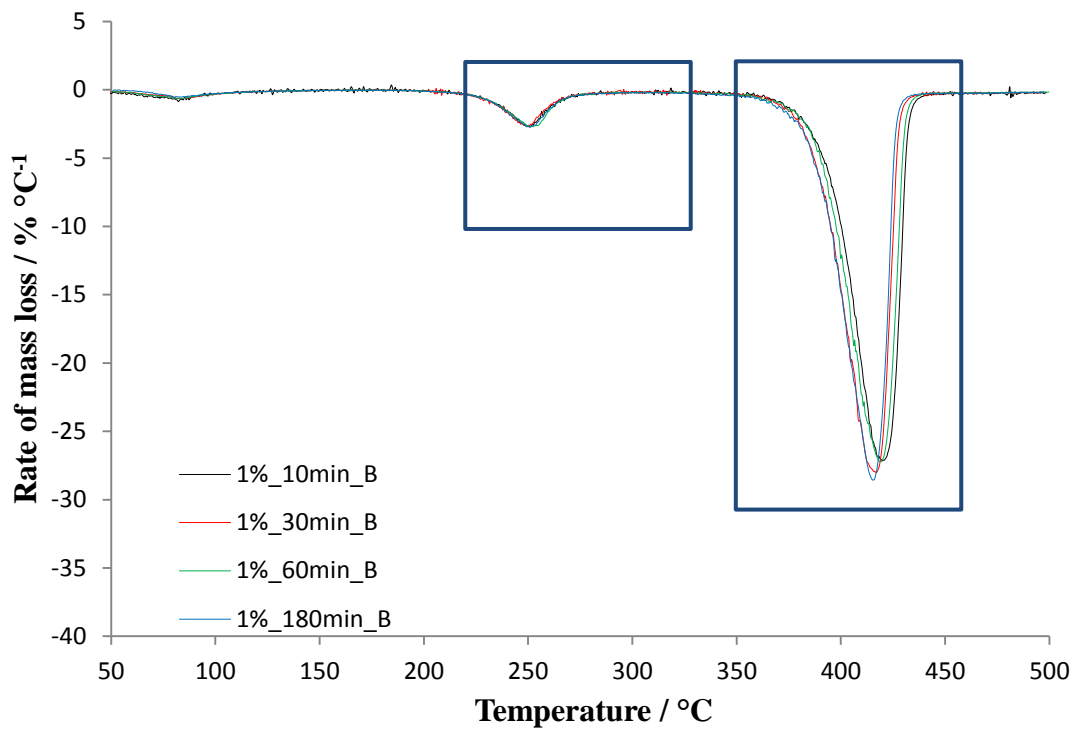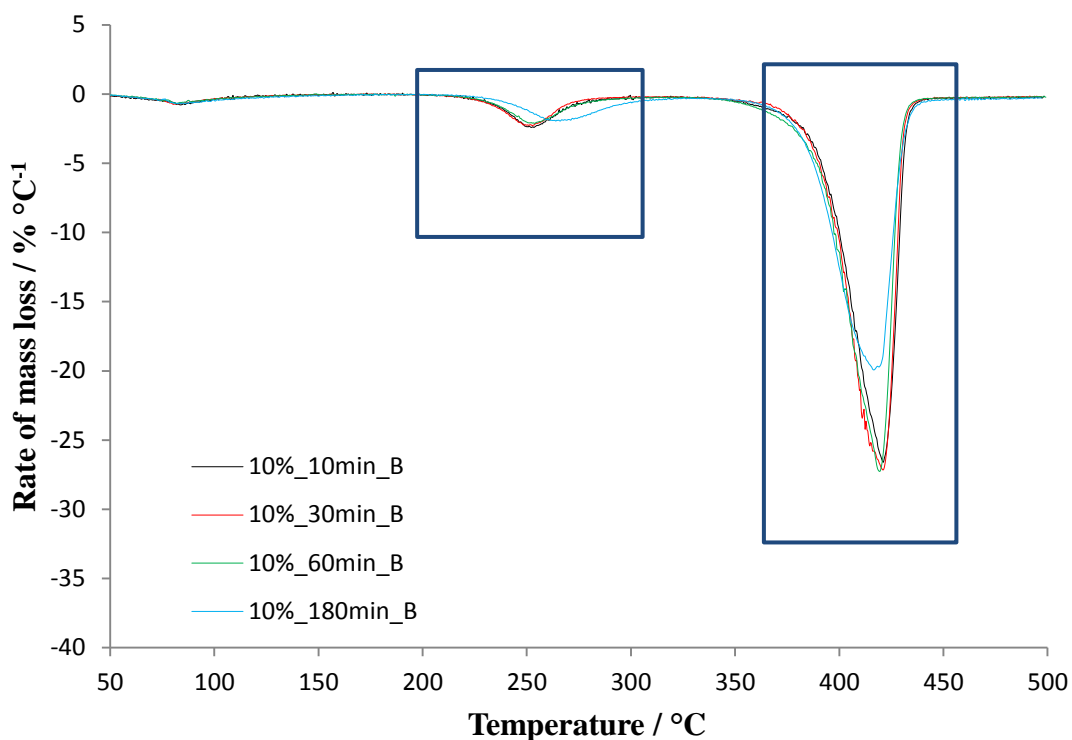
Figure 69. DTG curves of the nonisothermal degradation for the films after immersion in 10% w/v CaCl₂ solution for 10, 30, 60 and 180 min with double rinse (B)
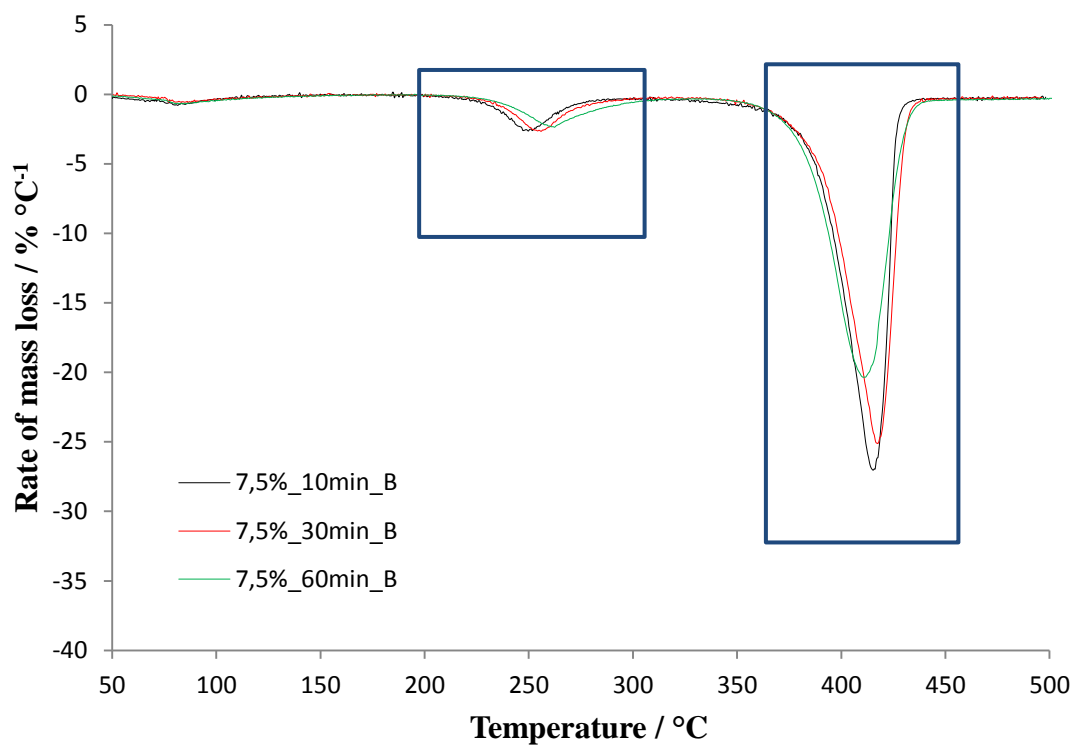
The TG and DTG curves of blend 80%PEO/20%NaAlg films after the cross-linkage procedure with Ca^{2+} ions are showed in Figures 59-58 and 60-69 while the obtained thermal characteristics are presented in Tables 15-22. Influence of different concentrations of $CaCl_2$ solutions, influence of immersion time or exposure time to Ca^{2+} ions and the number of rinses with methanol after treatment was investigated.

Comparison of all curves in the Figures and all obtained thermal characteristics in the Tables led to the following conclusions. The cross-linked films have also three degradation stages like the referent film. Thermal stability of NaAlg (the second degradation stage) in the cross-linked films is higher from the untreated film, but the films treated with concentration of 2.5, 5, 7.5 and 10% w/v $CaCl_2$ solutions during exposure time of 180 min has higher thermal stability compared to treated films during lower exposer time at the same concentration of the solution. This is clearly visible from the movement of the TG and DTG curves toward higher, Figures 59-58 and 60-69. If the results are compared at the same time but different concentration than the significant change could be observed with the concentrations higher from 5% w/v $CaCl_2$ solution. The value of T_{onset} and T_{max} increases for up to 15 °C and 20 °C, respectively (Table 15-

22). This can be attributed due to the structural changes that happens when Na^+ ions in the alginate are exchanged with Ca^{2+} ions. The structure that originates from this ion exchange is so called egg-box structure.[21] This structure makes these modified films thermally more stable and this obtained results agrees well with the previous DSC results. This does not mean that the cross-linkage in all other samples did not took place but just that was not high enough to significantly move the thermal stability of the alginate. The value of $(dm/dT)_{max}$ in the third degradation stage has generally lower values (DTG curve peak was smaller) for the films modified by the concentration of 5, 7.5 and 10% w/v $CaCl_2$ solutions during exposure time of 60 and 180 min. The value of $(dm/dT)_{max}$ decrease for up to 8 % °C^{-1}, degradation of PEO was decreased. All treated films with Ca^{2+} ions have higher values of m_f, but the films treated with concentration of 5, 7.5 and 10% w/v $CaCl_2$ solutions during exposure time of 180 min have the highest values in comparison to the referent film (the values have almost doubled). This results also pointed out that cross-linkage with Ca^{2+} ions happened, the presence of CaAlg makes degradation of alginate more stable while at the same time it decreased degradation of PEO and increased the amount of the residue after degradation process in the temperature interval of investigated TG measurement. This fact can be attributed to the CaAlg which is more stable than the NaAlg and during degradation forms thermally stable substances such as $Ca(OH)_2$, $CaCO_3$ and CaO.[21,50]

It is important to emphasize that number of rinses of the films with methanol did not make any significant change. The similar conclusion was made from FT-IR and DSC analysis. Two time rinsing was done to remove any excess of $CaCl_2$ that may remain on the films surface after ion exchange, as well as to remove NaCl which was produced during ion exchange.[21, 51, 52] In the future investigation more measuring techniques, like X-ray diffraction and X-ray micro Computed tomography, will be used to see what is happening with the mass and the surface of the films considering this residues that cannot be detected with used techniques. This additional analysis will provide information about efficiency of single and double rinse which will help to optimise the cross-linkage procedure.

Table 14. TG and DTG thermal characteristics of pure NaAlg, pure PEO and referent polymer blend 80%PEO/20%NaAlg film

Sample	Temperature area	$T_{5\%}$ / °C	T_{onset} / °C	m_{onset} / %	T_{max} / °C	m_{max} / %	$(dm/dT)_{max}$ / % °C^{-1}	Δm / %	m_f / %
NaAlg	I	37	66	98.7	86	95.3	1.8	12.2	38.6
	II		239	86.6	247	68.3	23.3	49.1	
PEO	III	366	380	100.0	404	40.3	26.0	96.1	3.9
80%PEO/20%NaAlg	I	234	64	100.0	85	98.5	0.8	3.2	11.3
	II		234	96.4	250	91.8	2.6	9.4	
	III		398	85.7	416	39.6	25.9	76.1	

Table 15. TG and DTG thermal characteristics of the films after immersion in 1, 2.5, 7.5 and 10% w/v $CaCl_2$ solutions for 10 min with single rinse

Sample	Temperature area	$T_{5\%}$ / °C	T_{onset} / °C	m_{onset} / %	T_{max} / °C	m_{max} / %	$(dm/dT)_{max}$ / % °C^{-1}	Δm / %	m_f / %
1%_10min_A	I	240	59	100.0	78	99.3	0.4	2.9	13.1
	II		235	96.6	251	92.5	2.7	8.3	
	III		395	87.4	414	35.1	28.3	75.7	
2.5%_10min_A	I	238	46	100.0	82	98.7	0.7	3.3	13.1
	II		236	96.0	248	92.8	2.6	8.8	
	III		369	86.4	416	32.0	27.5	74.7	
7.5%_10min_A	I	244	66	100.0	85	98.8	0.6	3.0	14.6
	II		237	96.4	251	93.6	2.0	8.4	
	III		399	86.6	417	35.9	28.5	73.8	
10%_10min_A	I	242	64	100.0	83	98.7	0.7	3.1	14.8
	II		236	96.5	252	93.0	2.3	8.5	
	III		396	86.6	417	32.7	27.8	73.5	

Table 16. TG and DTG thermal characteristics of the films after immersion in 1, 2.5, 5, 7.5 and 10% w/v CaCl$_2$ solutions for 10 min with double rinse

Sample	Temperature area	$T_{5\%}$ / °C	T_{onset} / °C	m_{onset} / %	T_{max} / °C	m_{max} / %	$(dm/dT)_{max}$ / % °C^{-1}	Δm / %	m_f / %
1%_10min_B	I	240	64	99.8	81	98.6	0.7	3.2	12.6
	II		236	96.7	251	92.5	2.7	8.6	
	III		400	86.8	420	36.4	27.1	75.7	
2.5%_10min_B	I	236	63	100.0	83	98.5	0.9	3.6	12.8
	II		236	95.8	253	91.4	2.6	9.5	
	III		400	85.1	420	31.9	27.1	74.1	
5%_10min_B	I	241	68	99.9	83	99.0	0.7	2.8	14.3
	II		236	96.9	251	92.8	2.8	9.2	
	III		400	86.1	420	32.3	27.8	73.7	
7.5%_10min_B	I	236	65	99.7	81	98.5	0.8	3.6	13.4
	II		236	95.9	251	92.0	2.5	9.8	
	III		397	83.6	416	33.3	27.0	73.1	
10%_10min_B	I	242	67	99.9	84	98.6	0.8	3.3	14.1
	II		237	96.7	253	92.7	2.4	9.1	
	III		401	85.3	422	32.5	26.3	73.6	

Table 17. TG and DTG thermal characteristics of the films after immersion in 1, 2.5, 5, 7.5 and 10% w/v $CaCl_2$ solutions for 30 min with single rinse

Sample	Temperature area	$T_{5\%}$ / °C	T_{onset} / °C	m_{onset} / %	T_{max} / °C	m_{max} / %	$(dm/dT)_{max}$ / % °C^{-1}	Δm / %	m_f / %
1%_30min_A	I	240	63	99.9	84	98.5	0.7	3.0	11.7
	II		234	96.8	250	92.8	2.6	8.7	
	III		400	86.1	420	32.0	27.6	76.5	
2.5%_30min_A	I	235	61	100.0	81	98.5	0.9	3.6	13.3
	II		235	96.0	250	92.2	2.5	9.9	
	III		398	84.3	416	35.3	28.7	76.2	
5%_30min_A	I	222	65	100.0	83	98.6	0.8	3.5	13.4
	II		238	95.7	259	87.3	3.9	15.5	
	III		390	74.6	413	28.7	20.2	67.5	
7.5%_30min_A	I	239	63	100.0	85	98.4	0.8	3.7	15.7
	II		239	96.1	254	92.2	2.7	9.6	
	III		395	85.1	416	36.6	237	71.0	
10%_30min_A	I	247	58	100.0	87	98.5	0.6	3.0	13.5
	II		240	96.7	256	93.3	2.1	7.9	
	III		401	87.7	423	30.8	27.5	75.8	

Table 18. TG and DTG thermal characteristics of the films after immersion in 1, 2.5, 5, 7.5 and 10% w/v $CaCl_2$ solutions for 30 min with double rinse

Sample	Temperature area	$T_{5\%}$ / °C	T_{onset} / °C	m_{onset} / %	T_{max} / °C	m_{max} / %	$(dm/dT)_{max}$ / % °C^{-1}	Δm / %	m_f / %
1%_30min_B	I	241	64	100.0	83	98.9	0.6	2.8	11.6
	II		233	97.0	250	92.9	2.6	8.7	
	III		398	87.4	417	32.2	28.0	76.9	
2.5%_30min_B	I	242	62	100.0	84	98.5	0.7	3.1	12.6
	II		239	96.3	254	92.4	2.6	9.1	
	III		401	86.2	423	30.8	26.6	75.2	
5%_30min_B	I	239	66	100.0	83	98.9	0.8	3.3	14.7
	II		239	96.4	253	91.6	3.2	10.4	
	III		399	84.3	420	31.1	26.6	71.7	
7.5%_30min_B	I	247	62	100.0	78	99.5	0.4	2.8	15.9
	II		240	97.0	255	93.0	2.6	10.1	
	III		399	84.9	418	36.6	24.9	71.1	
10%_30min_B	I	242	63	100.0	81	98.9	0.7	3.0	12.8
	II		236	96.7	250	93.4	2.3	8.7	
	III		401	86.6	422	29.4	26.9	75.5	

Table 19. TG and DTG thermal characteristics of the films after immersion in 1, 2.5, 5, 7.5 and 10% w/v $CaCl_2$ solutions for 60 min with single rinse

Sample	Temperature area	$T_{5\%}$ / °C	T_{onset} / °C	m_{onset} / %	T_{max} / °C	m_{max} / %	$(dm/dT)_{max}$ / % °C^{-1}	Δm / %	m_f / %
1%_60min_A	I	238	63	100.0	83	98.6	0.8	3.1	12.8
	II		240	96.4	250	92.4	2.7	8.8	
	III		398	86.8	417	33.8	27.4	75.2	
2.5%_60min_A	I	240	65	100.0	82	98.8	0.7	3.0	12.5
	II		234	96.6	250	93.0	2.5	8.3	
	III		396	87.1	416	32.5	28.0	76.2	
5%_60min_A	I	240	62	99.9	83	98.6	0.7	3.6	14.5
	II		240	96.0	255	91.9	2.9	9.9	
	III		401	84.0	419	32.2	29.2	72.0	
7.5%_60min_A	I	245	74	99.6	90	98.4	0.8	3.8	17.8
	II		248	96.1	264	91.2	2.9	10.3	
	III		389	84.8	410	43.2	20.4	68.1	
10%_60min_A	I	240	69	100.0	84	99.1	0.6	2.8	12.9
	II		238	96.4	258	91.0	3.0	11.3	
	III		392	80.4	412	32.6	24.0	72.9	

Table 20. TG and DTG thermal characteristics of the films after immersion in 1, 2.5, 5, 7.5 and 10% w/v $CaCl_2$ solutions for 60 min with double rinse

Sample	Temperature area	$T_{5\%}$ / °C	T_{onset} / °C	m_{onset} / %	T_{max} / °C	m_{max} / %	$(dm/dT)_{max}$ / % °C^{-1}	Δm / %	m_f / %
1%_60min_B	I	241	63	100.0	82	98.8	0.6	2.9	12.6
	II		236	96.8	253	92.4	2.7	9.1	
	III		400	86.6	419	34.0	27.2	75.4	
2.5%_60min_B	I	240	62	100.0	83	98.8	0.7	2.9	12.4
	II		235	96.7	251	92.5	2.7	8.8	
	III		397	86.8	417	32.0	28.0	75.8	
5%_60min_B	I	239	62	100.0	82	98.9	0.7	3.4	14.8
	II		238	96.2	251	92.3	3.1	9.5	
	III		394	85.4	415	30.8	27.3	72.4	
7.5%_60min_B	I	244	65	100.0	83	98.9	0.7	3,6	17.3
	II		245	96.1	263	91.8	2.4	11.0	
	III		392	83.4	412	42.7	20.3	68.1	
10%_60min_B	I	245	65	100.0	81	99.0	0.6	3.1	13.9
	II		239	69.5	253	93.6	2.1	8.7	
	III		399	86.3	420	31.3	27.1	74.4	

Table 21. TG and DTG thermal characteristics of the films after immersion in 1, 2.5, 5, 7.5 and 10% w/v CaCl$_2$ solutions for 180 min with single rinse

Sample	Temperature area	$T_{5\%}$ / °C	T_{onset} / °C	m_{onset} / %	T_{max} / °C	m_{max} / %	$(dm/dT)_{max}$ / % °C^{-1}	Δm / %	m_f / %
1%_180min_A	I		63	100.0	83	98.6	0.8	3.3	
	II	241	239	96.3	254	92.4	2.5	8.9	12.5
	III		401	86.2	421	33.4	27.1	75.3	
2.5%_180min_A	I		61	100.0	81	98.8	0.9	3.7	
	II	242	240	96.0	257	92.4	2.1	9.2	14.2
	III		399	84.8	421	31.2	25.0	72.8	
5%_180min_A	I		64	99.9	81	98.6	0.8	4.5	
	II	233	249	95.1	266	90.6	2.5	11.2	19.9
	III		390	82.4	409	45.8	18.4	64.3	
7.5%_180min_A	I		58	100.0	83	97.9	1.0	5.0	
	II	207	246	94.8	266	90.5	2.2	11.2	19.8
	III		397	81.1	416	45.2	18,1	63.9	
10%_180min_A	I		67	99.8	84	98.5	0.8	3.8	
	II	256	244	96.0	266	91.9	2.0	10.3	19.6
	III		393	84.2	416	43.5	19.0	66.3	

Table 22. TG and DTG thermal characteristics of the films after immersion in 1, 2.5, 5 and 10% w/v $CaCl_2$ solutions for 180 min with double rinse

Sample	Temperature area	$T_{5\%}$ / °C	T_{onset} / °C	m_{onset} / %	T_{max} / °C	m_{max} / %	$(dm/dT)_{max}$ / % °C^{-1}	Δm / %	m_f / %
1%_180min_B	I		66	100.0	81	99.4	0.5	2.4	
	II	244	235	97.3	255	930	2.7	9.5	13.2
	III		397	86.1	416	33.7	28.5	74.9	
2.5%_180min_B	I		63	100.0	84	99.4	0.4	2.2	
	II	251	240	97.4	257	93.8	2.2	8.9	13.7
	III		399	86.9	418	39.5	25.2	75.1	
5%_180min_B	I		67	100.0	84	99.0	0.6	3.8	
	II	246	248	95.8	270	90.8	2.4	12.0	20.4
	III		393	82.2	412	47.0	18.7	63.7	
10%_180min_B	I		64	100.0	82	98.9	0.7	3.8	
	II	247	246	95.8	265	92.3	2.0	10.4	19.1
	III		394	84.1	417	40.0	19.9	66.7	

4. CONCLUSION

> The experiment of the structural change of NaAlg in the referent blend 80%PEO/20%NaAlg film treated with different concentration of CaCl$_2$ solution in methanol, different time during which the film was exposed or immersed in the solution and different number of the rinse with methanol was done successfully.

> FT-IR analysis showed that change in the stretching vibrations of O–H bonds of alginate in the treated films are attributed to the successful cross-linkage with Ca^{2+} ions and that the greatest results are obtained at the highest concentration of CaCl$_2$ solution (10% w/v) and the highest exposure time to the solution (180 min).

> DSC analysis showed that the ability of NaAlg to cross-link with Ca^{2+} changed the crystallization process of PEO and at the same time decreased the amount of crystalline phase of PEO. The best results are obtained for the treated films at the highest exposure time (180 min) to solutions of all concentrations.

> TG analysis showed that the films treated with concentration of 5, 7.5 and 10% w/v CaCl$_2$ solution during exposure time of 180 min makes the alginate in the treated films more stable while at the same time it decreased degradation of PEO and increased the amount of the residue after degradation process.

> The number of rinses of the films with methanol did not make any significant change according to all analysis. In the future investigation, more measuring techniques will be used to provide information about efficiency of single and double rinse which will help in the optimization of the cross-linkage procedure.

> According to all analysis only conditions that consistently yielded good results of the treated films are at the highest concentration of CaCl$_2$ solution (10% w/v) and the highest exposure time to the solution (180 min). hence, in the future investigations cross-linkage of NaAlg with Ca^{2+} ions in 80%PEO/20%NaAlg film will be carried out only at these conditions.

> The aim of this research was to find the best conditions to obtain better polymer film for the preparation of the solid polymer electrolyte that will be used in a lithium or some other battery. Therefore, it is also necessary in the future work

to investigate how will addition of the salt affect to the conductivity of 80%PEO/20%NaAlg film before and after cross-linkage with Ca^{2+} ions.

5. REFERENCES

1. *Y. Zhao, Z. Huang, J. Zhang, W. Wu, M. Wang, L. Fan,* Thermal Degradation of Sodium Alginate- Incorporated Soy Protein Isolate/Glycerol Composite Membranes, 17th IAPRI World Conf. Packag., SciRes (2010) 402-405

2. *G. Ilia, E. Fagadar-Cosma, S. Iliescu, L. Macarie, N. Plesu, G. Fagadar-Cosma, A. Popa*, Solid polymer electrolites for batteries, Editura Mirton, Timisoara (2013) 8-13

3. https://sciencing.com/what-do-batteries-do-to-the-environment-if-not-properly-recycled-12730824.html

4. *J. Gurusiddappa, W. Madhuri, R. Padma Suvarna, K. Priya Dasan,* Electrical Properties of PEO – Based Electrolytes, International Journal of Innovative Research in Science, Engineering and Technology, IJIRSER **4** (2015) 11447-11454

5. *C. E. Carraher, Jr.,* Polymer Chemistry, sixth edition USA (2003) 37-53

6. *M. Rubinstein, R. H Colby,* Polymer Physics (Chemistry), Oxford University Press Inc, New York (2003) 380

7. https://iupac.org/polymer-edu/what-are-polymers/

8. *R. G. Jones, J. Kahovec, R. Stepto, E. S. Wilks,* Compendium of Polymer Terminology and Nomenclature, IUPAC Recommendations (2008) 1-16

9. https://byjus.com/jee/polymers/

10. *T. A. Osswald, G. Menges,* Materials science of Polymers for Engineers , 3rd edition, Munich(1996) 59-72

11. https://preparatorychemistry.com/Bishop_Chapter_Maps.htm

12. http://www.polymerdatabase.com/polymer%20chemistry/Condensation%20Polymerization.html

13. https://www.slideserve.com/dmitri/condensation-polymers

14. *T.I. Sogolova,* The supramolecular structure of polymers and its effect on their mechancal properties, Mekhanika polimerov, Vol. **I** (1965) 5-16

15. *H. V. Boenig,* Structure and Properties of Polymers, Stuttgart (1973) 127

16. http://www.dynamicscience.com.au/tester/solutions1/chemistry/crystallinestructures.html

17. *L. Yue*, *J. Ma*, *J. Zhang*, *J. Zhao*, *S. Dong*, *Z. Lin*, *G. Cui*, *L. Chen*, All solid-state polymer electrolytes for high-performance lithium ion batteries, Energy Storage Materials **5** (2016) 139–164

18. *S. B. Upadhye, A. R. Rajabi-Siahboom,* Properties and Applications of Polyethylene Oxide and Ethylcellulose for Tamper Resistance and Controlled Drug Delivery, Melt Extrusion **9** (2013) 145-158

19. *Lu Ren*, Production of Alginate Beads , New Zeland(2008) 1-10

20. https://pubchem.ncbi.nlm.nih.gov/compound/5102882

21. *P. dos Santos Araújo, G. Bertoni Belini,G. Pimenta Mambrini, F. Minoru Yamaji, W. Ruggeri Waldman,* Thermal degradation of calcium and sodium alginate: A greener synthesis towards calcium oxide micro/nanoparticles, International Journal of Biological Macromolecules **140** (2019) 749-760

22. *S. Peretz, M. Florea-Spiroiu, D. F. Anghel, C. Stoian, G. Zgheria,* Preparation of Porous Calcium Alginate Beads and Their Use for Adsorption of O-Nitrophenol from Aqueous Solutions, Romania (2014) 123-134

23. *A.S. Waldman, L. Schechinger, G. Govindarajoo, J. S. Nowick, L. H. Pignolet,* The alginate demonstration: polymers, food science, and ion exchange. J. Chem. Educ. **11** (1998) 1639-1646

24. *J.Y. Song*, *Y.Y. Wang*, *C.C. Wan*, Review of Gel-Type Polymer Electrolytes for Lithium-Ion Batteries, Power Sources **77** (1999) 183-197

25. *R. C. Agrawal*, *G. P. Pandey*, Solid polymer electrolytes: Materials designing and all solid state battery application: an overview, Journal of Physics. D: Applied Physics **41** (2008) 1-18

26. *B. Smitha*, *S. Sridhar*, *A.A. Khan*, Solid polymer electrolyte membranes for fuel cell applications-a review, Journal of Membrane Science **259** (2005) 10-26

27. *F. Zia, M. N. Anjum, M. J. Saif, T. Jamil, K. Malik, S. Anjum, I. BiBi, M. A. Zia*, Alginate-Poly(Ethylene) Glycol and Poly(Ethylene) Oxide Blend Materials, , Elsevier, Amsterdam (2017) 581-594

28. *J. W. Rhim*, Physical and mechanical properties of water resistant sodium alginate films, Lebensm.-Wiss. u.-Technol. **37** (2004) 323–330

29. *L.V. Gregov*, Physics of thin films, **3** (1966), 144

30. *G. H. Jackson*, Thin solid films (1970), 209

31. *E. B. Mana*, *L. K. Durow*, Impedance spectroscopy Emphsizing Solid material and system, Wiley, New York (1987)

32. *J. B. Whiteand*, *C. Wagner*, Thin Solid Films (1973) 157

33. *B. Jinisha*, *K. M. Anilkumar*, *M. Manoj*, *V. S. Pradeep*, *S. Jayalekshmi*, Development of a novel type of solid polymer electrolyte for solid state lithium battery applications based on lithium enriched poly (ethylene oxide)(PEO)/poly (vinyl pyrrolidone)(PVP) blend polymer, Electrochimica Acta **235** (2017) 210-222

34. *A. Sesar,* Utjecaj natrijevog alginate na pripravu I toplinska svostva filmova poli(etilen-oksida), Diplomski rad, Kemijsko-tehnološki fakultet, Split (2019)

35. *M. Jakić,* Studij međudjelovanja komponenata u polimernim mješavinama poli(vinil-klorid)/poli(etilen-oksid), Doktorska disertacija, Kemijsko-tehnološki fakultet, Split (2014) 7-8, 37.

36. *C.R. Badita, D. Aranghel, C. Burducea, P. Mereuta,* Characterization of sodium alginate based films, Romania, (2019)

37. *K. Kulasekarapandian, S. Jayanthi, A. Muthukumari, A. Arulsankar, B. Sundaresan,* Preparation and Characterization of PVC – PEO Based Polymer Blend Electrolytes Complexed With Lithium Perchlorate, International Journal of Engineering Research and Development, **5** (2013) 30-39

38. *G. Patel, M. B. Sureshkumar, P. Patel,* Spectroscopic Investigation and Characterizations of PAM/PEO Blends Films, Soft **4** (2015) 9–24

39. *H. Daemi, M. Barikani,* Synthesis and characterization of calcium alginate nanoparticles, sodium homopolymannuronate salt and its calcium nanoparticles, Scientia Iranica F **19** (2012) 2023-2028

40. *J. Nastaj, A. Przewłocka, M. Rajkowska-Myśliwiec,* Biosorption of Ni(II), Pb(II) and Zn(II) on calcium alginate beads: equilibrium, kinetic and mechanism studies, Polish Journal of Chemical Technology **18** (2016) 81-87

41. *M. J. Costa, Arlete M. Marques, L. M. Pastrana, J. A. Teixeira, S. M. Sillankorva, M. A. Cerqueira,* Physicochemical properties of alginate-based films: Effect of ionic crosslinking and mannuronic and guluronic acid ratio, Food Hydrocolloids **81** (2018) 442-448

42. *V. Wan-Ping, L. Boon-Beng, I. Ani, I. Aminul, T. Beng-Ti, C. Eng-Seng,* Production of ultra-high concentration calcium alginate beads with prolonged dissolution profile, RSC Adv. **5** (2015) 36687–36695

43. *A. Grossi Santos de Laia, E. de Souza Costa Júnior, H. de Souza Costa,* A study of sodium alginate and calcium chloride interaction through films for intervertebral disc regeneration uses, Brasil (2014)

44. *J. P. Soares, J. E. Santos, G. O. Chierice, E. T. G. Cavalheiro,* Thermal behavior of alginic acid and its sodium salt, Eletica Quimica **29** (2004) 57-63

45. *A. G. Pereira*, *A. T. Paulino*, *A. F. Rubira*, *E. C. Muniz*, Polymer-Polymer Miscibility in PEO/Cationic Starch and PEO/Hydrophobic Starch Blends, EXPRESS Polym. Lett. **4** (2010) 488–499

46. *R. M. Ramos Wellen*, *M. Silveira Rabello*, *I. C. Araujo Júnior*, *G. J. Macedo Fechine*, *E. L. Canedo*, Melting and crystallization of poly(3-hydroxybutyrate): effect of heating/cooling rates on phase transformation, Polímeros **25** (3) (2015) 296–304

47. *M. L. Di Lorenzo*, *P. Sajkiewicz*, *P. La Pietra*, *A. Gradys*, Irregularly shaped DSC exotherms in the analysis of polymer crystallization, Polymer Bulletin **57** (2006) 713–721

48. *S. Kuo*, Hydrogen-bonding in polymer blends. J. Polym. Res. **15** (2008) 459–486

49. *Y. Qi, M. Jiang, Y.-L. Cui, L. Zhao, X. Zhou*, Synthesis of Quercetin Loaded Nanoparticles Based on Alginate for Pb(II) Adsorption in Aqueous Solution, Nanoscale Research Letters **10** article 408 (2015) 1-9

50. *T. S. Pathak, J. S. Kim, S.-J. Lee, D.-J. Beak, K.-J. Paeng*, Preparation of Alginic Acid and Metal Alginate from Algae and their Comparative Study, J Polym Environ **16** (2008) 198–204

51. *R. S. Herme, R. Narayani,* For all polymer films treated with Ca^{2+} ions with all used concentration, exposure time and number of rinsing, Trends Biomater. Artif. Organs. **15** (2002) 54-56

52. *C. Remunan-Lopez, R. Bodmeier,* Mechanical, water uptake and permeability properties of cross-linked chitosan glutamate and alginate films, Journal of Controlled Release **44** (1997) 215-225